Source Test of Steam-Assisted Flare Tips with Passive FTIR – BP Whiting

Final Report
November 14, 2014

BP Products North America
Whiting Refinery
2815 Indianapolis Boulevard
Whiting, IN 46394

Prepared by
Clean Air Engineering, Inc.
Project No: 12359

Contents

1.0 Background and Summary

1.1 Overview

As required by Paragraph 38 of BP Products North America's (BP) Flare Consent Decree (No. 2:12-cv-00207-PPS-APR), BP conducted source testing on the Whiting ALKY and DDU flares at the Whiting Refinery (Whiting) from July 10th to July 16th, 2014. As a result of this work, BP can establish operating envelopes for its flares to ensure its traditional steam-assisted elevated flares perform at high combustion efficiency.

It should be noted that the testing was performed according to the submitted test protocol with the following exception. DDU flare testing was ended prior to achieving 93% combustion efficiency. This was necessary because when the maximum available of supply steam was applied to the flare the resulting combustion efficiency measured was ~95%. No other deviations from the submitted protocol were made during testing.

Appendix D paragraph 38 of the CD sets forth several requirements for scheduling of the testing covered in this report. Table 1.1-1 presents both schedule requirements and the date this compliance requirement was satisfied.

Test Scheduling Requirement	Date/Time Specified in CD	Date Requirement Met
Submit PFTIR Test Protocol	At least 60 days prior to each test	Submitted 4/15/2014
Conduct PFTIR testing	No later than 9/1/2014	PFTIR testing completed on 7/17/14
Submit Test Report	No later than 4 months after completion of PFTIR testing	Submitted on 11/11,2014

Table 1.1-1: PFTIR Test Scheduling Compliance

Appendix D paragraph 39 of the CD sets forth several requirements related to the contents of this test report. Table 1.1-2 presents the consent decree requirements and the corresponding section of this test report that fulfills each compliance requirement.

Consent Decree Requirement	Consent Decree Reference	Corresponding Test Report Section
Minute by minute electronic data in Excel format for all measurements and process data.	App D, ¶39.a	Appendices A.5 thru A.13
Description of the extent to which the NHV_{cz} affects combustion efficiency	App D, ¶39.b	Figs 3.1-2 & 3.2.1 Sect. 3.4-1
Range of NHV_{cz} that the covered flares must be operated at to ensure 98% combustion efficiency	App D, ¶39.c	Sect. 3.4-1
The "A" combustion efficiency multiplier for calculating $NHV_{cz\text{-}limit}$ which BP proposes to operate the covered flares	App D, ¶39.d	Sect. 3.4-1
Evaluation of the impact of the "A" combustion efficiency multiplier for calculating NHVcz-limit at the six covered flares not subject to PFTIR testing	App D, ¶39.e	Sect. 3.4-1

Table 1.1-2: Correlation of Report Content with Consent Decree Requirements

The operating envelope of a flare is bounded by excess smoke (too little assist) on one side and by decreased combustion efficiency resulting in excess emissions of volatile organic compounds (VOCs) (too much assist) on the other. Smoke suppression is easily monitored by visually observing whether smoke is present. However, the ability to measure or even identify excess emissions caused by over-assisting is a more difficult task. Standard emission estimation techniques have generally assumed a 98% combustion efficiency or higher when calculating VOC emissions from flares regardless of assist rate.

Regulatory requirements for flares are contained in 40 CFR §60.18 and §63.11. These requirements were developed from a series of flare emissions tests led by the United States Environmental Protection Agency (US EPA) from 1983 – 1986. The requirements include maintaining a flare pilot, operating with a minimum net heating value of 300 BTU/scf in the vent gas, operating at exit velocities of less than 60 ft/s (or up to 400 ft/s depending upon the vent gas net heating value), and operating with a limited amount of visible emissions. However, a flare can be operated in compliance with these requirements and still have low combustion efficiency due to over-assisting.

Prior to the recent refinery tests of flare performance, including the US EPA tests in the mid-1980s, flare tests were conducted on pilot-scale test flares or on flares operating at moderate to high vent gas loads. However, a flare typically operates at low vent gas loads (i.e. high turndown) under normal conditions until a process upset or other operating condition requires the operator to flare waste gas. Thus, the flare normally operates at high turndown for the majority of the operating year, a condition for which there was little to no available performance data.

In the past, measuring the combustion products from a flare was difficult and dangerous. However, recent technological advances have produced remote sensing instruments capable of measuring combustion products such as carbon dioxide, carbon monoxide, and select

hydrocarbons without the safety hazards introduced by physically sampling a flare plume. One such instrument is the PFTIR, which characterizes a plume's chemical make-up (carbon dioxide, carbon monoxide, and total hydrocarbons) in units of concentration × pathlength. Using this technology, the absolute concentration cannot be determined from a flare plume, but the product of concentration × pathlength (e.g., ppmv × meters), can be used in combustion efficiency calculations. The PFTIR is a relatively new tool and was recently blind-validated against extractive sampling results for flare plume testing by TCEQ and the University of Texas in 2010. The PFTIR was first used for refinery flare testing at MPC Texas City in 2009. Several accuracy, precision, and bias checks were performed during the recent flare tests to better characterize the PFTIR measurement technique.

The flare tests were conducted using Passive Fourier Transform Infrared (PFTIR) instruments. The specific analytical method used for these tests is the same method used and validated during testing conducted by the Texas Commission on Environmental Quality (TCEQ) in 2010. This report summarizes the test results and compares them to results from previous flare tests.

Figure 1.1-1: DDU (Left) and ALKY (Right) Flare Tips

Combustion efficiency was measured under base load vent gas conditions and various steam rates. Each of these combinations is referred to as a "test condition" in this report. The following test conditions were used during this project.

ALKY Base Load Flow and Composition. Variable Steam Rate.
Objective: To determine the performance curve of the ALKY flare under base load conditions. Fuel flow was set to base load flow rate and base load composition. The initial test condition targeted the incipient smoke point. Subsequent test conditions increased the steam rate to achieve successively lower NHVcz values until a combustion efficiency of <93% was measured. The steam rate that achieved <93% CE was the final test condition of this series. Two replicates were performed for each test condition.

DDU Base Load Flow and Composition. Variable Steam Rate.
Objective: To determine the performance curve of the DDU flare under base load conditions. Fuel flow was set to base load flow rate and base load composition. The initial test condition targeted the incipient smoke point. Subsequent test conditions increased the steam rate to achieve successively lower NHVcz values until the capacity of the steam-assist system was reached. Two replicates were performed for each test condition.

The PFTIR performance test conducted on Whiting's DDU and ALKY Flare systems produced valuable insights into the efficiency performance of the two flares under typical operating conditions. Tests were conducted while flaring fuel gases containing hydrocarbons, hydrogen, and nitrogen. For the results presented below, relationships between combustion efficiency (CE) and other parameters were analyzed:

- **NHVcz** – Net heating value of the combustion zone gas (BTU/scf).
- **LFLcz** – Lower flammability limit of the combustion zone gas (volume fraction)
- **Ccz** – Combustibles fraction of the combustion zone gas (volume fraction)
- **S/VG –** Actual steam to vent gas ratio (lb steam/lb vent gas) or (scf steam/scf vent gas)

1.2 Results

Table 1.2-1 lists the key parameters of each test run. Figures 1.2-1 through 1.2-5 below show the results of all of the test runs.

A Tracerco study conducted at Whiting indicated that the reported flow rates of steam and vent gas may not be accurate. Adjustment factors were applied to these measurements. All data contained in the main body of this report uses the flow correction factors obtained from the Tracerco study. Appendix A.12 contains detailed information on the impact of the adjustment factors on key parameters.

Test --	NHVcz BTU/scf	LFLcz Vol. Fraction	Ccz Vol. Fraction	S/VG lb/lb	S/VG scf/scf	CE %
DDU-1 1	223	0.194	0.110	2.18	2.36	99.3
DDU-1 2	184	0.234	0.093	2.82	3.06	99.6
DDU-2 1	169	0.235	0.099	2.82	3.06	96.5
DDU-2 2	144	0.271	0.085	3.40	3.69	96.1
DDU-3 1	127	0.313	0.075	4.21	4.49	96.4
DDU-3 2	114	0.351	0.068	4.91	5.16	95.6
DDU-4 1	107	0.373	0.063	5.30	5.59	98.1
DDU-4 2	76	0.523	0.046	7.85	8.27	96.1
DDU-5 1	134	0.336	0.080	4.63	4.99	97.4
DDU-5 2	160	0.253	0.096	3.29	3.53	97.1
DDU-6 1	178	0.224	0.107	2.89	3.01	97.8
DDU-6 2	183	0.229	0.092	2.88	3.12	98.1
ALKY-1 1	327	0.143	0.146	0.42	0.68	99.7
ALKY-1 2	357	0.134	0.160	0.33	0.54	99.0
ALKY-2 1	236	0.201	0.106	0.81	1.32	97.5
ALKY-2 2	232	0.203	0.104	0.86	1.40	98.0
ALKY-3 1	213	0.224	0.095	0.99	1.60	93.7
ALKY-3 2	189	0.256	0.084	1.15	1.89	96.3
ALKY-4 1	207	0.242	0.093	0.89	1.48	95.4
ALKY-4 2	222	0.228	0.100	0.78	1.29	94.2
ALKY-5 1	216	0.237	0.096	0.85	1.41	96.6

Table 1.2-1: Key Parameters for Each Test Run

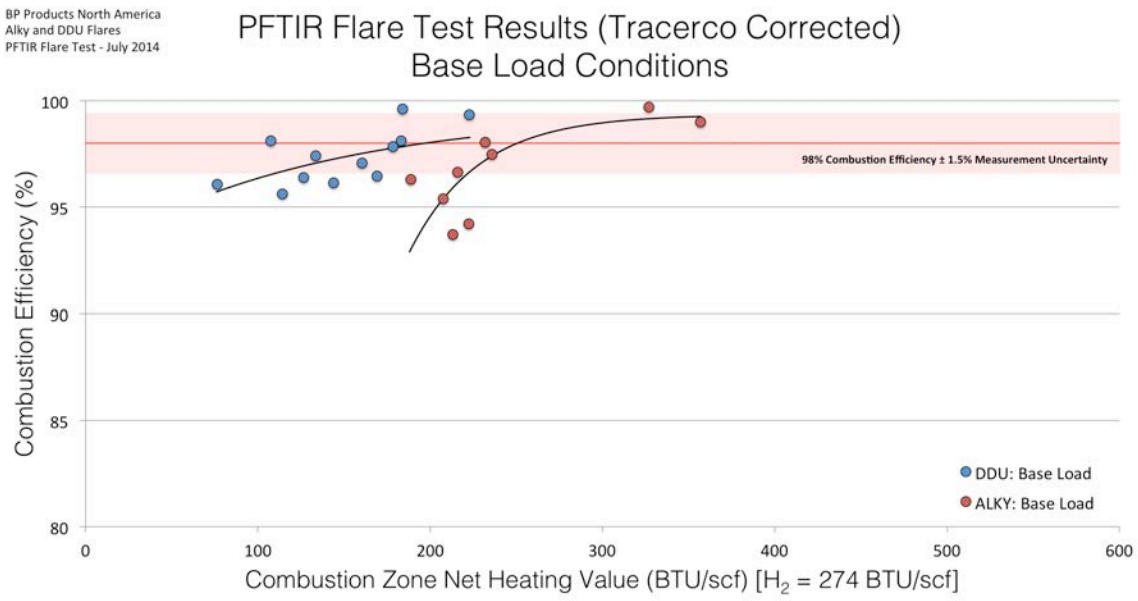

Figure 1.1-1: NHVcz vs. CE for All Test Runs

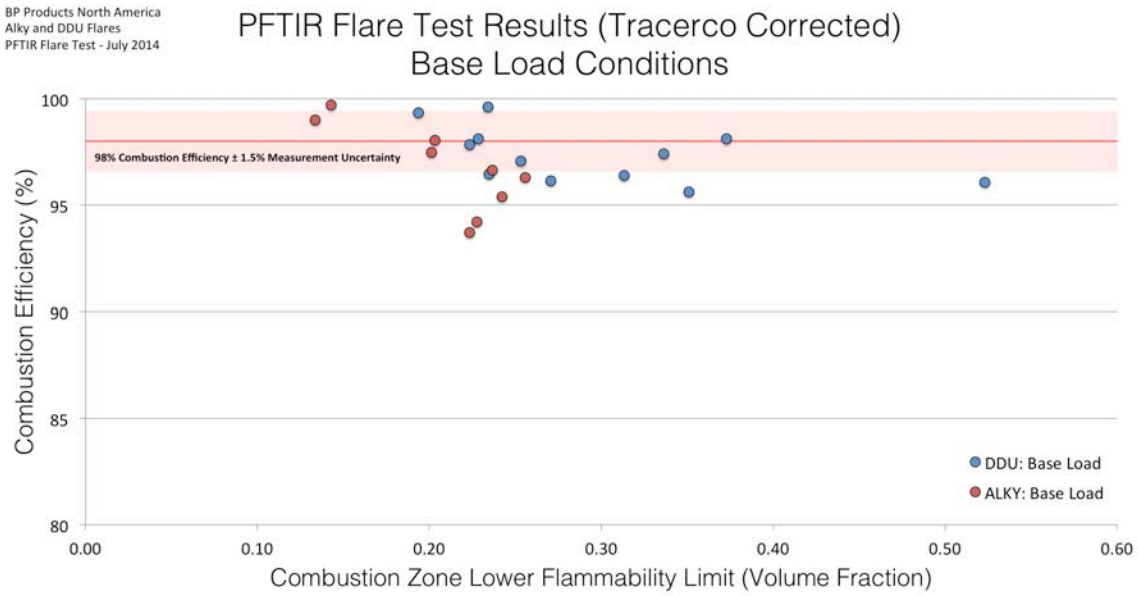

Figure 1.1-2: LFLcz vs. CE for All Test Runs

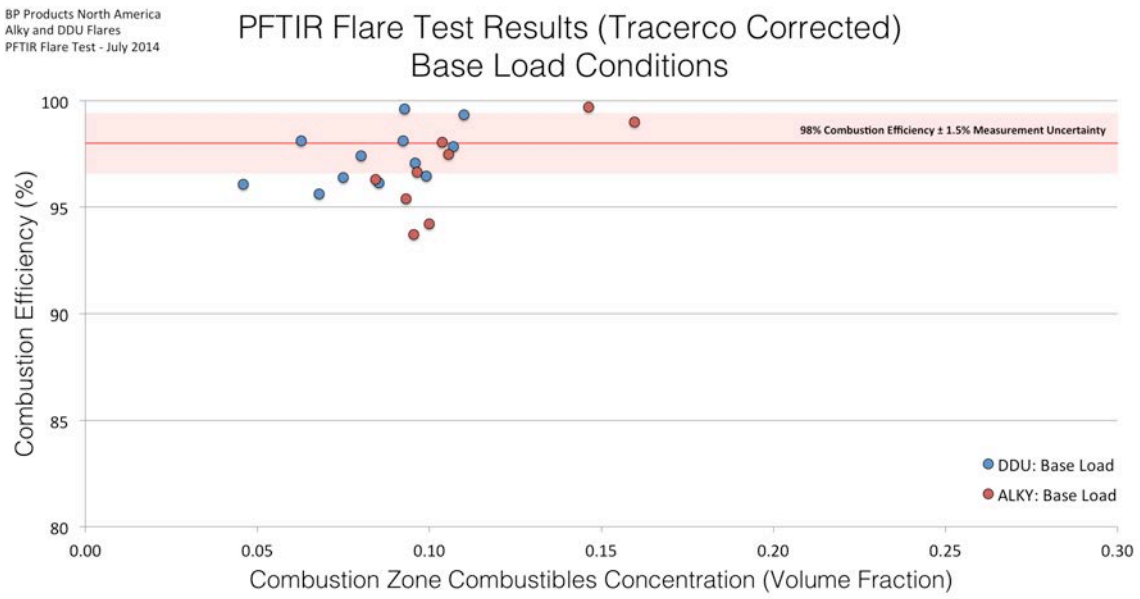

Figure 1.1-3: Ccz vs. CE for All Test Runs

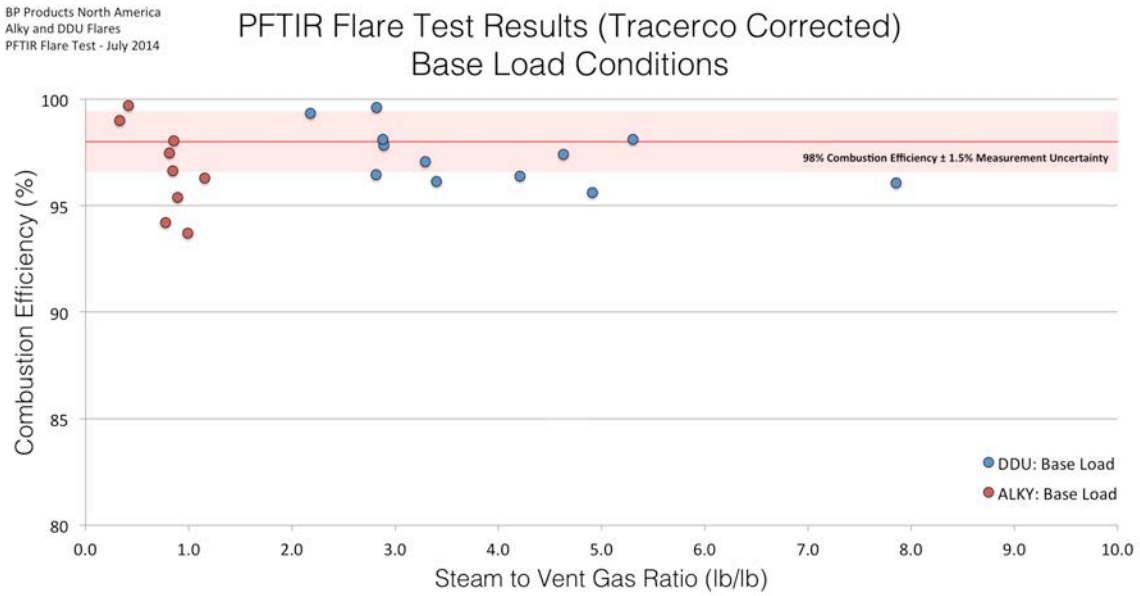

Figure 1.1-4: S/VG (Mass Basis) vs. CE for All Test Runs

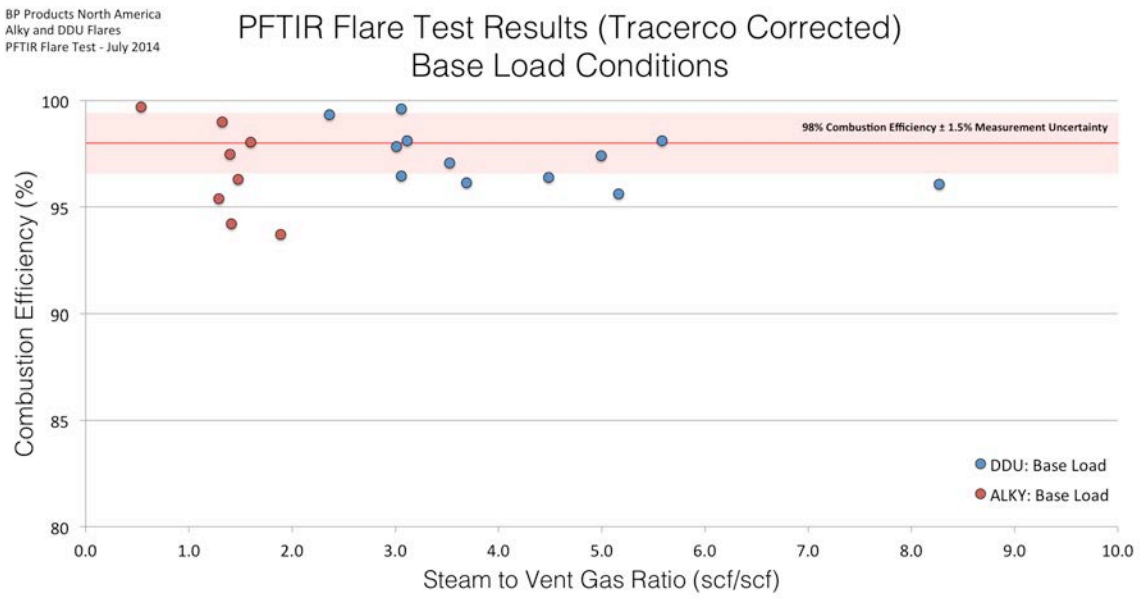

Figure 1.1-5: S/VG (Volume Basis) vs. CE for All Test Runs

Additional details for each of these tests are found in Sections 3.0 and 4.0 within the main body of this report.

1.2.1 Conclusions

The PFTIR test of the DDU and ALKY Flares provided data to support the following conclusions.

1.2.1.1 Relationship of Combustion Efficiency and NHVcz

The general relationships between combustion efficiency and other key parameters that were observed during the DDU and ALKY Test Series are consistent with previous PFTIR tests on steam-assisted flare tips.

When the DDU flare is operating under base load conditions, high combustion efficiency (98% ±1.5%) is maintained until NHVcz falls to less than 110 BTU/scf. When the ALKY flare is operating under base load conditions, high combustion efficiency is maintained until NHVcz falls to less than 220 BTU/scf. On past PFTIR base load tests on elevated steam-assisted refinery flare tips high combustion efficiency is generally maintained until NHVcz falls below 300 BTU/scf. Therefore, the combustion efficiency performance of the DDU and ALKY flares is above average for their class.

1.2.1.2 Operating Ranges for Covered Flares to Assure 98% combustion Efficiency

The above average combustion efficiency performance of flares is a function of several inter-related process variables, notably S/VG ratio and NHVvg, and the composition of the vent gas. S/VG is a controlled process variable at Whiting Refinery. The current control scheme limits S/VG ratios to 3:1. The scheme is in compliance with the consent decree requirements in Appendix D, ¶34.a.

The source test data presented in this report suggests that an "A" combustion efficiency multiplier of 2.84 would be required to maintain high combustion efficiency on the DDU Flare and an "A" combustion efficiency multiplier of 4.38 would be required to maintain high combustion efficiency on the ALKY Flare. There is a significant difference in the Combustion Efficiency Multipliers due to differences in vent gas compositions and the levels of NHVcz where combustion efficiency on the DDU and ALKY flares begins to decline. The multipliers were calculated with vent gas compositions specific to each flare and could vary greatly for flares with different vent gas compositions. Section A.1.6 discusses the details of how the "A" combustion multiplier is calculated.

NHVvg and LFLvg are generally inherent to the sources tied into a specific flare. Table 1.2.1-1 presents the long-term average composition along with the calculated values of NHVvg and LFLvg for each covered flare at Whiting. Figure 1.2.1-1 shows the NHVvg against the LFLvg computed from the average composition of each covered by the BP Flare Consent Decree. The plot shows that characteristics of the ALKY and VRU flares are very similar. It also shows that the characteristics of the FCU and DDU flares are very similar. Because of these relationships, it is possible that an "A" combustion efficiency multiplier of 2.84 can be used for the FCU flare and an "A" combustion efficiency multiplier of 4.38 can be used on the VRU flare. The plot shows the remaining covered flares, GOHT, 4UF, UIU and South with higher NHVvg and lower LFLvg.

Compound	Alky Flare	DDU Flare	South Flare	VRU Flare	FCU Flare	UIU Flare	4UF Flare	GOHT Flare
Nitrogen (mol %)	21.80	69.88	7.20	58.20	37.70	13.50	13.20	22.40
Oxygen (mol %)	0.03	0.05	0.00	0.20	1.00	0.00	0.10	0.00
Water (mol %)	1.06	0.34	0.60	0.40	1.80	0.00	0.50	0.10
Carbon dioxide (mol %)	0.86	0.10	0.80	0.90	0.50	0.80	0.10	0.40
Carbon monoxide (mol %)	0.23	0.00	0.00	0.10	0.00	0.10	0.00	0.00
Hydrogen sulfide (mol %)	0.00	0.00	0.40	0.00	0.00	0.00	0.10	0.00
Methane (mol %)	48.97	7.42	6.60	2.40	14.70	30.00	66.60	35.80
Ethane (mol %)	6.66	0.48	67.20	21.50	19.60	42.10	9.10	35.40
Hydrogen (mol %)	13.68	0.31	4.50	2.60	3.40	6.40	4.70	2.30
Ethylene (mol %)	1.85	0.13	0.80	2.60	1.90	2.00	0.20	0.30
Acetylene (mol %)	0.48	0.00	0.00	0.00	0.00	0.00	0.00	0.00
Propane (mol %)	1.36	3.03	1.50	0.50	2.80	2.20	2.80	0.50
Isobutane (mol %)	0.21	3.95	0.60	0.20	0.10	0.30	0.30	0.10
n-Butane (mol %)	0.35	2.57	2.00	0.10	0.00	1.00	0.70	0.10
Butenes (combined) (mol %)	0.06	0.05	0.20	0.10	0.10	0.20	0.00	0.00
Propylene (mol %)	0.80	6.20	0.80	0.80	1.60	1.20	0.50	0.30
n-Pentane+ (mol %)	0.50	1.05	6.10	1.00	0.70	0.50	2.40	0.20
Other Parameters								
NHVvg (BTU/scf)	705	536	1478	515	696	1093	932	922
LFLvg (Volume Fraction)	0.05	0.09	0.03	0.08	0.06	0.04	0.05	0.05

Table 1.2.1-1: Long Term Average Composition Data for Vent Gas of Covered Flares

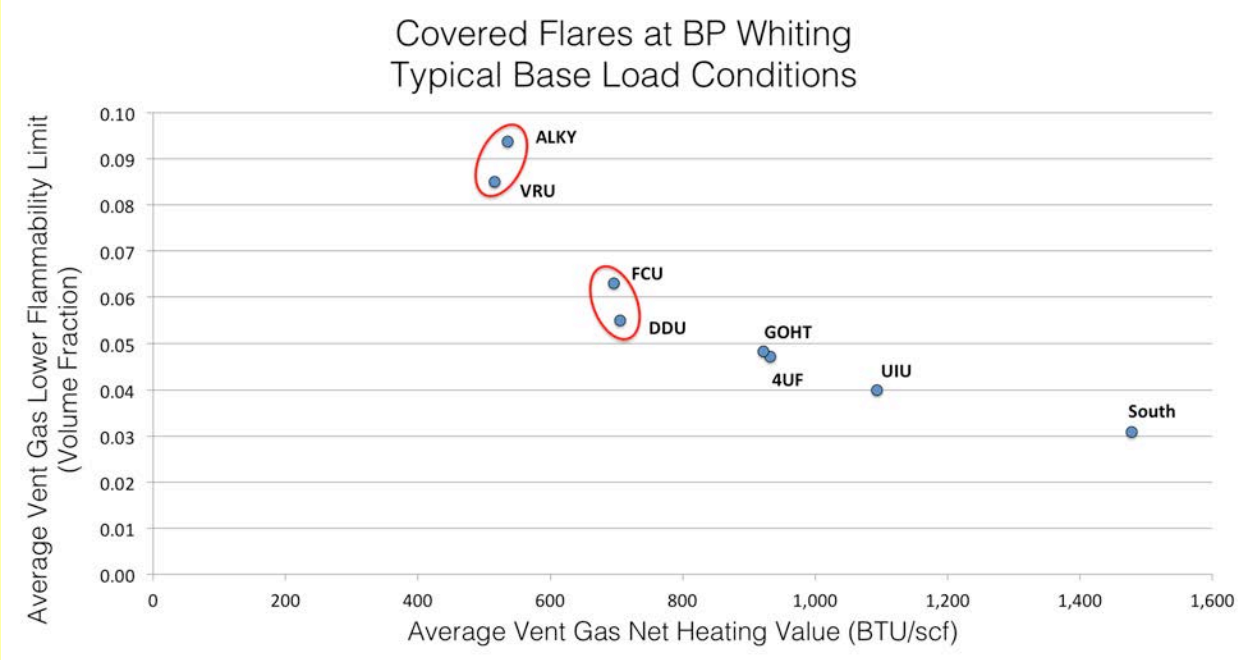

Figure 1.2.1-1: Average NHVvg vs. Average LFLvg for Covered Flares

2.0 Introduction

2.1 Objectives of Test Program

The overall objectives of the Whiting test program were as follows:

1. Determine the impact various steam rates have on the ALKY flare when operating at base load conditions. This will provide the proper operating envelope for the ALKY flare during typical operation.

2. Determine the impact various steam rates have on the DDU flare when operating at base load conditions. This will provide the proper operating envelope for the DDU flare during typical operation.

2.2 Testing Organization

The test was conducted with the assistance of Clean Air Engineering (CleanAir)

Clean Air Engineering
500 W Wood St.
Palatine, IL 60067

A cross-functional team was formed between CleanAir and BP in order to staff, advise, monitor, and record test results.

2.3 Flare System Components

2.3.1 Purpose

A flare is one of the most important safety devices in use at a refinery. Its purpose is to safely combust gases generated by emergency or upset conditions within a process unit. As a result, a flare must function over a large and variable range of operating scenarios. These vary from typical stand-by operation at minimum flow conditions to efficiently combusting gases generated from a full power outage or other process safety relief scenario.

Like previous Passive FTIR flare tests, the Whiting test addressed the normal (i.e., high turndown) operating range.

2.3.2 Tip Design and Control

2.3.2.1 DDU Flare

Table 2.3.2.1-1 lists DDU flare system design specifications.

Date of Original Flare Installation	July 1993
Date of Installation of Current Flare Tip	2005
Manufacturer	Callidus
Flare Tip Model Number	BTZ-US-60/24C
Nominal Tip Diameter (inches)	60.0
Effective Tip Diameter (inches)	56.4

Table 2.3.2.1-1: DDU Flare Description

DDU Flare Tip

The function of the flare tip is to mix the flare gas and assist gas at velocities, turbulence, and concentrations required to establish and maintain proper ignition and stable combustion for the maximum specified relief gas flow rates at the system-allowable pressure drop. Although the flare has a low baseline flow rate of flare gas during normal operations, the flare system is designed to handle potentially large emergency flaring events.

The current flare tip was installed shortly after the shipping date of June 6, 2005. The unobstructed cross-sectional area of the tip is approximately 2,500 square inches. The tip consists of a single burner equipped with multiple steam injection points. Steam assist can be supplied radially using the upper external steam ring, as well as in the center of the flare stack, just above the velocity seal.

DDU Steam Assist System

Assist gas is added to the flare tip to promote flame zone turbulence, improve air entrainment, and thus, improve combustion efficiency and the reduction of smoke formation.

The DDU flare is a steam-assisted flare, meaning steam is injected at the flare tip in two locations: ring and center. The total steam capacity for the injection points is 65,000 pounds per hour (lb/hr). The total flow of steam is monitored by an ultrasonic flow meter installed on the main steam header. Each injection point is monitored by a flow transmitter and controlled through a tiered arrangement of control valves and restriction orifices.

Ring steam is supplied through a 6-inch steam supply pipe from an 8-inch riser pipe from the main steam header. The ring steam ring has a diameter approximately equal to the diameter of the flare tip and is equipped with 30 star-shaped steam diffusers on the outside of the flare stack circumference. Ring steam is used to aspirate air into the perimeter of the flame bundle, in order to keep the vent gas inside the combustion zone and assist in smoke control. The minimum flow of ring steam is 400 lb/hr, which is controlled by a restriction orifice. The maximum flow of ring steam is 60,000 lb/hr (59,600 lb /hr through the control valve plus 400 lb/hr through the restriction orifice).

Steam addition adjustments to the tip are made based upon a programmed distributed control system (DCS) logic, which limits the steam-to-vent gas (S/VG) ratio to less than or equal to 3.0 for the tip steam.

DDU Ignition System

A pilot light is required to ensure that a flame remains constantly present. The ignition equipment functions to reliably light the Pilot. The DDU flare is equipped with a flame front generator (FFG) to ignite the pilots. Compressed air and fuel are introduced into a mixing chamber at grade through orifices. Piping connects the mixing chamber, which is equipped with a sparking device, with the pilot tip. The piping is filled with a combustible mixture, and then a flame front is generated that travels to the pilot through the piping when the gas stream is ignited by the sparking device. There are two (2) types of ignition sources for the FFG used at the Refinery:

1. Ignition Transformer – The primary source of ignition for the DDU Flare is the 120 V AC ignition transformer.

2. Piezo Igniter – The piezo igniter acts as a backup to the ignition transformer and ensures that an ignition source is available even it electrical power is not available.

DDU Sweep Gas

Sweep gas is injected into the flare header to reduce the likelihood of stratification of gases and localized corrosion in the header. Additionally, sweep gas provides a positive gauge pressure such that ambient oxygen does not have the opportunity to leak into the header.

There are 15 sweep gas injection points in the DDU flare header. Refinery fuel, nitrogen, and natural gas are used as sweep gas. The sweep gas is typically injected at the furthest point upstream of a long header run, in order to sweep the highest percentage of the header pipe.

DDU Supplemental Gas

Supplemental gas is introduced to the flare in order to comply with the net heating value (NHV) requirements of 40 CFR 60.18(b) and 40 CFR 63.11(b). Supplemental gas is used as a caloric boost to the vented gas to ensure adequate combustion. When combustible gases are used for sweep gas, they simultaneously function as supplemental gas.

2.3.2.2 ALKY Flare

Table 2.3.2.2-1 lists ALKY flare system design specifications.

Date of Original Flare Installation	1961
Date of Installation of Current Flare Tip	2006
Manufacturer	NAO
Flare Tip Model Number	30-NFF-RC-HS
Nominal Tip Diameter (inches)	30.0
Effective Tip Diameter (inches)	25.2

Table 2.3.2.2-1: ALKY Flare Description

ALKY Flare Tip

The function of the flare tip is to mix the flare gas and assist gas at velocities, turbulence, and concentrations required to establish and maintain proper ignition and stable combustion for the maximum specified relief gas flow rates at the system-allowable pressure drop. Although the flare has a low baseline flow rate of flare gas during normal operations, the flare system is designed to handle potentially large emergency flaring events. The design of the flare tip is an integral part of the flare system because it enables the refinery to handle large variances in the volume, pressure drop, concentration, and temperature of the flare gas streams.

The current flare tip was installed shortly after the shipping date of September 13, 2006. The unobstructed cross-sectional area of the Tip is approximately 500 square inches. The tip consists of a single burner equipped with multiple steam injection points. Steam assist can be supplied radially using the upper external steam ring, as well as in the center of the flare stack, just above the velocity seal.

ALKY Assist System

Assist gas is added to the flare tip to promote flame zone turbulence, improve air entrainment, and thus, improve combustion efficiency and the reduction of smoke formation. Care must be taken to ensure the combustible mixture of the combined gases is not diluted by excess use of assist gas.

The ALKY flare is a steam-assisted flare, meaning steam is injected at the flare tip in two locations: ring and center. The total steam capacity for the injection points is 22,500 pounds per hour (lb/hr). The total flow of steam is monitored by an ultrasonic flow meter installed on the main steam header. Each injection point is monitored by a flow transmitter and controlled through a tiered arrangement of control valves and restriction orifices.

Ring steam is supplied through a 3-inch steam supply pipe from a 6-inch riser pipe from the main steam header. The ring steam ring has a diameter approximately equal to the diameter of the flare tip and is equipped with 18 star-shaped steam diffusers on the outside of the flare stack circumference. Ring steam is used to aspirate air into the perimeter of the flame bundle, in order to keep the vent gas inside the combustion zone and assist in smoke control. The minimum flow of ring steam is 400 lb/hr, which is controlled by a restriction orifice.
The center steam injection includes a single internal steam injection nozzle using a 3-inch supply pipe centered inside the stack just above the velocity seal from the main steam header.

Center steam prevents burn back at low gas flows and aids in flame stability. When in use, Center steam is supplied at 3,750 lb/hr.

ALKY Ignition System

A Pilot Light is required to ensure that a flame remains constantly present. Therefore, Pilot ignition is a critical concern because without a flame, there will be no Flare Gas combustion. The ignition equipment functions to reliably light the Pilot. The ALKY flare is equipped with a flame front generator (FFG) to ignite the Pilots. Compressed air and fuel are introduced into a mixing chamber at grade through orifices. Piping connects the mixing chamber, which is equipped with a sparking device, with the pilot tip. The piping is filled with a combustible mixture, and then a flame front is generated that travels to the Pilot through the piping when the gas stream is ignited by the sparking device. There are two (2) types of ignition sources for the FFG used at the Refinery:

1. Ignition Transformer – The primary source of ignition for the DDU Flare is the 120 V AC ignition transformer.

2. Piezo Igniter – The piezo igniter acts as a backup to the ignition transformer and ensures that an ignition source is available even it electrical power is not available.

ALKY Pilot Gas

Pilot gas is introduced through the flare pilot tips in order to provide a flame to reliably ignite the vent gases. The ALKY flare has three (3) pilot lights, each of which is paired with three (3) dual element thermocouples. The pilot lights are spaced at 120 degree intervals around the flare tip. The pilot lights are fueled by purchased natural gas.

ALKY Purge Gas

The ALKY flare systems is designed to prevent flashback, in-line detonation, and potential explosion in the flare stack by preventing oxygen from entering the flare tip and traveling down the flare stack. A continuous purge is therefore necessary to prevent atmospheric oxygen from entering down through the Flare burners. The purge is an injected gas designed to provide a minimum continuous momentum flux upward through the flare tip, ensuring no reversal of flow and such that no intrusion of air that could create an ignitable mixture.

Because the ALKY flare system is equipped with a water seal, the system maintains both purge gas and sweep gas. Purge gas is injected downstream of the water seal to condition the velocity seal and to prevent air intrusion into the flare stack. Natural Gas is used as Purge Gas in the ALKY flare system.

ALKY Sweep Gas

Sweep gas is injected upstream of the water seal into the flare header to reduce the likelihood of stratification of gases and localized corrosion in the header. Additionally, sweep gas provides a positive gauge pressure such that ambient oxygen does not have the opportunity to leak into the header.

There are ten (10) sweep gas injection points in the ALKY flare header. Nitrogen gas is used as sweep gas at different points. The sweep gas is typically injected at the furthest point upstream of a long header run, in order to sweep the highest percentage of the header pipe.

ALKY Supplemental Gas

Supplemental gas is introduced to the flare in order to comply with the net heating value (NHV) requirements of 40 CFR 60.18(b) and 40 CFR 63.11(b). Supplemental gas is used as a caloric boost to the vented gas to ensure adequate combustion. When combustible gases are used for sweep gas or purge gas, they simultaneously function as supplemental gas. Supplemental gas, which consists of natural gas, is connected to the flare header downstream of the water seal.

2.3.3 Instrumentation

Process data was provided by plant operations and includes process data, vent gas composition data, and meteorological data. Table 2.3.3-1 lists the parameters and time interval that were recorded and delivered by plant operations. The gas chromatograph (GC) used for measuring flare gas composition reported the compounds listed in Table 2.

Parameter	Unit	Frequency	Instrumentation
Flare Gas Volumetric Flow Rate	scf/hr	1 minute	OSI OFS-2000FW Optical Scintillation
Flare Gas Mass Flow Rate	lb/hr	1 minute	GE DigitalFlow GF868 Ultrasonic
Flare Gas Molecular Weight	lb/lbmol	1 minute	Calculation (~8 minute cycle time)
Flare Gas Composition	vol %	15 minutes	Siemens Maxum II Gas Chromatograph with TCD (~8 minute cycle time)
Estimated Pilot Gas Mass Flow Rate	lb/hr	N/A	Estimation
Steam Mass Flow Rate	lb/hr	1 minute	Sick Flowsic-100 Ultrasonic
Steam Temperature at Flow Measurement Point	°F	1 minute	Type K thermocouple
Flare Gas Combustion Zone Net Heating Value	BTU/scf	1 minute	Calculation (~8 minute cycle time)
Vent Gas Net Heating Value	BTU/scf	15 min	Calculation (~8 minute cycle time)
Actual Total Steam to Vent Gas Ratio	--	1 min	Calculation
Hydrocarbon Mass Flow Rate	lb/hr	1 min	Orifice Meter
Flare Exit Velocity	fps	1 min	Calculation
Wind Direction	° (N = 0)	1 min	Wind Vane
Wind Speed	mph	1 min	Anemometer
Ambient Barometric Pressure	psia	1 min	Silicon Capacitance transducer
Ambient Temperature	°F	1 min	CMOS sensor
Ambient Humidity	%	1 min	CMOS sensor
Momentum Flux Ratio	--	1 min	Calculation

Table 2.3.3-1: Operating Parameters Measured During Testing

Compound	Molecular Weight (lb/lb-mol)	Range	Units
Hydrogen	2.02	0 - 100	mole %
Nitrogen	28.02	0 - 100	mole %
Oxygen	32.00	0 - 100	mole %
Carbon Dioxide	44.01	0 - 100	mole %
Carbon Monoxide	28.01	0 - 100	mole %
Methane	16.04	0 - 100	mole %
Ethane	30.07	0 - 100	mole %
Ethylene	28.06	0 - 100	mole %
Acetylene	26.04	0 - 100	mole %
Propane	44.10	0 - 100	mole %
Propylene	42.08	0 - 100	mole %
Iso-Butane	58.12	0 - 100	mole %
Normal Butane	58.12	0 - 100	mole %
iso-Butene, Butene-1, cis-butene-2, transbutene-2 and 1,3 Butadiene combined	56.11	0 - 100	mole %
Pentane-Plus (C5+)	72.15	0 - 100	mole %
Water	18.02	0 - 100	mole %

Table 2.3.3-2: Compounds reported by the GC for Flare Gas Composition

2.4 Video Cameras

During the test program, a total of six video cameras recorded flare activity from the two PFTIR locations. Four infrared cameras and two visible light cameras were used. This appendix describes the video cameras used. Appendix A.11 contains the video taken by these cameras.

2.4.1 NEC/Mikron TH5104

This infrared camera was used as an aiming camera for PFTIR 2. It was mounted on the PFTIR telescope. The PFTIR operator used the image from this camera to aim the instrument. An examination of this video stream gives an indication of PFTIR aiming accuracy. Figure 2.4.1-1 shows an example image from this camera. The crosshair (added for this report) shows the area analyzed by PFTIR 2 (see Appendix A.4.2 for location descriptions).

Figure 2.4.1-1: Image from NEC/Mikron TH5104

2.4.2 NightSight Palm IR 250

This infrared camera was used as an aiming camera for PFTIR 1. It was mounted on the PFTIR telescope. The PFTIR operator used the image from this camera to aim the instrument. An examination of this video stream gives an indication of PFTIR aiming accuracy. Figure 2.4.2-1 shows an example image from this camera. The crosshair (added for this report) shows the area analyzed by PFTIR 1 (see Appendix A.4.2 for location descriptions).

Figure 2.4.2-1: Image from NightSight Palm IR 250

2.3.3 FLIR A320

This infrared camera was used as a stationary thermal camera at both PFTIR locations. It captured a general thermal view of the flare during the test program. It has a broad spectral range from 7.5 to 13 microns (1333 to 769 wavenumbers). The temperature scale on the camera was not calibrated for transparent gases, so any temperatures shown were considered relative indicators only. Figure 2.4.3-1 shows an example image from the FLIR A320 camera.

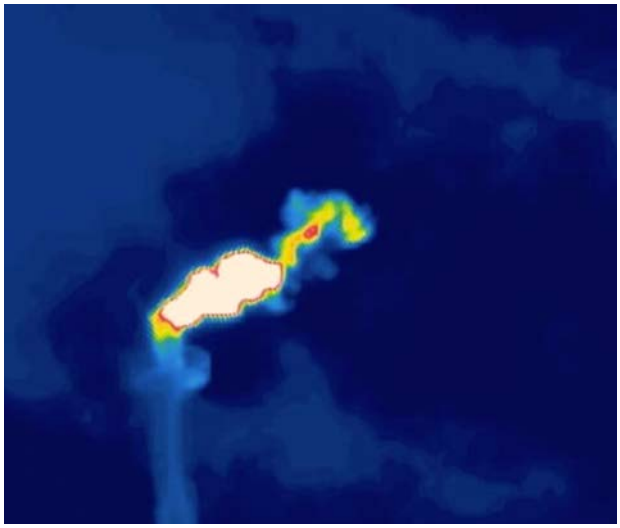

Figure 2.4.3-1: Image from FLIR A320 – Stationary

2.4.4 Axis Q1755

This visible light camera was used as a stationary visual camera at both PFTIR locations. The HD cameras provided a detailed visible light image of the flare operation. The purpose of the Axis Q1755 cameras was to provide a visual image corresponding to the PFTIR locations during testing. Figure 2.4.4-1 shows an example image from the Axis Q1755 camera.

Figure 2.4.4-1: Image from Axis Q1755

2.5 PFTIR

PFTIR instruments from CleanAir were used to measure combustion efficiency of the flare. The PFTIR instruments were equipped with dual sensors - mercury-cadmium-telluride (HgCdTe) and indium-antimonide (InSb). If two PFTIR instruments were used to conduct measurements during a test run, then each instrument will be located 90° around the base of the flare to the other. The perpendicular placement of the two instruments will allow one instrument to have an adequate plume cross-section for any wind direction.

PFTIR data was logged into the data acquisition system supplied by the PFTIR contractor. PFTIR measurements were provided for analysis on a minute-by-minute timeline. The reported values constitute an average of several analytical cycles over each test run. The software used by the PFTIR contractor is proprietary but will perform analyses and report data in accordance with the specifications found in Appendix A.2. Table 2.5-1 lists the compounds that were measured.

Compound	Unit
Carbon Dioxide (CO2) at 765 wavenumber	ppm x m
Carbon Dioxide (CO2) at 2000 wavenumber	ppm x m
Carbon Monoxide (CO)	ppm x m
Methane (CH4)	ppm x m
Ethylene (C2H4)	ppm x m
Propane (C3H8)	ppm x m
Propylene (C3H6)	ppm x m
1, 3 – Butadiene	ppm x m
n-Butane	ppm x m
C5+	ppm x m
Total Hydrocarbon (THC)[1]	ppm x m

1. Calculated during data reduction

Table 2.5-1: Compounds Reported by the PFTIR

2.6 Flare Test Program

2.6.1 Test Series Descriptions

Combustion efficiency was measured under base load vent gas conditions and various steam rates. Each of these combinations is referred to as a "test condition" in this report. The following test conditions were used during this project.

ALKY Base Load Flow and Composition. Variable Steam Rate.

Objective: To determine the performance curve of the ALKY flare under base load conditions. Fuel flow was set to base load flow rate and base load composition. The initial test condition targeted the incipient smoke point. Subsequent test conditions increased the steam rate to achieve successively lower NHVcz values until a combustion efficiency of <93% was measured. The steam rate that achieved <93% CE was the final test condition of this series. Two replicates were performed for each test condition.

DDU Base Load Flow and Composition. Variable Steam Rate.

Objective: To determine the performance curve of the DDU flare under base load conditions. Fuel flow was set to base load flow rate and base load composition. The initial test condition targeted the incipient smoke point. Subsequent test conditions increased the steam rate to achieve successively lower NHVcz values until the capacity of the steam-assist system was reached. Two replicates were performed for each test condition.

2.6.2 PFTIR Locations

Two PFTIR instruments were used for this test program. These locations were chosen based on their unobstructed views of the flare tip, easy access to electricity, and the ability to lay data cables in a safe manner. The locations of the PFTIR instruments were set up at a roughly 90 degree angle.

Figures 2.6.2-1 and 2.6.2-2 show maps of the PFTIR locations in relation to the ALKY and DDU flare tips. Section 4.0 contains more detailed information about each PFTIR location.

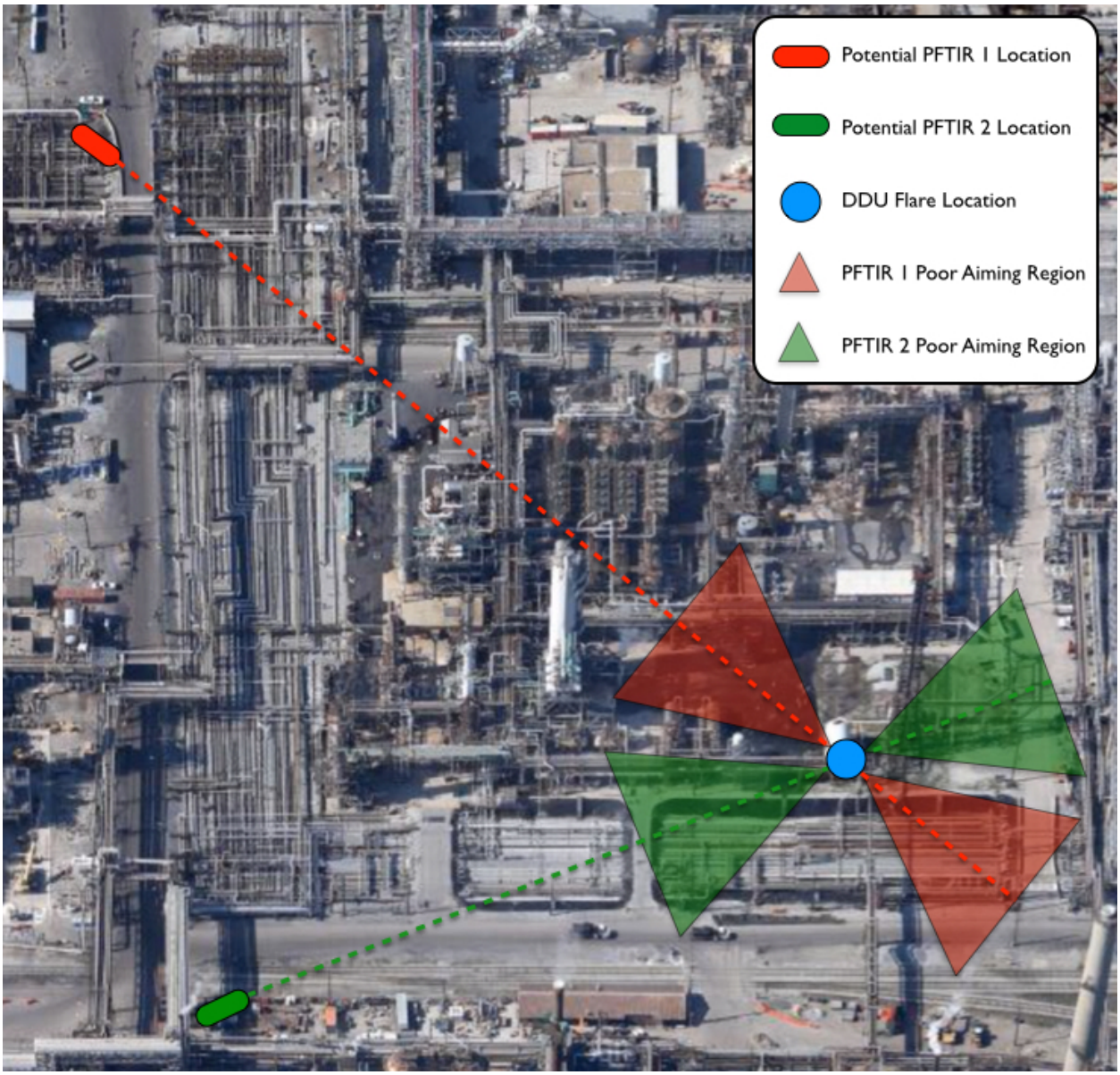

Figure 2.6.2-1: Map of the PFTIR Locations in Relation to the ALKY Flare Tip

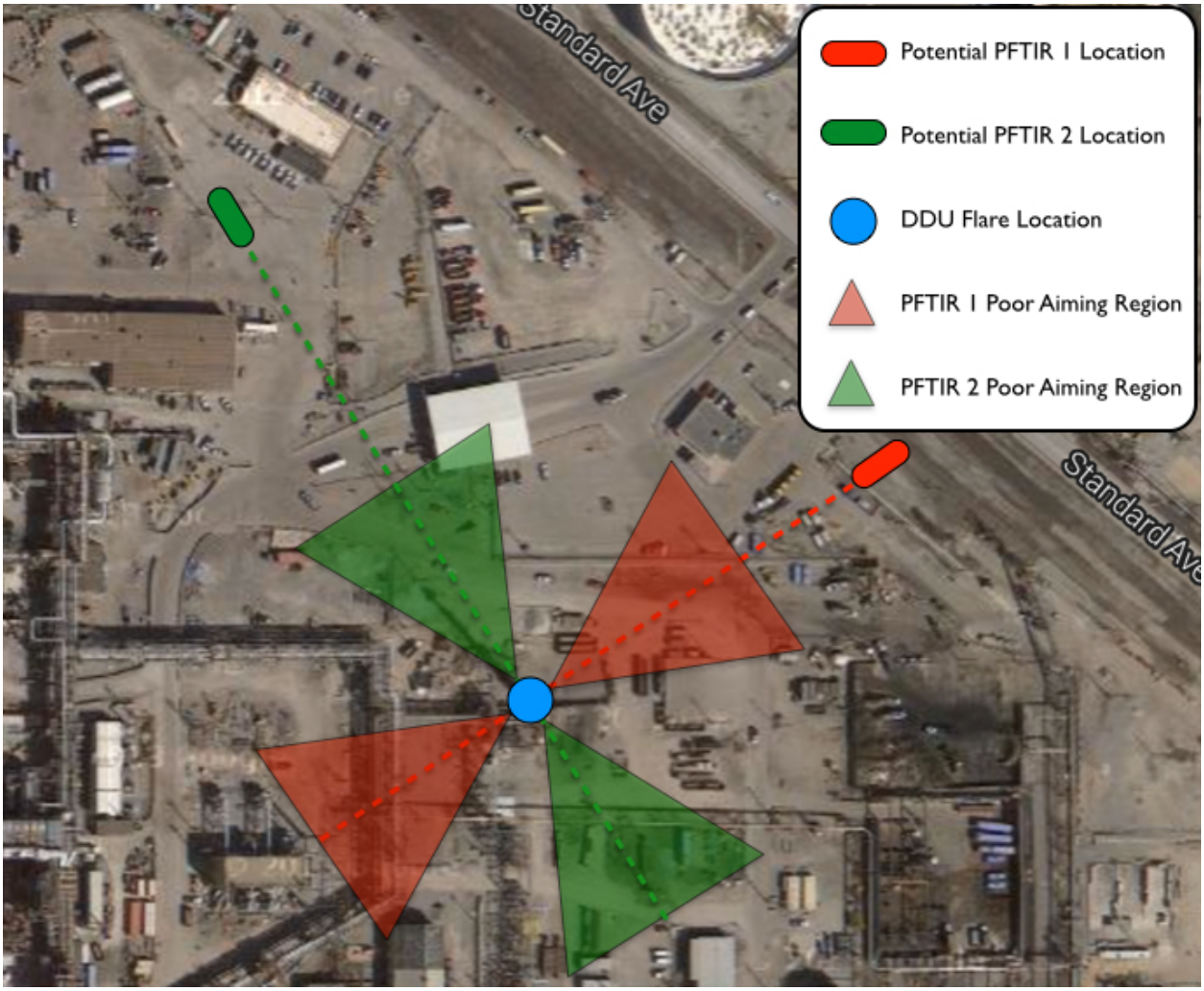

Figure 2.6.2-2: Map of the PFTIR Locations in Relation to the DDU Flare Tip

2.6.3 Run Lengths and Replicates

Table 2.6.3-1 below shows the run length for each test run.

Test Condition	Replicate 1 Length	Replicated 2 Length
DDU-1	20 minutes	20 minutes
DDU-2	27 minutes	20 minutes
DDU-3	21 minutes	21 minutes
DDU-4	22 minutes	23 minutes
DDU-5	20 minutes	21 minutes
DDU-6	11 minutes[1]	10 minutes[1]
ALKY-1	25 minutes	26 minutes
ALKY-2	21 minutes	22 minutes
ALKY-3	21 minutes	22 minutes
ALKY-4	23 minutes	21 minutes
ALKY-5[2]	22 minutes	N/A

1. Run lengths were less than 20 minutes because these runs were not included in the test protocol and were conducted only as check on previous results
2. Only one replicate was conducted because this run was not included in the test protocol and was conducted only as a check on previous results.

3.0 Summary of Results

3.1 Summary and Key Data Trends by Varied Parameter

Both the DDU and ALKY Test Series were conducted with the flare operating at base load conditions. The steam assist rates were varied to achieve different combustion efficiencies. The objectives of the test were to define operating envelopes for the DDU and ALKY flares based on data collected. Combustion efficiency showed significant decline on the DDU flare around an NHVcz level of 110 BTU/scf, an LFLcz level of 0.25, a Ccz level of 0.08, and S/VG levels of 5 lb/lb and 5 scf/scf. Combustion efficiency showed significant decline on the ALKY flare around an NHVcz level of 220 BTU/scf, an LFLcz level of 0.21, a Ccz level of 0.10, and S/VG levels of 1 lb/lb and 1.3 scf/scf. Overall, the general trends are consistent with previous PFTIR tests on steam-assisted flare tips.

Figure 3.0-1 shows the relationship between NHVcz and CE for the ALKY and DDU tests. Figure 3.0-2 shows the relationship between NHVcz and CE for all base load test series. Figure 3.0-3 shows the relationship between LFLcz and CE for the ALKY and DDU tests. Figure 3.0-4 shows the relationship between LFLcz and CE for all base load test series. Figure 3.0-5 shows the relationship between Ccz and CE for the ALKY and DDU tests. Figure 3.0-6 shows the relationship between Ccz and CE for all base load test series. Figure 3.0-7 shows the relationship between S/VG (mass basis) and CE for the ALKY and DDU tests. Figure 3.0-8 shows the relationship between S/VG (mass basis) and CE for all base load test series. Figure 3.0-9 shows the relationship between S/VG (volume basis) and CE for the ALKY and DDU tests. Figure 3.0-10 shows the relationship between S/VG (volume basis) and CE for all base load test series.

Paragraph 39d of the BP Flare Consent Decree requires BP to propose a Combustion Efficiency Multiplier for calculating the $NHV_{cz\text{-}limit}$ for the DDU and ALKY Flares. Using the average gas composition data from the tests, an average net heating value of the vent gas at its lower flammability limit ($NHV_{vg\text{-}lfl}$) was determined. $NHV_{vg\text{-}lfl}$ can be used to determine appropriate Combustion Efficiency Multipliers for the flares when operating with base load compositions. Table 3.1-1 contains average vent gas concentrations and other calculated parameters for the DDU and ALKY flares. The test data suggests that a Combustion Efficiency Multiplier of 2.84 would be required to maintain high combustion efficiency on the DDU Flare and a Combustion Efficiency Multiplier of 4.38 would be required to maintain high combustion efficiency on the ALKY Flare. There is a significant difference in the Combustion Efficiency Multipliers due to differences in vent gas compositions and the levels of NHVcz where combustion efficiency on the DDU and ALKY flares begins to decline. It may not be appropriate to use these multipliers on other flares. The multipliers were calculated with vent gas compositions specific to each flare and could vary greatly for flares with different vent gas compositions. The calculation for the "A" combustion multipliers is outlined in Appendix A.1.6.

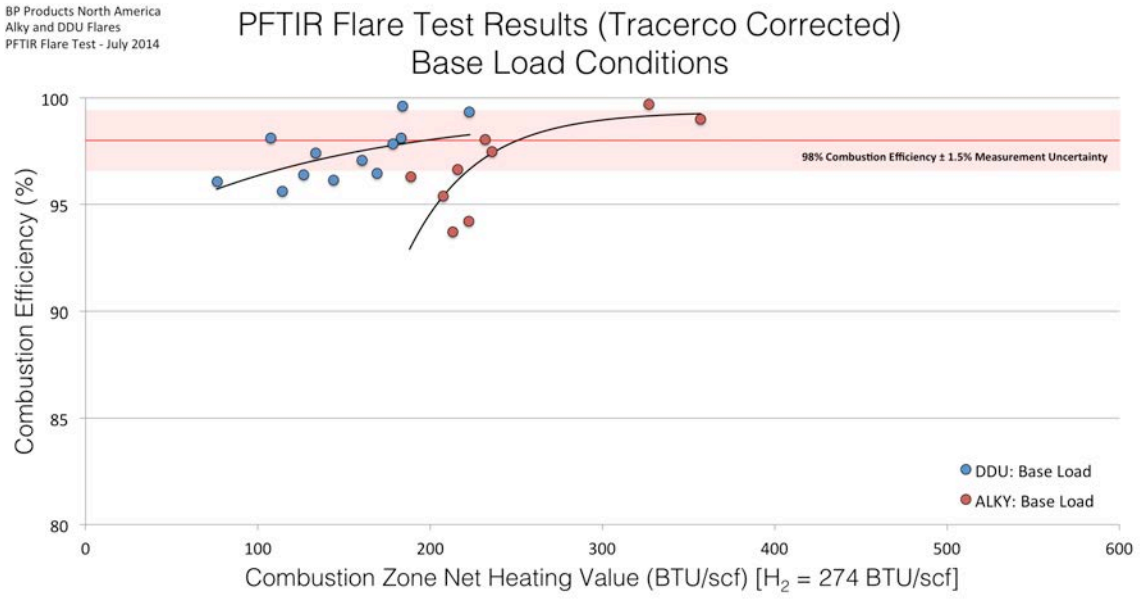

Figure 1.1-1: NHVcz vs. CE for All BP Test Runs

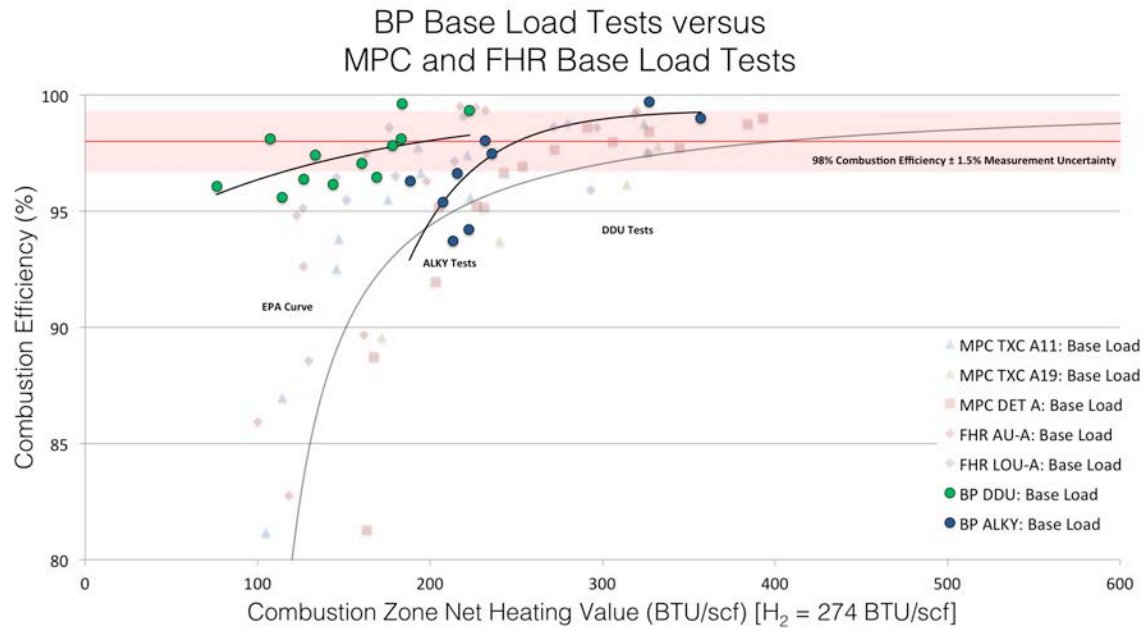

Figure 3.1-2: NHVcz vs. CE for All Base Load Test Series

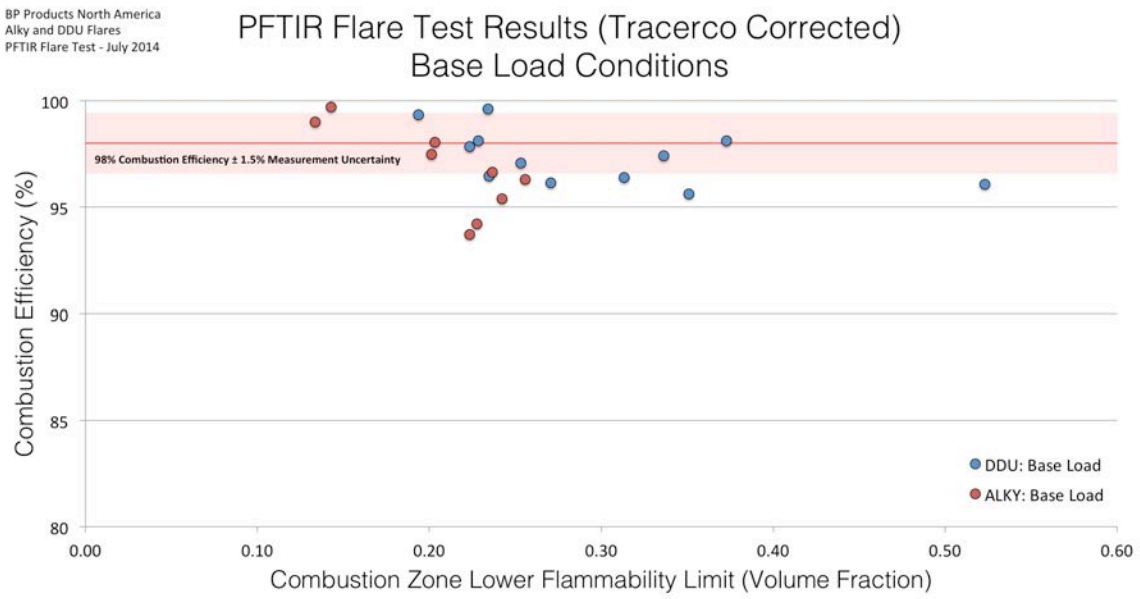

Figure 3.1-3: LFLcz vs. CE for All BP Test Runs

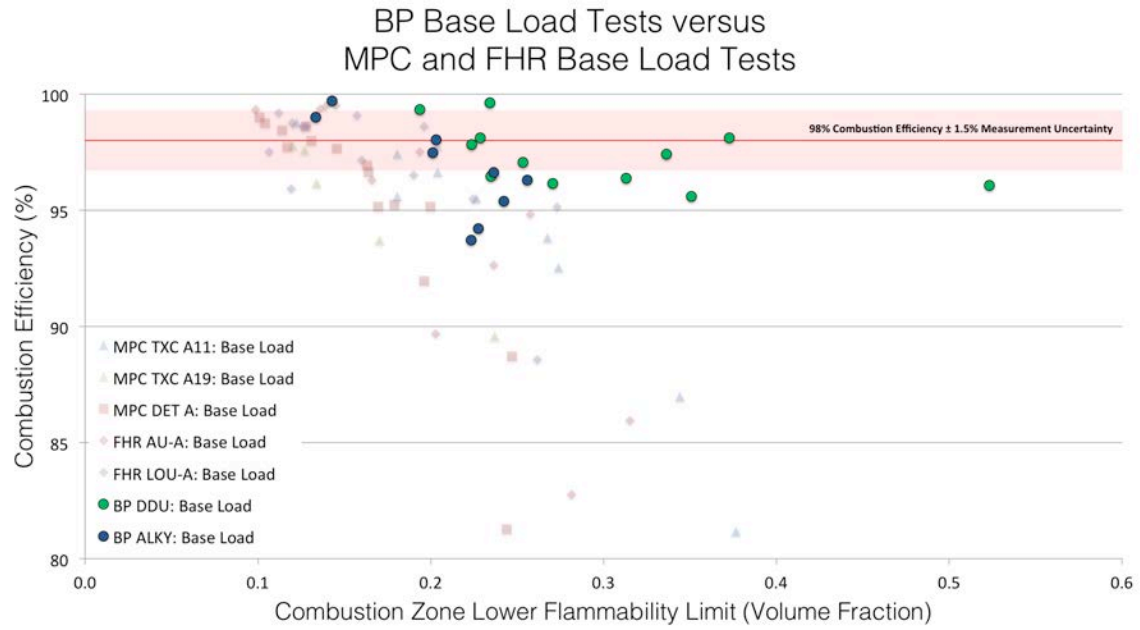

Figure 3.1-4: LFLcz vs. CE for All Base Load Test Series

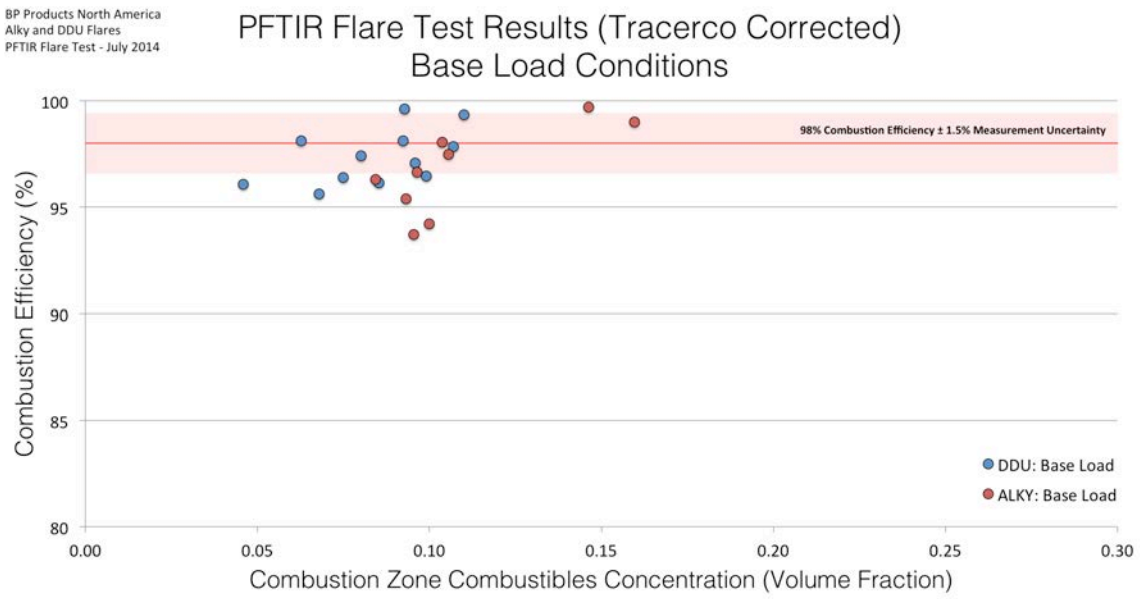

Figure 3.1-5: Ccz vs. CE for All BP Test Runs

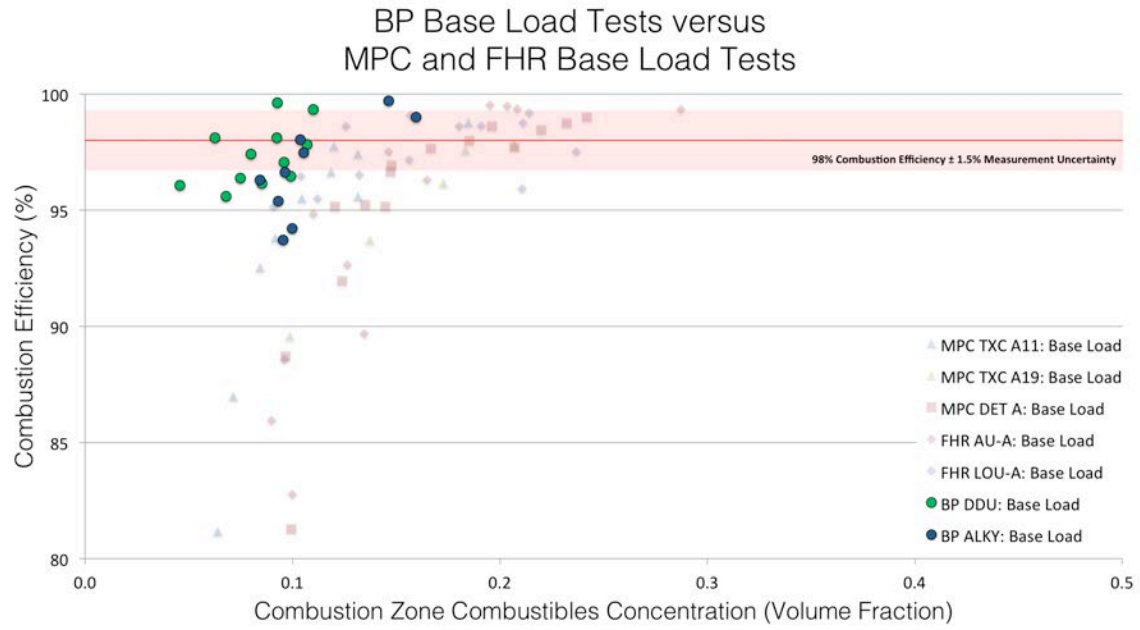

Figure 3.1-6: Ccz vs. CE for All Base Load Test Series

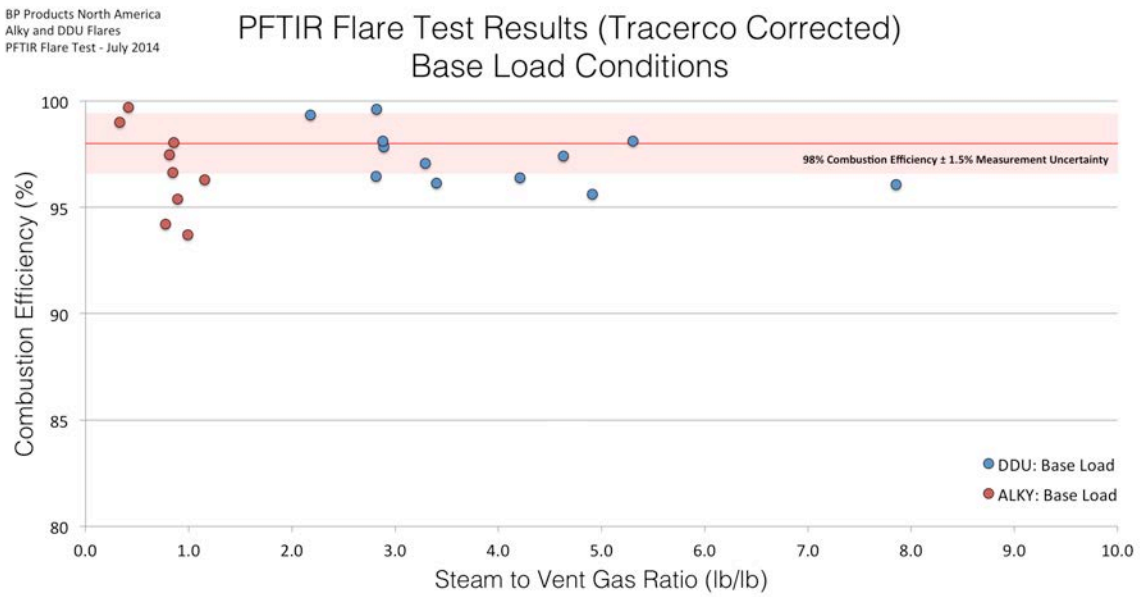

Figure 3.1-7: S/VG (Mass Basis) vs. CE for All BP Test Runs

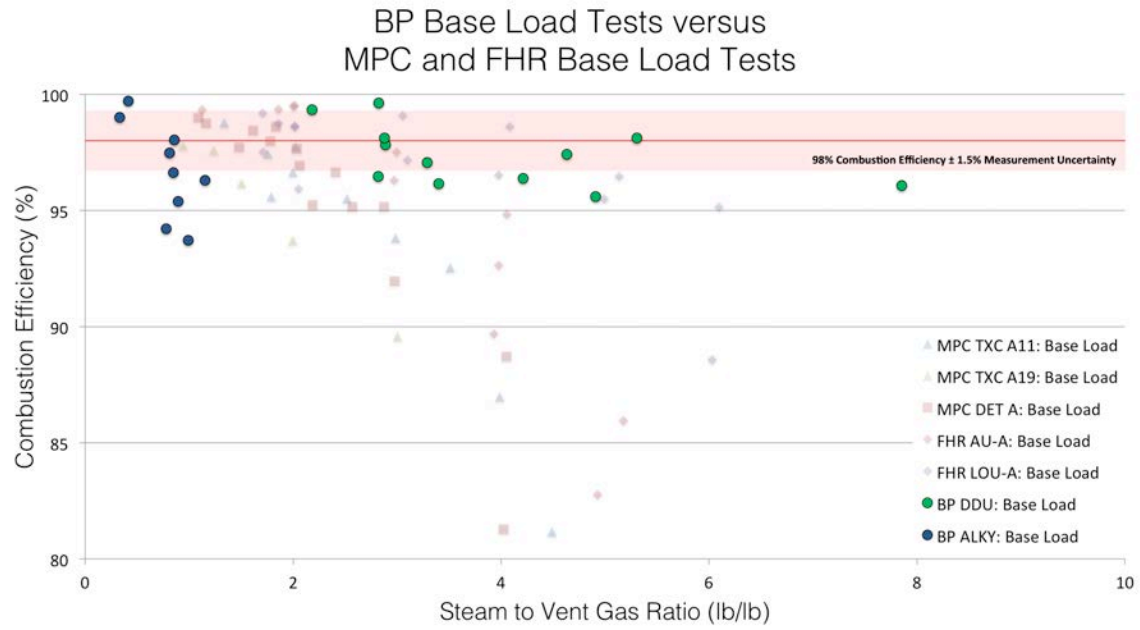

Figure 3.1-8: S/VG (Mass Basis) vs. CE for All Base Load Test Series

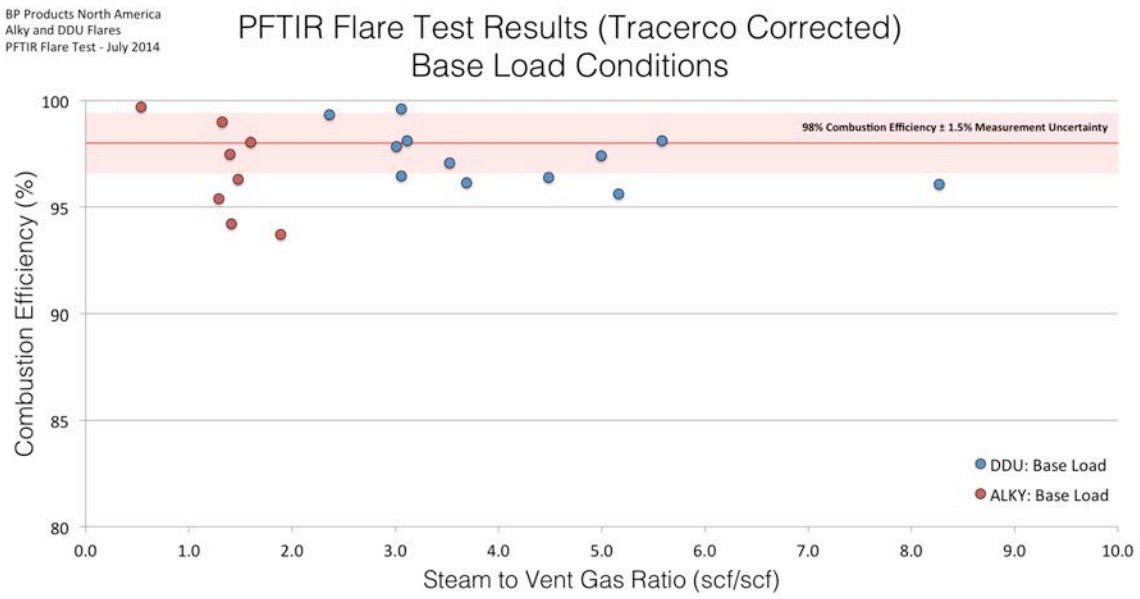

Figure 3.1-9: S/VG (Volume Basis) vs. CE for All BP Test Runs

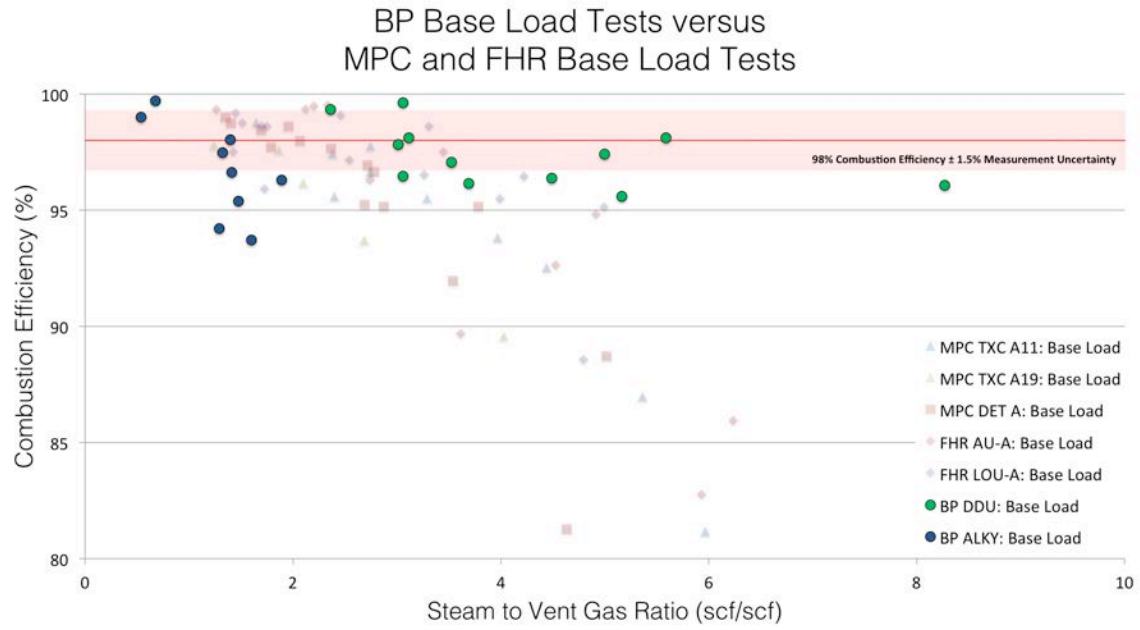

Figure 3.1-10: S/VG (Volume Basis) vs. CE for All Base Load Test Series

Compound	DDU Base Load Composition	ALKY Base Load Composition
Nitrogen (mol %)	21.80	69.88
Oxygen (mol %)	0.03	0.05
Water (mol %)	1.06	0.34
Carbon dioxide (mol %)	0.86	0.10
Carbon monoxide (mol %)	0.23	0.00
Hydrogen sulfide (mol %)	0.00	0.00
Methane (mol %)	48.97	7.42
Ethane (mol %)	6.66	0.48
Hydrogen (mol %)	13.68	0.31
Ethylene (mol %)	1.85	0.13
Acetylene (mol %)	0.48	0.00
Propane (mol %)	1.36	3.03
Isobutane (mol %)	0.21	3.95
n-Butane (mol %)	0.35	2.57
Butenes (combined) (mol %)	0.06	0.05
Propylene (mol %)	0.80	6.20
n-Pentane+ (mol %)	0.50	1.05
Other Parameters		
Vent Gas Volume %	98.91	95.57
NHVvg (BTU/scf)	705.30	535.58
LFLvg (Volume Fraction)	0.055	0.094
NHVvg-lfl (BTU/scf)	38.72	50.20
Proposed NHVcz-limit (BTU/scf)	110	220
Appropriate Combustion Efficiency Multiplier	2.84	4.38

Table 3.1-1: Average VG Compositions, Calculated Parameters, and Appropriate Combustion Efficiency Multipliers for the DDU and ALKY Flares based on Base Load Fuel Composition

3.2 Summary and Key Data Trends of Whole Data Set

3.2.1 Composite of All Hydrocarbons Tested

Figures 3.2-1 through 3.2-5 show the results of the Whiting tests with the results of previous PFTIR tests on steam-assisted flare tips conducted by Marathon Petroleum Company (MPC), Flint Hills Resources (FHR) and the Texas Commission on Environmental Quality (TCEQ). The data from the Whiting tests follow the same general trends as data from the previous tests. However, combustion efficiency on the DDU Flare appears to drop off at 110 BTU/scf. This is a lesser value than the other base load tests. Generally, combustion efficiency dropped off at around 300 BTU/scf during past PFTIR tests on steam-assisted flare tips operating under base load conditions.

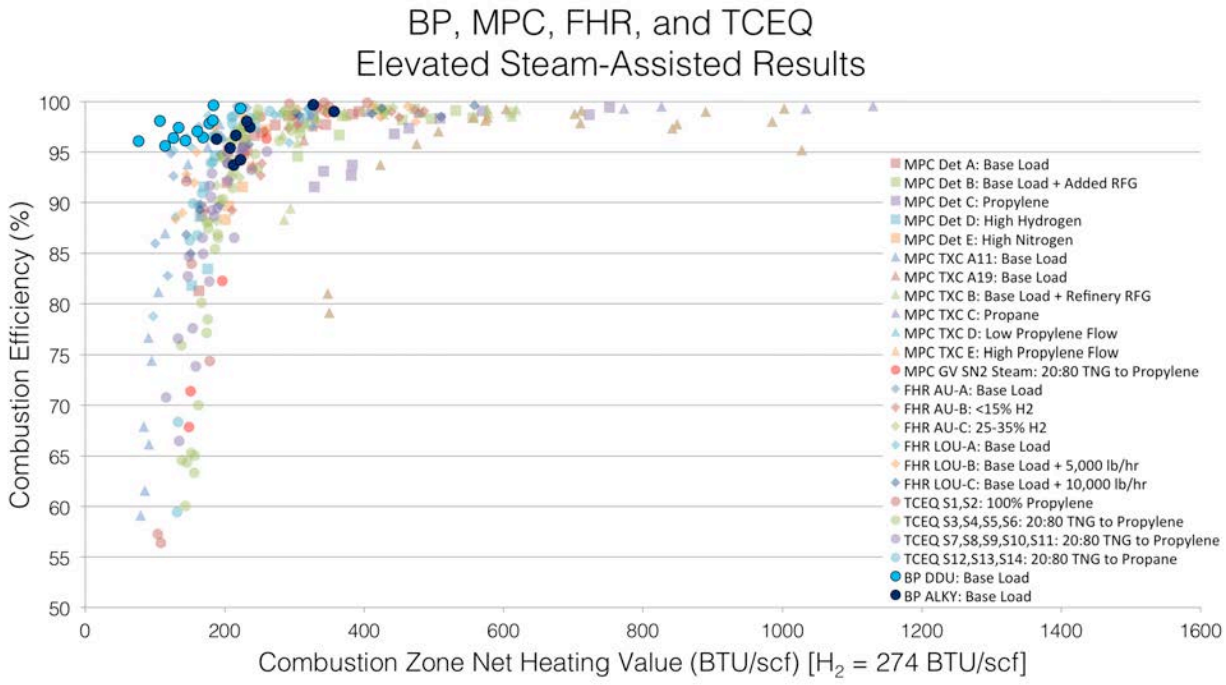

Figure 3.2-1: NHVcz vs. CE for All Elevated, Steam-Assisted Test Runs

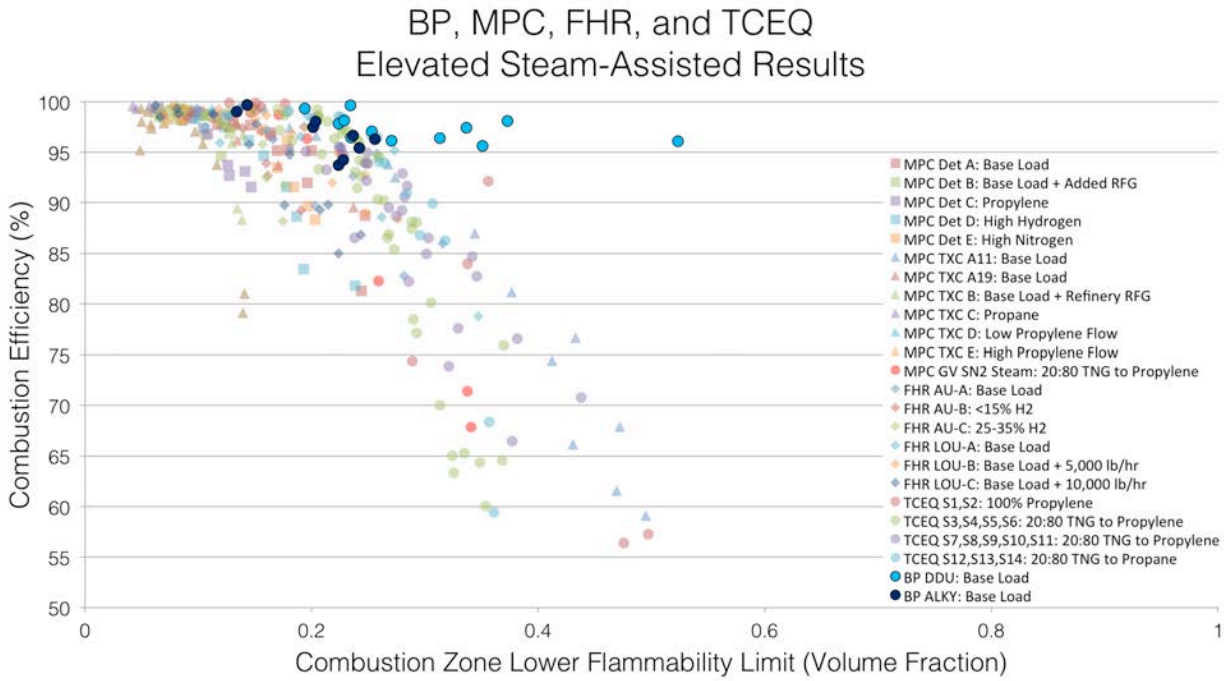

Figure 3.2-2: LFLcz vs. CE for All Elevated, Steam-Assisted Test Runs

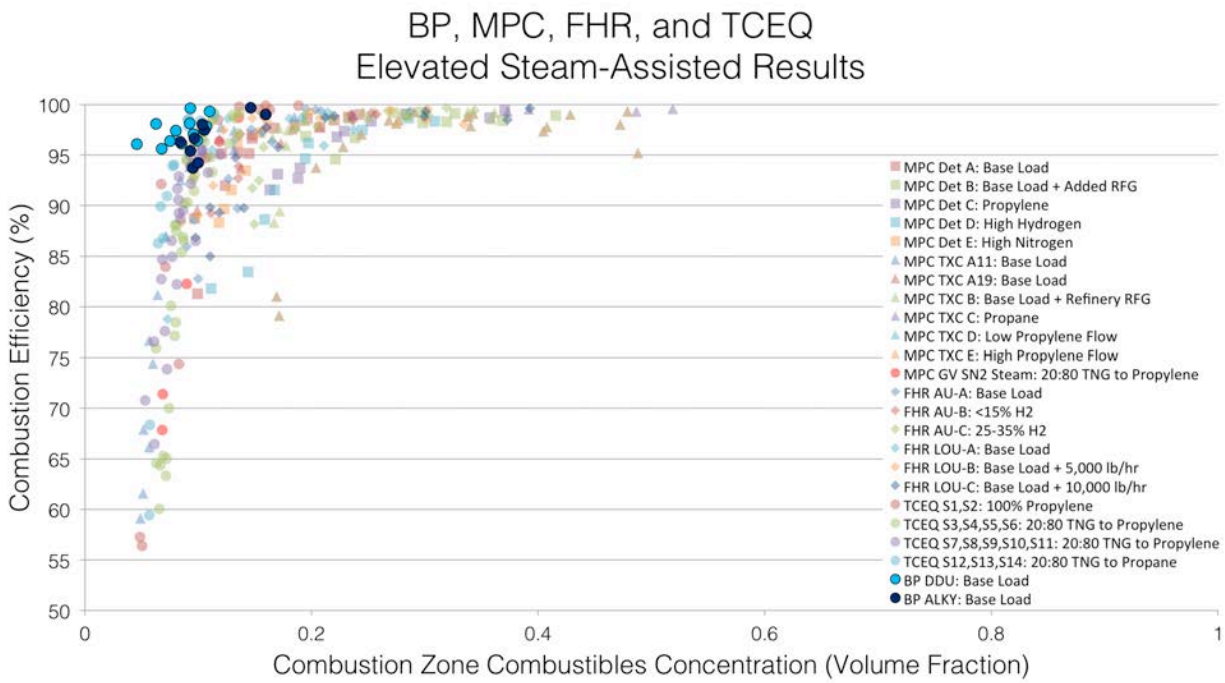

Figure 3.2-3: Ccz vs. CE for All Elevated, Steam-Assisted Test Runs

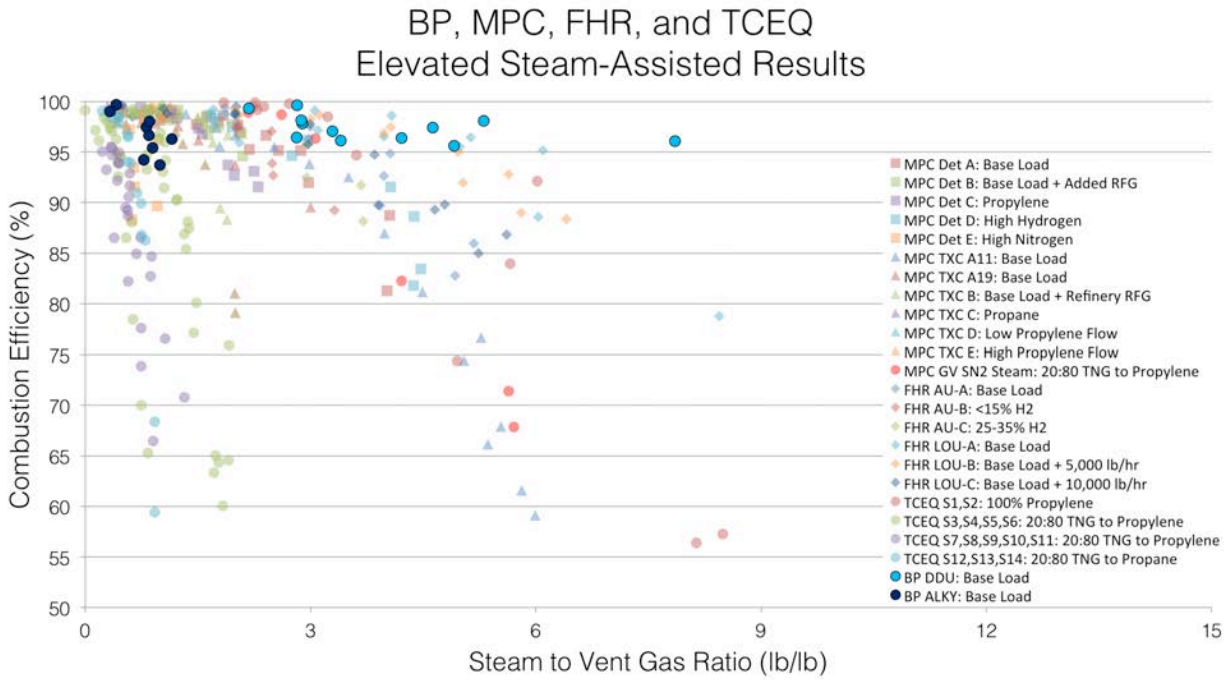

Figure 3.2-4: S/VG (Mass Basis) vs. CE for All Elevated, Steam-Assisted Test Runs

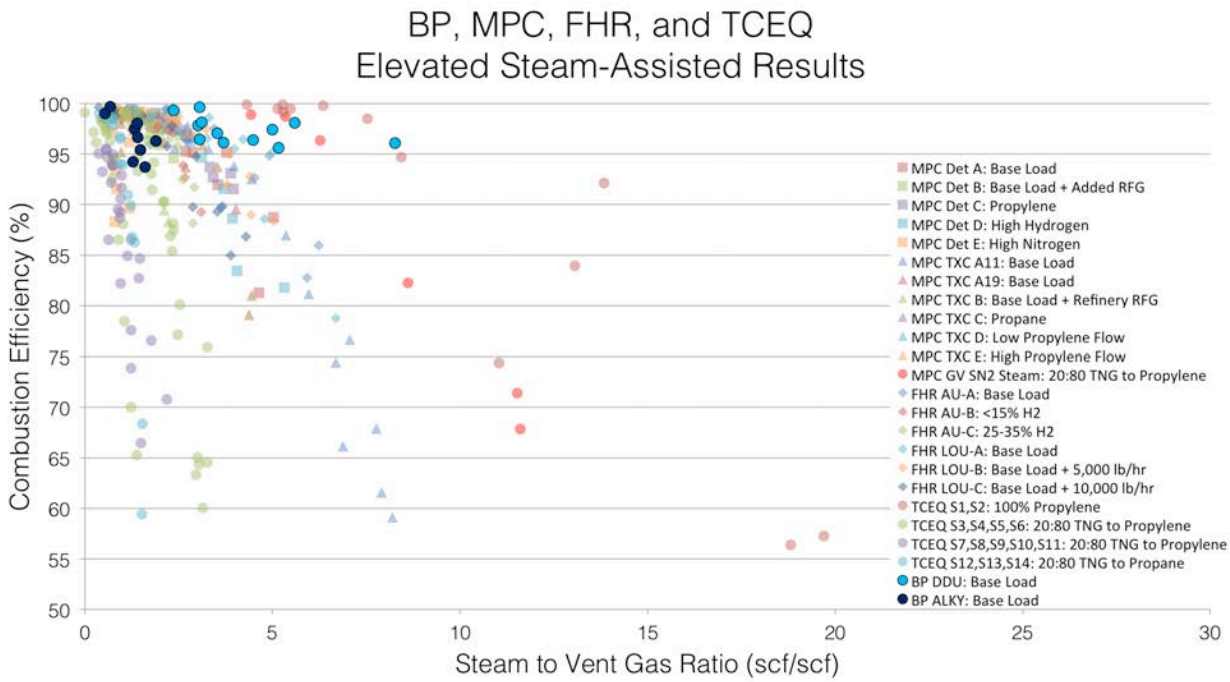

Figure 3.2-5: S/VG (Volume Basis) vs. CE for All Elevated, Steam-Assisted Test Runs

3.2.2 Visible Emissions and Combustion Efficiency

Visible emissions play a key role in environmental compliance for refinery flares. New Source Performance Stands (NSPS) and Maximum Achievable Control Technology (MACT) standards contain time limits for allow visible emissions or "smoke." As such, the point at which visible emissions begin to form is one operating bound on the proper operating envelope for a refinery flare.

During previous flare tests, a visible emissions scale was developed and implemented as part of the test program in order to quantitatively grade the visual flame characteristics. The scale is shown in Table 3.2.2-1. The incipient smoke point was designated as the number 5 (the scale center), and represents the point at which the flare flame displays a "marbley" texture, indicative of small carbon and soot particles forming in the flame zone but quickly completing the combustion process. As such, no visible soot particles are present outside the flame boundary.

Flame ratings above 5 indicate an increasing amount of visible emissions extending beyond the flame boundary observed by increasing amounts of a trailing smoke plume. Flame ratings less than 5 indicate a visible flame decreasing in intensity until it becomes invisible. Ratings of 4 to 2 indicated a visible flame and a rating of 1 indicated a transparent or invisible flame. A flame rating of 0 indicated that the flare was extinguished with steam visually present.

Flame Rating	Flame Characteristic
0	Steam plume
1	Transparent
2	Mostly transparent, with occasional yellow flame.
3	Mostly yellow flame, with occasional transparency.
4	Yellow to orange flame.
5	Orange flame with some dark areas in the flame. (Incipient smoke point)
6	Orange flame with light smoke trail.
7	Clear steam at the flare tip, with an orange flame and a light smoke trail.
8	Orange flame with dark smoke trail leaving the flame.
9	Orange flame with heavy dark smoke trail leaving the flame.
10	Billowing black smoke

Table 3.2.2-1: Visual Emissions Scale

Previous PFTIR studies have shown that when a steam-assisted flare is operating at its incipient smoke point, combustion efficiency is high and that a bright orange flame is an indicator of good combustion efficiency. However, visual characteristics alone cannot be relied upon to determine whether or not a flare is operating at high combustion efficiency. Flares with vent gas streams containing large quantities of nitrogen and hydrogen may be mostly transparent, yet they may operate at high combustion efficiency.

Visual emissions data sheets for the ALKY and DDU flare tests are contained in Appendix A.10.

3.3 Factors Influencing Test Results

3.3.1 Run Lengths

As the length of a Passive FTIR flare test run is extended, the relative variability in the results becomes less. Comparing the combustion efficiency averages of 5 minute and 10 minute intervals to the average combustion efficiency of a flare test run supports this trend. Table 3.3.1-1 shows the 5 minute interval averages and Table 3.3.1-2 shows the 10 minute interval averages. If the variation between the run average combustion efficiency and the interval combustion efficiency is 0.5% or greater, the values are flagged red. These results show that the 10 minute interval averages show less variation from the run averages.

Test	Run Average CE	0-5 Minute Average	0-5 Minute Deviation	5-10 Minute Average	5-10 Minute Deviation	10-15 Minute Average	10-15 Minute Deviation	15-20 Minute Average	15-20 Minute Deviation	20-25 Minute Average	20-25 Minute Deviation
DDU-1 1	99.3	98.7	-0.6	99.4	0.0	99.6	0.3	99.6	0.3		
DDU-1 2	99.6	99.7	0.0	99.5	-0.1	99.8	0.2	99.6	-0.1		
DDU-2 1	96.5	97.5	1.1	96.5	0.0	96.3	-0.2	95.4	-1.0	96.6	0.13
DDU-2 2	96.1	96.3	0.1	96.8	0.6	95.9	-0.2	95.5	-0.6		
DDU-3 1	96.4	96.3	-0.1	96.1	-0.3	97.4	1.0	95.7	-0.7		
DDU-3 2	95.6	95.9	0.3	93.9	-1.7	96.9	1.3	96.2	0.6		
DDU-4 1	98.1	98.2	0.1	98.5	0.3	97.9	-0.2	97.9	-0.2		
DDU-4 2	96.1	96.6	0.6	95.8	-0.3	96.0	0.0	95.9	-0.1		
DDU-5 1	97.4	97.1	-0.3	97.1	-0.3	97.7	0.3	97.7	0.3		
DDU-5 2	97.1	97.2	0.1	96.9	-0.2	96.9	-0.1	97.2	0.1		
DDU-6 1	97.8	97.8	-0.1	97.9	0.0						
DDU-6 2	98.1	98.2	0.1	98.0	-0.1						
ALKY-1 1	99.7	99.7	0.0	99.8	0.1	99.7	0.0				
ALKY-1 2	99.0	98.7	-0.3	99.0	0.0	98.9	-0.1	99.2	0.2		
ALKY-2 1	97.5	97.9	0.4	96.9	-0.6	97.8	0.3				
ALKY-2 2	98.0	98.3	0.3	97.8	-0.3						
ALKY-3 1	93.7	95.7	2.0	91.8	-1.9	93.9	0.2				
ALKY-3 2	96.3	98.7	2.4	95.0	-1.3	95.7	-0.6	96.3	0.0		
ALKY-4 1	95.4	98.7	3.3	97.6	2.2	91.3	-4.1	94.9	-0.5		
ALKY-4 2	94.2	97.5	3.3	94.2	0.0	92.3	-2.0				
ALKY-5 1	96.6	97.1	0.5	96.2	-0.4	98.0	1.3	95.8	-0.9		

Table 3.3.1-1: Run Average CE with 5 Minute Averaging Interval CE and Deviations

Test	Run Average CE	0-10 Minute Average	0-10 Minute Deviation	10-20 Minute Average	10-20 Minute Deviation
DDU-1 1	99.3	99.0	-0.3	99.6	0.3
DDU-1 2	99.6	99.6	-0.1	99.7	0.1
DDU-2 1	96.5	96.9	0.5	96.2	-0.3
DDU-2 2	96.1	96.5	0.4	95.7	-0.4
DDU-3 1	96.4	96.2	-0.2	96.6	0.2
DDU-3 2	95.6	94.8	-0.8	96.5	0.9
DDU-4 1	98.1	98.4	0.2	97.9	-0.2
DDU-4 2	96.1	96.1	0.1	96.0	-0.1
DDU-5 1	97.4	97.1	-0.3	97.7	0.3
DDU-5 2	97.1	97.0	0.0	97.1	0.0
DDU-6 1	97.8				
DDU-6 2	98.1				
ALKY-1 1	99.7				
ALKY-1 2	99.0	98.8	-0.2	99.1	0.1
ALKY-2 1	97.5				
ALKY-2 2	98.0				
ALKY-3 1	93.7				
ALKY-3 2	96.3	96.7	0.4	96.0	-0.3
ALKY-4 1	95.4	98.1	2.7	93.5	-1.9
ALKY-4 2	94.2				
ALKY-5 1	96.6	96.6	0.0	96.7	0.0

Table 3.3.1-1: Run Average CE with 10 Minute Averaging Interval CE and Deviations

3.3.2 Wind Effects

Wind did not impact the ability of the Passive FTIR to measure combustion efficiency because two instruments were situated at a 90 degree angle to ensure at least one instrument had a good view of the flare plume. During the Whiting tests, PFTIR 2 almost always had an acceptable vantage point.

3.3.2.1 Momentum Flux Ratio

Figure 3.3.2.1-1 shows combustion efficiency as a function of momentum flux ratio (MFR). The data show that lower MFR values do not necessarily result in low combustion efficiency. The data points with lower combustion efficiency were a result of over-steaming, not wind effects.

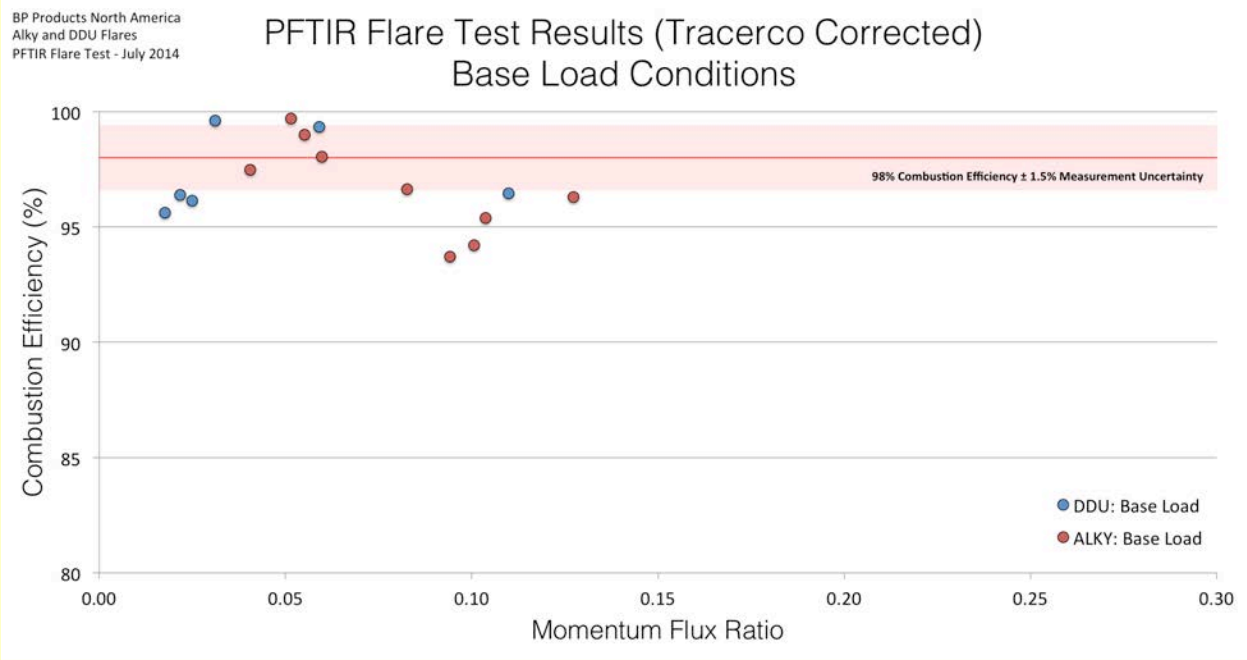

Figure 3.3.2.1-1: Momentum Flux Ratio vs. Combustion Efficiency

3.3.3 PFTIR Aiming

Proper aiming of the Passive FTIR is critical to acquisition of valid data. Ideally, the PFTIR should be aimed near the centerline of the flare plume about one flame length away from the flame tip. At this distance, it is believed that all thermal destruction reactions have been completed. However, the plume is a moving target. Therefore, in an attempt to maintain the aim of the PFTIR at this optimal sampling point, the instrument must be continually adjusted by the operator. This can become increasingly difficult when wind direction and shifting.

3.3.4 Overall Test Variability

3.3.4.1 Long Term Stability

A long term stability test was not conducted. All of the DDU testing was completed in one day and the ALKY testing was completed in two days. Because the PFTIRs were not set up for testing at a single flare for more than two days, no long term stability test could be conducted.

3.3.4.2 Replicate Analysis

Replicate runs were performed for many of the test conditions. Table 3.3.4.2-1 below shows the combustion efficiency for each run and the variation between replicate runs.

	1st Replicate	2nd Replicate	
Condition	**CE (%)**	**CE (%)**	**ΔCE (%)**
DDU-1	99.3	99.6	0.3
DDU-2	96.5	96.1	0.6
DDU-3	96.5	95.6	0.9
DDU-4	98.1	96.1	2.0
DDU-5	97.4	97.1	0.3
DDU-6	97.8	98.1	0.3
ALKY 1	99.7	99.0	0.7
ALKY 2	97.5	98.0	0.5
ALKY 3	93.7	96.3	2.6
ALKY 4	95.4	94.2	1.2
ALKY 5	96.6		N/A

Table 3.3.4.2-1: Combustion Efficiencies of Replicate Runs

3.3.4.3 Dual PFTIR Simultaneous Measurements

Only data from PFTIR 2 was used in analysis. The wind conditions were favorable for PFTIR 2 for the entire test program. Because of this, PFTIR 1 data is not reliable and is not used in any of the analysis.

3.3.4.4 Dilution Assumption

Because the flare plume is constantly moving during the test, it is impossible to collect all spectra at exactly the same point in the plume. As the gases in the plume move farther from the combustion zone, they are increasingly diluted by the ambient air. This means that the absolute concentration of the plume components will vary based solely on where in the plume the PFTIR is aimed and collecting data.

Since the calculation of combustion efficiency is based on the ratio of CO_2 to total carbon in the plume (i.e. the sum of CO_2, CO, and TH), it is the ratios of the components that matter rather than their absolute concentrations. Therefore, even though absolute concentrations vary at different measurement points due to dilution, the ratios should be the same because, in theory, all plume components are diluted equally at any given sampling point.

3.3.4.5 PFTIR Field Hot Cell Calibrations

See Section 4.4.1 for details.

3.3.5 PFTIR Calibration

3.3.5.1 Background Radiance Calibrations

See Section 4.4.1 for details.

3.3.5.2 Atmospheric Radiance and Transmission Calibrations

See Section 4.4.1 for details.

3.3.5.3 Hot Cell Calibrations

See Section 4.4.1 for details.

3.3.6 PFTIR Detectors

PFTIR instruments from CleanAir were used to measure combustion efficiency of the flare. The PFTIR instruments were equipped with dual sensors - mercury-cadmium-telluride (HgCdTe) and indium-antimonide (InSb).

3.3.6.1 Spectral Regions for CO_2

Figure 3.3.6.1-1 shows the spectral regions where CO_2 is detected with the dual detector. CO_2 is detected in two regions. CO_2 can be detected near 2000 wavenumbers (CO_2 2K) and near 765 wavenumbers (CO_2 765).

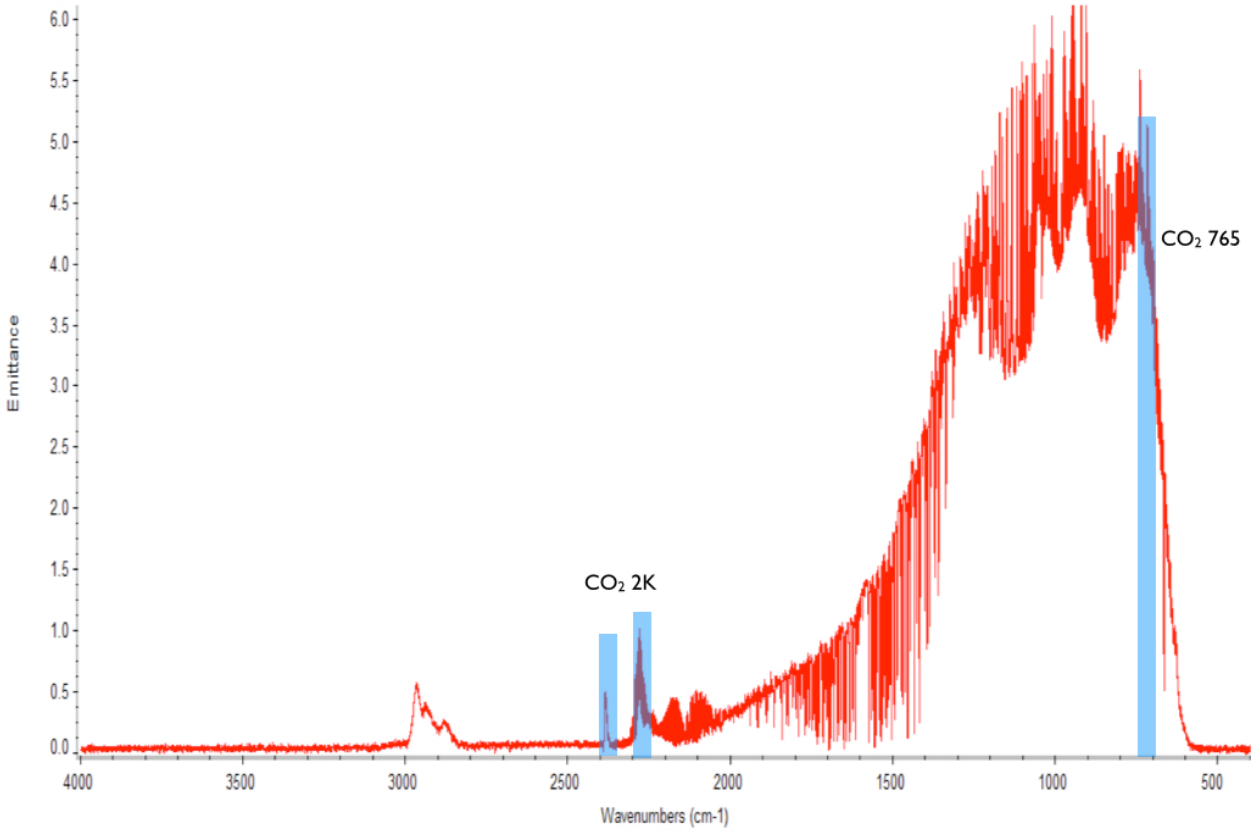

Figure 3.3.6.1-1 Spectral Regions for CO2

3.4 Conclusions

The PFTIR test of the DDU and ALKY Flares provided data to support the following conclusions.

3.4.1 Relationship of Combustion Efficiency and NHVcz

The general relationships between combustion efficiency and other key parameters that were observed during the DDU and ALKY Test Series are consistent with previous PFTIR tests on steam-assisted flare tips.

When the DDU flare is operating under base load conditions, high combustion efficiency (98% ±1.5%) is maintained until NHVcz falls to less than 110 BTU/scf. When the ALKY flare is operating under base load conditions, high combustion efficiency is maintained until NHVcz falls to less than 220 BTU/scf. On past PFTIR base load tests on elevated steam-assisted refinery flare tips high combustion efficiency is generally maintained until NHVcz falls below 300 BTU/scf. Therefore, the combustion efficiency performance of the DDU and ALKY flares is above average for their class.

3.4.2 Operating Ranges for Covered Flares to Assure 98% combustion Efficiency

The above average combustion efficiency performance of flares is a function of several inter-related process variables, notably S/VG ratio and NHVvg, and the composition of the vent gas. S/VG is a controlled process variable at Whiting Refinery. The current control scheme limits S/VG ratios to 3:1. The scheme is in compliance with the consent decree requirements in Appendix D, ¶34.a.

The source test data presented in this report suggests that an “A” combustion efficiency multiplier of 2.84 would be required to maintain high combustion efficiency on the DDU Flare and an “A” combustion efficiency multiplier of 4.38 would be required to maintain high combustion efficiency on the ALKY Flare. There is a significant difference in the Combustion Efficiency Multipliers due to differences in vent gas compositions and the levels of NHVcz where combustion efficiency on the DDU and ALKY flares begins to decline. The multipliers were calculated with vent gas compositions specific to each flare and could vary greatly for flares with different vent gas compositions. Section A.1.6 discusses the details of how the “A” combustion multiplier is calculated.

NHVvg and LFLvg are generally inherent to the sources tied into a specific flare. Table 3.4.2-1 presents the long-term average composition along with the calculated values of NHVvg and LFLvg for each covered flare at Whiting. Figure 3.4.2-1 shows the NHVvg against the LFLvg computed from the average composition of each covered by the BP Flare Consent Decree. The plot shows that characteristics of the ALKY and VRU flares are very similar. It also shows that the characteristics of the FCU and DDU flares are very similar. Because of these relationships, it is possible that an “A” combustion efficiency multiplier of 2.84 can be used for the FCU flare and an “A” combustion efficiency multiplier of 4.38 can be used on the VRU flare. The plot shows the remaining covered flares, GOHT, 4UF, UIU, and South, with higher NHVvf and lower LFLvg.

Compound	Alky Flare	DDU Flare	South Flare	VRU Flare	FCU Flare	UIU Flare	4UF Flare	GOHT Flare
Nitrogen (mol %)	21.80	69.88	7.20	58.20	37.70	13.50	13.20	22.40
Oxygen (mol %)	0.03	0.05	0.00	0.20	1.00	0.00	0.10	0.00
Water (mol %)	1.06	0.34	0.60	0.40	1.80	0.00	0.50	0.10
Carbon dioxide (mol %)	0.86	0.10	0.80	0.90	0.50	0.80	0.10	0.40
Carbon monoxide (mol %)	0.23	0.00	0.00	0.10	0.00	0.10	0.00	0.00
Hydrogen sulfide (mol %)	0.00	0.00	0.40	0.00	0.00	0.00	0.10	0.00
Methane (mol %)	48.97	7.42	6.60	2.40	14.70	30.00	66.60	35.80
Ethane (mol %)	6.66	0.48	67.20	21.50	19.60	42.10	9.10	35.40
Hydrogen (mol %)	13.68	0.31	4.50	2.60	3.40	6.40	4.70	2.30
Ethylene (mol %)	1.85	0.13	0.80	2.60	1.90	2.00	0.20	0.30
Acetylene (mol %)	0.48	0.00	0.00	0.00	0.00	0.00	0.00	0.00
Propane (mol %)	1.36	3.03	1.50	0.50	2.80	2.20	2.80	0.50
Isobutane (mol %)	0.21	3.95	0.60	0.20	0.10	0.30	0.30	0.10
n-Butane (mol %)	0.35	2.57	2.00	0.10	0.00	1.00	0.70	0.10
Butenes (combined) (mol %)	0.06	0.05	0.20	0.10	0.10	0.20	0.00	0.00
Propylene (mol %)	0.80	6.20	0.80	0.80	1.60	1.20	0.50	0.30
n-Pentane+ (mol %)	0.50	1.05	6.10	1.00	0.70	0.50	2.40	0.20
Other Parameters								
NHVvg (BTU/scf)	705	536	1478	515	696	1093	932	922
LFLvg (Volume Fraction)	0.05	0.09	0.03	0.08	0.06	0.04	0.05	0.05

Table 3.4.2-1: Long Term Average Composition Data for Vent Gas of Covered Flares

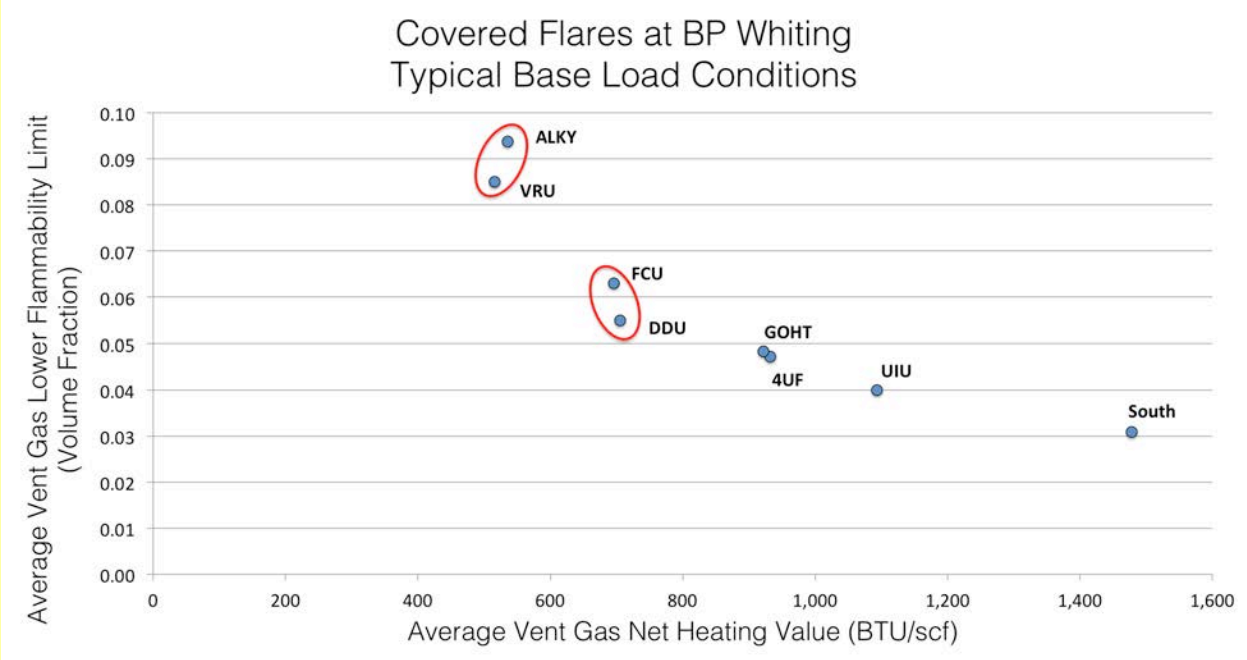

Figure 3.4.2-1: Average NHVvg vs. Average LFLvg for Covered Flares

3.5 Recommendations for Further Study

Appendix D paragraph 48 of the consent decree requires BP Whiting to perform PFTIR testing of the LPG flare if the 2015 annual average flow rate equals or exceeds 35 scfm. If the average flow rate remains below 35 scfm in 2015, there is no reason to conduct PFTIR testing of this flare because LPG flare will have very little impact on flare emissions at BP Whiting. If triggered, the testing must be completed by September 2016. BP intends to perform this testing only if the average flow rate for 2015 exceeds 35 scfm.

Based on BP's proposal to continue to use the more conservative "A" combustion efficiency multiplier in section FLR-3 of the consent decree, no further study of flare combustion efficiency is recommended.

4.0 PFTIR Testing Method and Procedure

4.1 Description and Principals of Passive FTIR

The instrument used to measure the gas composition of the flare plume is the Passive Fourier Transform Infrared (PFTIR) analyzer. To monitor elevated flares, standard "active" IR spectroscopy could be used. However, it is difficult from a practical standpoint to pass a beam of IR light through an elevated flare plume and then capture the transmitted light. A flare plume is constantly moving and would require that the IR light beam constantly move to remain inside the flare plume. Therefore, for this project, a "passive" approach is used that does not require an independent IR light source. PFTIR analysis operates on the principle of spectral analysis of thermal radiation emitted by hot gases. "Passive" means that no "active" infrared light source is used. Instead, the hot gases of the flare are the infrared source. The spectrometer is a receiver only.

Most stack test and fence-line measurement technologies either physically extract a sample of gas from a stack into a sample cell or "shoot" a reference beam across the stack or along the fence-line. These technologies measure how much of a reference IR beam is absorbed by the gas at various wavelengths. This process generates an "absorption spectrum". Since these techniques are a mature technology, many references and software tools available for analyzing absorption spectra.

The PFTIR approach is possible because hot gases emit radiation at the same frequencies as they absorb. The result is referred to as a "radiance spectrum." Since the infrared radiance spectra of hot gases have the same patterns or "fingerprints" as the absorption spectra, it is possible to convert radiance spectra to absorption spectra and then to use the many available analytical tools to determine gas concentrations. Figure 4.1-1 shows a schematic of a PFTIR measuring a flare plume.

For this test program, Dr. Robert Spellicy of Industrial Monitor and Control Corporation (IMACC) oversaw the PFTIR operation and data analysis. Dr. Spellicy and IMACC developed both the PFTIR instrument and the analytical software.

Figure 4.1-1: Schematic of PFTIR Measuring a Flare Plume

There is one main difference between the two approaches: the radiance spectrum from hot gases is proportional to the concentration of the gas (as it is absorption), but it also affected by gas temperature. In standard absorption FTIR, the temperature of the gas is known and controlled. With PFTIR measurements on a flare plume, the temperature is unknown. Therefore, when conducting PFTIR measurements, the temperature of the flare plume must be determined. Details of how this temperature determination is made are found in Appendix A.2.

Consequently, unlike absorption spectroscopy, the PFTIR signal must be calibrated in absolute units of radiance. This requires that the instrument be calibrated utilizing an IR source of known spectral radiance. This calibration is accomplished with a commercial black body calibrator. This calibrator produces a known IR distribution as predicted by the Planck function. Details of the calibration are found in Appendix A.2.

Calibrations were performed each day at the beginning and end of testing. Calibration results are found in Appendix A.7.

A more detailed treatment of PFTIR theory is found in Appendix A.2. In order to perform calibrations on the PFTIR, a calibration cart is used. See Figure 4.1-2. This cart consists of a telescope, identical to the telescope on the PFTIR. At the focal point of the telescope is a mount where various calibration materials are placed as described below. The telescope acts as a collimator providing a collimated beam with the same diameter as the PFTIR telescope. When the collimator and the PFTIR are aligned, the calibration source fills the PFTIR field of view. To perform the calibrations, the calibration cart was placed next to the base of the flare and aimed toward the PFTIR. The two were then aligned and each calibration source, in turn, was placed in the collimator. The PFTIR then collected data from each source. This data is then used in the analytical software to calibrate the raw signal and to correct for interferences.

Figure 4.1-2: The Calibration Cart

Several calibrations were performed throughout the test program to account for the effects of sky background and atmospheric radiance and transmittance. Three radiant sources with various characteristics were placed at the focal point of the collimator at roughly the same distance from the PFTIR as the flare. Precise alignment of the PFTIR with the collimator was critical during

these calibrations. The sky background calibrations were performed as needed during testing. Calibration files are found in Appendix A.7.

Black Body Calibration
To calibrate the PFTIR signal in absolute units of radiance, a black body with an IR source of known spectral radiance was used. A commercial black body calibrator was placed in the collimator at the base of the flare, which produced a known IR spectrum as predicted by the Planck function. The calibration of this black body standard is traceable to the National Institute for Standards and Technology (NIST). This calibration was done at least once each day.

IR Source Calibration
To determine the atmospheric transmission loss between the flare plume and the PFTIR, an infrared (IR) source was placed in the collimator at the base of the flare. It created a strong IR signal that the PFTIR could detect to determine atmospheric transmission. This calibration was done at the beginning and end of each day.

Cold Source Calibration
Since the air and PFTIR are not at absolute zero, they radiate also. This radiation will be detected by the PFTIR. To determine the atmospheric radiance generated by the air between the flare plume and the PFTIR and from the PFTIR instrument itself, a cold source of liquid nitrogen in a windowed cup was placed in the collimator at the base of the flare. It zeroed any radiance except for that created by the atmosphere and the PFTIR. This calibration was done at the beginning and end of each day.

Sky Background Calibration
Background radiance calibrations were conducted as needed during the test program. When the background changed behind the flare plume, such as when clouds were passing, backgrounds were taken more often. It was not uncommon to take a background every 10 minutes during a run. During the background calibration, the PFTIR would swing off the flare plume and collect a reading for approximately one minute, then swing back to the flare plume and continue collecting data. Background times are included in the PFTIR raw data in Appendix A.7.

4.2 Passive FTIR Sitting Configuration

Two PFTIR instruments were used for this test program. These locations were chosen based on their unobstructed views of the flare tip, easy access to electricity, and the ability to lay data cables in a safe manner. The locations of the PFTIR instruments were set up at a roughly 90 degree angle.

Figures 4.2-1 and 4.2-2 show maps of the PFTIR locations in relation to the ALKY and DDU flare tips.

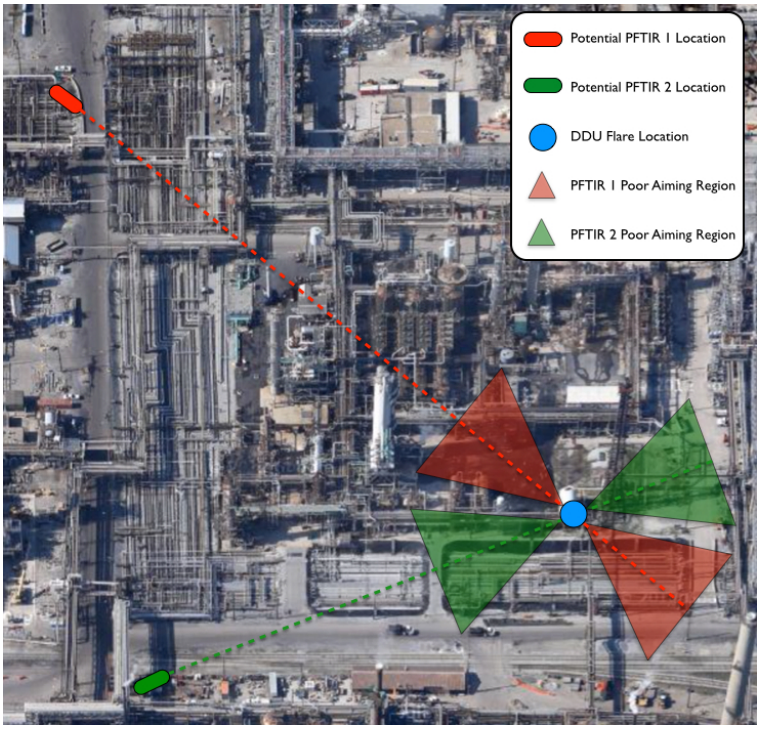

Figure 4.2-1: Map of the PFTIR Locations in Relation to the ALKY Flare Tip

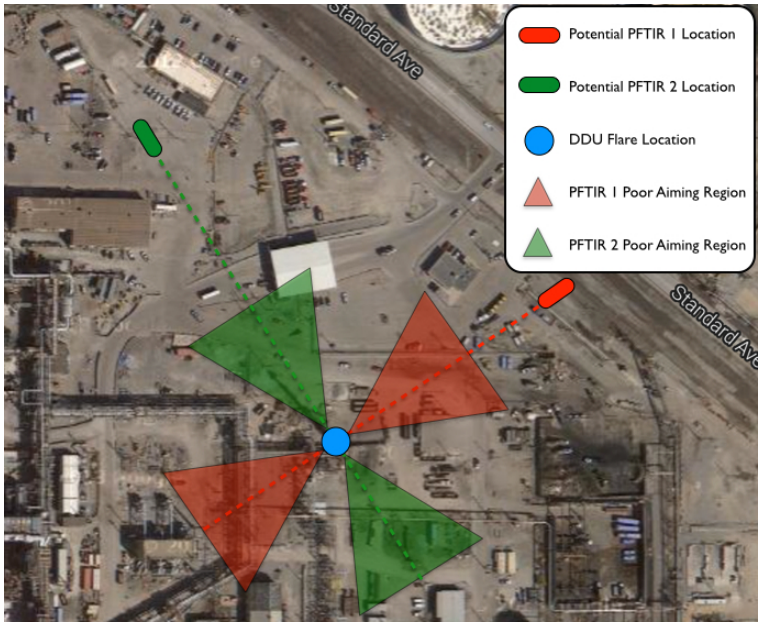

Figure 4.2-2: Map of the PFTIR Locations in Relation to the DDU Flare Tip

4.3 Background

Prior to the recent refinery tests of flare performance, including the US EPA tests in the mid-1980s, flare tests were conducted on pilot-scale test flares or on flares operating at moderate to

high vent gas loads. However, a flare typically operates at low vent gas loads (i.e. high turndown) under normal conditions until a process upset or other operating condition requires the operator to flare waste gas. Thus, the flare normally operates at high turndown for the majority of the operating year, a condition for which there was little to no available performance data.

In the past, measuring the combustion products from a flare was difficult and dangerous. However, recent technological advances have produced remote sensing instruments capable of measuring combustion products such as carbon dioxide, carbon monoxide, and select hydrocarbons without the safety hazards introduced by physically sampling a flare plume. One such instrument is the PFTIR, which characterizes a plume's chemical make-up (carbon dioxide, carbon monoxide, and total hydrocarbons) in units of concentration × pathlength. Using this technology, the absolute concentration cannot be determined from a flare plume, but the product of concentration × pathlength (e.g., ppmv × meters), can be used in combustion efficiency calculations. The PFTIR is a relatively new tool and was recently blind-validated against extractive sampling results for flare plume testing by TCEQ and the University of Texas in 2010. The PFTIR was first used for refinery flare testing at MPC Texas City in 2009. Several accuracy, precision, and bias checks were performed during the recent flare tests to better characterize the PFTIR measurement technique.

The flare tests were conducted using Passive Fourier Transform Infrared (PFTIR) instruments developed by Industrial Monitor and Control Corporation (IMACC). The specific analytical method used for these tests is the same method used and validated during testing conducted by the Texas Commission on Environmental Quality (TCEQ) in 2010.

4.4 PFTIR Operation

Each PFTIR was housed in a trailer. These trailers were positioned to obtain the best view of the flare plumes regardless of wind conditions. Calibrations for each PFTIR were performed at least once each day. Results of these daily calibrations are found in Appendix A.7. After calibration was completed, the equipment was ready to begin testing. Before each test run, a sky background was obtained. Additional sky backgrounds were taken approximately every 20 minutes or as sky conditions changed during testing.

Both PFTIRs collected data during a run for simultaneous readings. However, for some runs only one PFTIR was operational due to poor vantage points and equipment malfunctions.

Wind speed changed the profile of the flare plume. When the wind speed was relatively low, the flare plume was more upright and compact. When the wind speed was relatively high, the flare plume was more horizontal and elongated. Aiming was adjusted for wind speed to capture a representative section of the flare plume that was not too close to the flare flame and not too cold for the PFTIR to be effective.

Proper aiming of the PFTIR is critical to acquisition of consistent, reliable data. Ideally, the PFTIR should be aimed near the centerline of the flare plume about one flame length away from the flame tip. At this distance, all thermal destruction reactions have reached completion. However, the plume is a moving target. Therefore, in an attempt to maintain an optimal view, the PFTIR operator must continually adjust the aiming position of the PFTIR. This task becomes

increasingly difficult when the wind is shifting, causing the plume to move in different directions. Aiming is poor and readings are invalid when the flare plume is blowing directly away from the PFTIR.

Because two PFTIRs were used at separate locations for the tests, at least one PFTIR always had a good view of the flare plume. Aiming videos were monitored during the test program to ensure that acceptable aiming was maintained. The best opportunity for the PFTIR to obtain a representative sample of the flare plume is when:

1. The flame is buoyant and plume is rising directly above the flame, or

2. The flame is "bent over" by the wind and the plume is roughly perpendicular to the PFTIR field of view. Figure A.4.5-1 shows a perpendicular view from a PFTIR location.

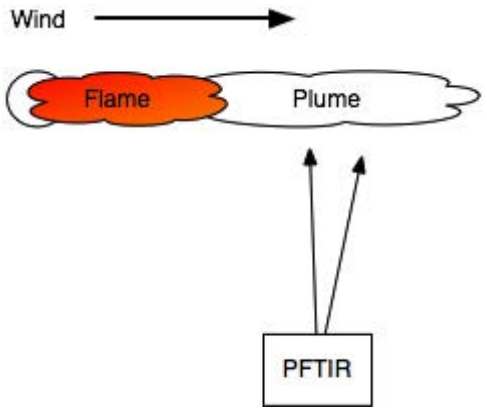

Figure 4.4-1: Example of Good Plume Alignment with PFTIR

The worst alignment occurs when the flame and plume are bent by the wind and blowing directly away from the PFTIR. Figure 4.4-2 shows an example of poor PFTIR alignment. When this occurs, the flare structure, tip, and flame block the view of the plume from the PFTIR, making it difficult to obtain a representative sample of the plume.

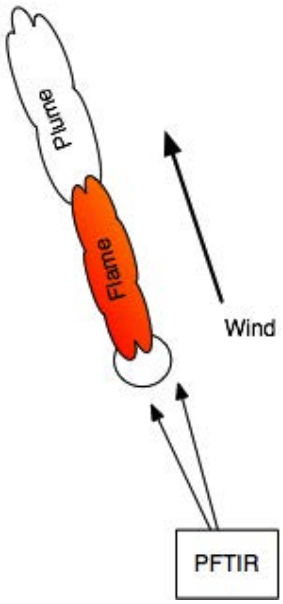

Figure 4.4-2: Example of Poor Plume Alignment with PFTIR

This effect can be seen visually on the PFTIR aiming camera. Figure 4.4-3 shows example images of good plume alignment and poor plume alignment, respectively. The crosshair on the images shows the PFTIR field aiming point. Data collected from a poorly aligned plume may result in invalid data.

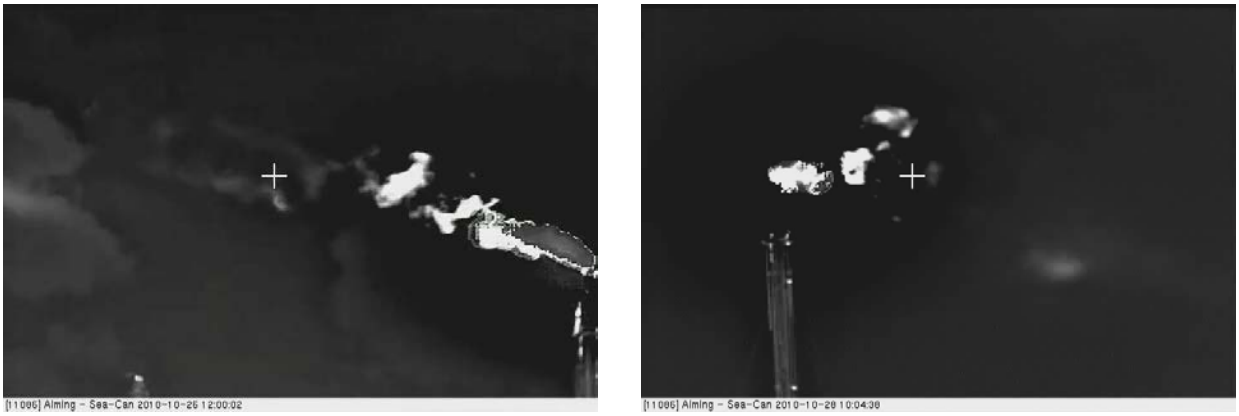

Figure 4.4-3: Left – Aiming Camera with Good Plume Alignment. Right – Aiming Camera with Poor Plume Alignment

To avoid the problem of poor plume alignment, two PFTIRs were placed at separate locations so at least one PFTIR had good plume alignment regardless of wind direction. However, because many of the test runs featured high exit velocities, wind speed and direction had little impact on the ability of the PFTIRs to get a good reading.

4.5 PFTIR Data Reduction

Once collected, the raw PFTIR data must be processed to yield the individual flare component concentrations. This data processing was performed by Dr. Robert Spellicy from IMACC. Data were compiled at approximately one minute intervals. Each one minute point consists of approximately 40 individual measurements averaged into a single spectrum.

The data analysis procedure has four major components:

1. Convert the raw interferogram to a single-beam spectrum using a Fourier Transform process.

2. Isolate the flare transmissivity from the other interferences listed above.

3. Convert the isolated flare transmissivity spectrum to an absorbance spectrum so it can be further analyzed with standard spectroscopic techniques.

4. Determine the concentrations of individual components of the flare plume from the absorbance spectrum.

Each of these steps is discussed briefly below. A more detailed treatment is found in Appendix A.2.

Step 1 – Convert the raw interferogram to a radiance spectrum

The raw data from the PFTIR are in the form of an interferogram, which is radiance as a function of FTIR scan position. The Fourier Transform (FT) process converts this data into a radiance spectrum, which is radiance as a function of wavelength or, in this case, wavenumber. The result is what is referred to as a "single beam" radiance spectrum. These single beam spectra have been supplied on the data hard drives that accompany this report. The FT process is a standard spectroscopic procedure and is not discussed in detail in this report.

Step 2 – Isolate the flare transmission spectrum

Once the radiance spectrum has been generated, the flare transmission must be isolated from all the interferants that the PFTIR also "sees". In order to accomplish this, each term in Equation A.4-1 above must be determined. This is done as follows:

Background radiance (N_{bkg}) – As described in Appendix A.3.3.5.1, at least once each day, the PFTIR was aimed at an unobstructed part of the sky. Since the background radiance is affected by conditions such as sun position and cloud cover, this procedure was repeated whenever a significant change in background was observed.

Flare transmissivity (τ_{flr}) – This is the value we are looking for and is the result when all competing factors are removed. It actually appears two places: 1) in transmitting the sky background through the flare to the PFTIR and 2) in the radiance term for the flare itself. The flare transmission must be extracted from the complex mixture of signals received by the PFTIR. This task is accomplished by the IMACC software.

Atmospheric transmissivity (τ_{atm}) – This value is determined by aiming the PFTIR at an IR source and taking the ratio of the value obtained (minus the atmospheric radiance) to a "synthetic background" spectrum. This synthetic background (referred to as I_0) represents the shape of the radiance spectrum that would be generated by the PFTIR in the absence of all gases. For this project the IR source was a SiC source operated at a temperature of 1250 K. This is a standard source used in most active FTIR systems. This source has sufficient signal throughout the infrared to allow for a transmission spectrum to be determined over the range of wavenumbers needed.

Flare plume radiance (N_{flr}) – Plume radiance is (1 – plume transmission) times the Planck function (evaluated at the temperature of the plume). The plume radiance is the desired measurement for flare testing. However, as discussed elsewhere, the plume radiance signal is mixed with other signals and so must be corrected with respect to this interference.

Atmospheric radiance (N_{atm}) – This value is determined by aiming the PFTIR at very cold source in the calibration telescope located at the same distance from the PFTIR as the flare. Any radiance observed will then be due to the intervening atmosphere plus any radiance from the PFTIR instrument itself. This measured value is referred to as M_n. For this project, the cold source was a windowed cup filled with liquid nitrogen where the level of the liquid nitrogen was just below the collimator inlet.

PFTIR radiance (N_f) – PFTIR radiance is the emissions of the instrument itself. It is measured together with atmospheric radiance and is part of the M_n measurement.

Once these values are known, they are applied to the total radiance spectrum by IMACC proprietary software to isolate the flare transmission spectrum. For a more detailed description of this process, see Appendix A.2.

Step 3 – Convert the transmission spectrum to an absorption spectrum
Once the flare transmission spectrum has been isolated, it must be converted to an absorbance spectrum so that standard spectroscopic techniques can be used for further analysis. Transmission and absorbance are related by the Beer-Lambert law through the following equation.

$$\tau_{plume} = e^{-K(\upsilon)*c*l} \qquad \text{Equation 4.5-2}$$

Essentially, absorbance is the negative log of transmission, thus:

$$\text{Absorbance}(\upsilon) = (0.434)K(\upsilon) * c * l \qquad \text{Equation 4.5-3}$$

See Appendix A.2 for further detail. This conversion is a standard spectroscopic procedure.

Step 4 – Determine the concentrations of individual components in the flare plume
Once the absorbance spectrum has been generated, there are several analytical techniques that may be used to estimate individual component concentrations. For this project, a modified Classical Least Squares (CLS) analysis was used. IMACC proprietary software was used for this step of the data analysis. The modifications to standard CLS include algorithms for linearizing the absorbance for each analyte with concentration, corrections for spectral baseline shifts, corrections for any spectral line shifts observed, and algorithms for dynamic reference spectra selection based upon observed concentrations of each compound.

The CLS technique compares measured spectra to combinations reference spectra of known concentration and interfering compounds and matches the absorbance of the data and the references to determine gas concentration. This process is performed for all components present to account for all spectral features present.

After fitting, CLS also determines the difference or residual between the measured and scaled references. The fitting process minimizes the residuals in each analysis region. The software used for this project uses dynamic reference selection to select reference spectra based upon measured gas concentrations. In most cases, this means different reference spectra will be chosen for each analyte in the measured spectrum. This process will be repeated up to four times to optimize all spectra compared to the measured data.

A flow chart of the PFTIR data analysis process is shown in Figure 4.5-1.

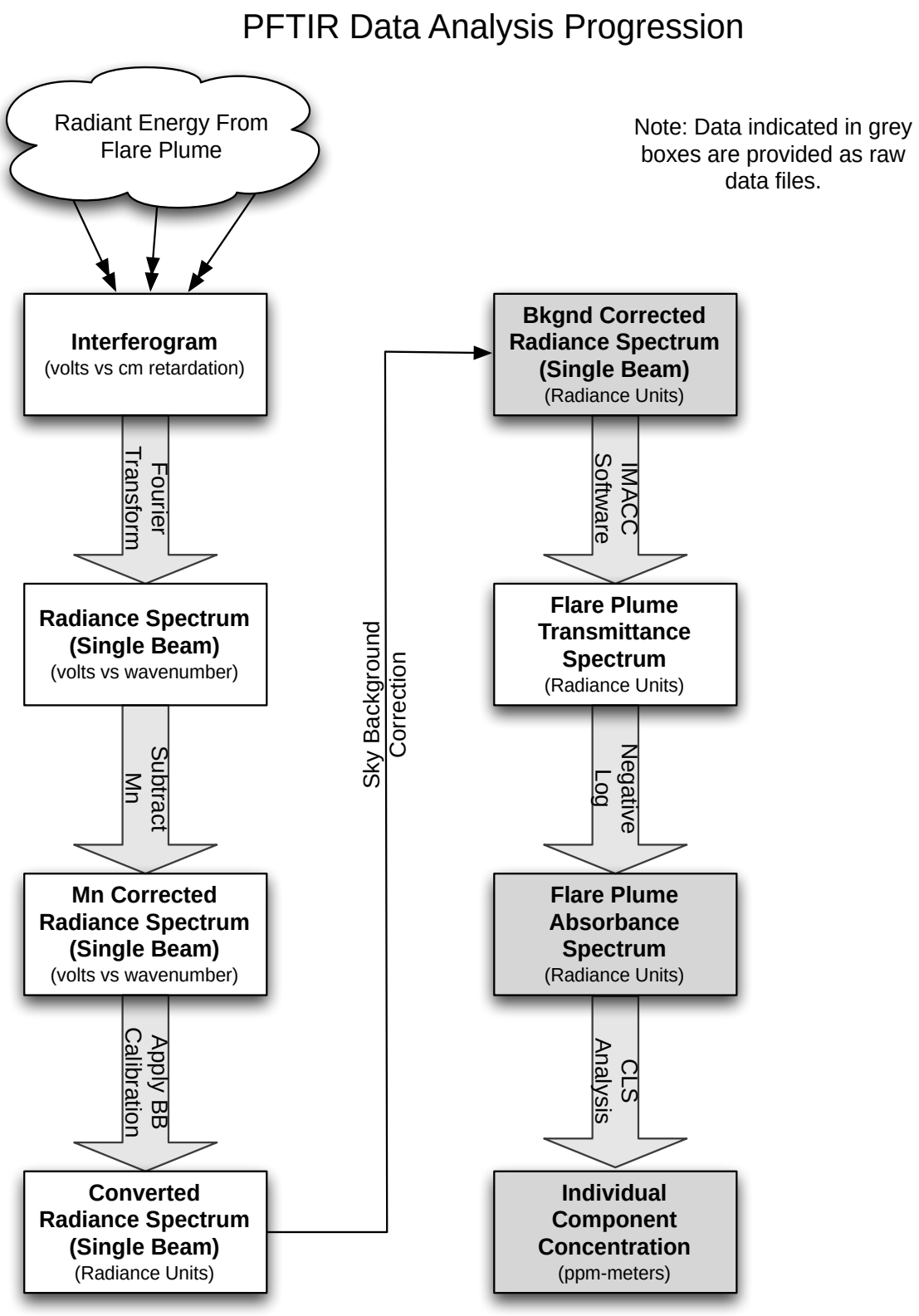

Figure 4.5-1: PFTIR Data Analysis Progression

The raw FTIR data (one minute averages) are reported from the analytical software with a 2-sigma (2σ) error calculated from the fit of the reference spectra to the sample spectra. Any individual component measurement that was less than 2 times this error (i.e., 4σ) was not used in calculating combustion efficiency.

This filtering eliminates non-detectable individual components from the combustion efficiency calculation. For very poor combustion efficiencies, the CO_2 region of the spectra is very weak and might not pass through the detection filter described above. Without a CO_2 reading, the combustion efficiency drops to zero. However, this does not mean that combustion is not occurring. It just means that the signal for CO_2 is too weak to detect. Evidence of combustion still appears with the detection of CO, a product of inefficient combustion, but this cannot be used to calculate combustion efficiency. Therefore, runs that do not have CO_2 readings but do have CO readings are marked as below the detection limit for CO_2. No combustion efficiency is listed for these runs, even though the flare is not snuffed.

5.0 Data Tables and Process Conditions

5.1 Data Summary Tables

Due to the large quantity of data collected for this project, three levels of data reduction are provided. Section 3 is the most concise summary providing run averages for a few key parameters at each test condition. This section provides more details on the individual test series, shows a large number of test parameters, and provides wind information. Appendices A.5 through A.7 contain raw run data collected during the test program and any additional calibration or support data.

Data Summary Table

The following data table includes summary data for each run. Column headings for this table are described below:

Condition: The designation for each test series and condition described in Section 2.6.1.
Run: The run number indicating the replicate
Run ID: The unique identifier assigned to each test run
Start Time: The date and time each run began.
End Time: The date and time each run ended.
Std Flare Gas Flow: The average vent gas flow in standard cubic feet per hour.
Flare Gas Flow: The average vent gas flow in pounds per hour.
Flare Tip Velocity: The average velocity at which the vent gas is exiting the tip in feet per second.
Flare Gas NHV: The average net heating value of the vent gas in BTU per standard cubic foot.
Steam Flow: The average steam flow to the flare tip in pounds per hour. This is the sum of the center steam flow, lower steam flow, and upper steam flow.
Hydrogen: The average mole percent hydrogen in the vent gas.
Nitrogen: The average mole percent nitrogen in the vent gas.
THC: The average mole percent of total hydrocarbons in the vent gas.
MWvg: The average molecular weight of the vent gas in pounds per pound-mole.
Wind Direction: The average wind direction during the run in degrees.
Wind Speed: The average wind speed during the run in miles per hour.
S/VG: The average steam to vent gas ratio during the run.
NHVcz: The average combustion zone gas net heating value in BTU per standard cubic foot.
LFLcz: The average combustion zone gas lower flammability limit in volume fraction.
Ccz: The average combustion zone gas combustibles fraction in volume fraction.
CE (weighted): The average weighted combustion efficiency for the run.

Test Conditions					Process Data					VG Composition Data				Weather		Calculations				
Condition	Run	Run ID	Start Time	End time	Std Flare Gas Flow	Flare Gas Flow	Flare Tip Velocity	Flare Gas NHV	Steam Flow	Hydrogen	Nitrogen	THC	MWvg	Wind Direction	Wind Speed	S/VG (calc)	NHVcz	LFLcz	Ccz	CE (weighted)
--	--	--	--	--	scf/hr	lb/hr	ft/s	BTU/scf	lb/hr	mol %	mol %	mol %	lb/lbmol	° (N=0, E=90)	mph	(lb/lb)	BTU/scf	vol. fraction	vol. fraction	%
DDU-1	1	1	7/10/2014 8:13:00	7/10/2014 8:33:00	136,210	6,901	2.49	749	15038	9.02	17.4	71.6	19.5	43	6.4	2.18	223	0.194	0.110	99.3
DDU-1	2	2	7/10/2014 8:37:00	7/10/2014 8:57:00	136,364	6,908	2.55	746	19489	9.74	17.8	70.5	19.5	35	8.8	2.82	184	0.234	0.093	99.6
DDU-2	1	3	7/10/2014 10:15:26	7/10/2014 10:31:00	136,962	6,949	2.82	686	19573	14.54	25.4	57.8	19.6	41	10.0	2.82	169	0.235	0.099	96.5
DDU-2	2	4	7/10/2014 10:54:00	7/10/2014 11:14:00	137,451	6,967	2.93	674	23701	14.83	25.7	56.9	19.5	43	9.4	3.40	144	0.271	0.085	96.1
DDU-3	1	5	7/10/2014 12:40:00	7/10/2014 13:01:00	144,156	7,182	3.22	694	30240	15.21	23.5	59.0	19.2	62	12.3	4.21	127	0.313	0.075	96.4
DDU-3	2	6	7/10/2014 13:04:00	7/10/2014 13:25:00	145,589	7,155	3.29	704	35134	15.65	22.4	59.6	18.9	62	12.3	4.91	114	0.351	0.068	95.6
DDU-4	1	7	7/10/2014 14:00:00	7/10/2014 14:22:00	149,195	7,346	3.38	704	38973	14.93	22.5	60.4	19.0	54	11.4	5.30	107	0.373	0.063	98.1
DDU-4	2	8	7/10/2014 14:25:00	7/10/2014 14:48:00	150,809	7,420	3.34	704	58310	16.03	22.7	58.9	19.0	58	12.3	7.85	76	0.523	0.046	96.1
DDU-5	1	9	7/10/2014 15:22:00	7/10/2014 15:42:00	154,320	7,775	3.24	677	35985	15.46	25.0	57.3	19.4	61	13.6	4.63	134	0.336	0.080	97.4
DDU-5	2	10	7/10/2014 15:47:00	7/10/2014 16:08:00	155,934	7,812	3.20	678	25722	15.34	25.0	57.5	19.3	59	12.1	3.29	160	0.253	0.096	97.1
DDU-6	1	11	7/10/2014 16:27:00	7/10/2014 16:38:00	158,116	7,702	3.14	715	22248	16.31	21.2	60.2	18.8	59	12.8	2.89	178	0.224	0.107	97.8
DDU-6	2	12	7/10/2014 17:00:00	7/10/2014 17:10:00	160,173	8,098	3.09	754	23325	9.85	17.2	71.2	19.5	51	11.4	2.88	183	0.229	0.092	98.1
ALKY-1	1	13	7/15/2014 12:15:00	7/15/2014 12:40:00	117,511	8,977	8.26	549	3728	0.30	72.7	26.5	29.5	292	12.2	0.42	327	0.143	0.146	99.7
ALKY-1	2	14	7/15/2014 12:43:00	7/15/2014 13:09:00	111,779	8,537	10.16	548	2809	0.30	72.7	26.5	29.4	64	304.7	0.33	357	0.134	0.160	99.0
ALKY-2	1	15	7/15/2014 13:35:00	7/15/2014 13:56:00	112,691	8,603	8.34	548	6973	0.30	72.7	26.5	29.4	305	12.9	0.81	236	0.201	0.106	97.5
ALKY-2	2	16	7/15/2014 13:59:00	7/15/2014 14:21:00	116,385	8,887	7.66	548	7606	0.30	72.7	26.5	29.4	301	12.1	0.86	232	0.203	0.104	98.0
ALKY-3	1	17	7/15/2014 15:10:00	7/15/2014 15:31:00	110,671	8,358	8.95	555	8281	0.31	72.3	26.8	29.1	275	11.3	0.99	213	0.224	0.095	93.7
ALKY-3	2	18	7/15/2014 15:38:00	7/15/2014 16:00:00	88,851	6,816	6.37	545	7852	0.30	72.8	26.3	29.6	67	286.6	1.15	189	0.256	0.084	96.3
ALKY-4	1	19	7/16/2014 10:22:00	7/16/2014 10:45:00	101,052	7,797	7.67	508	6971	0.40	74.1	25.0	29.7	308	10.0	0.89	207	0.242	0.093	95.4
ALKY-4	2	20	7/16/2014 10:50:00	7/16/2014 11:11:00	116,922	9,068	9.05	507	7053	0.41	74.2	24.9	29.9	126	9.8	0.78	222	0.228	0.100	94.2
ALKY-5	1	21	7/16/2014 11:30:00	7/16/2014 11:52:00	120,520	9,376	8.68	519	7935	0.29	73.9	25.4	30.0	41	8.7	0.85	216	0.237	0.096	96.6

Table 5.1-1: Data Summary for All Test Runs

5.2 Long Term Stability Test Data

5.2.1 DDU Test Process and Wind Conditions

The purpose of the DDU Test Series was to determine the performance curve of the DDU flare tip under base load conditions.

Process Conditions

Figure 5.2.1-1 to 5.2.1-3 shows vent gas composition and process conditions for the DDU Test Series. Figures 5.2.1-4 through 5.2.1-15 show wind speed and wind direction for the DDU Test Runs.

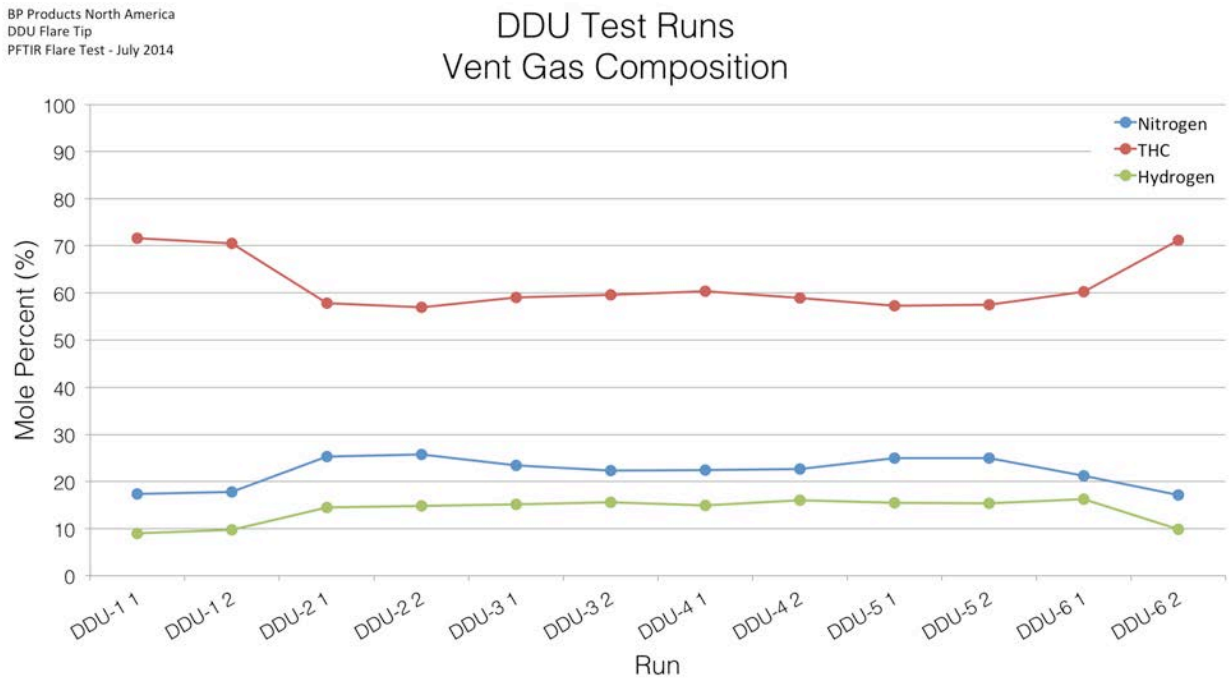

Figure 5.2.1-1: DDU Test Series Vent Gas Composition

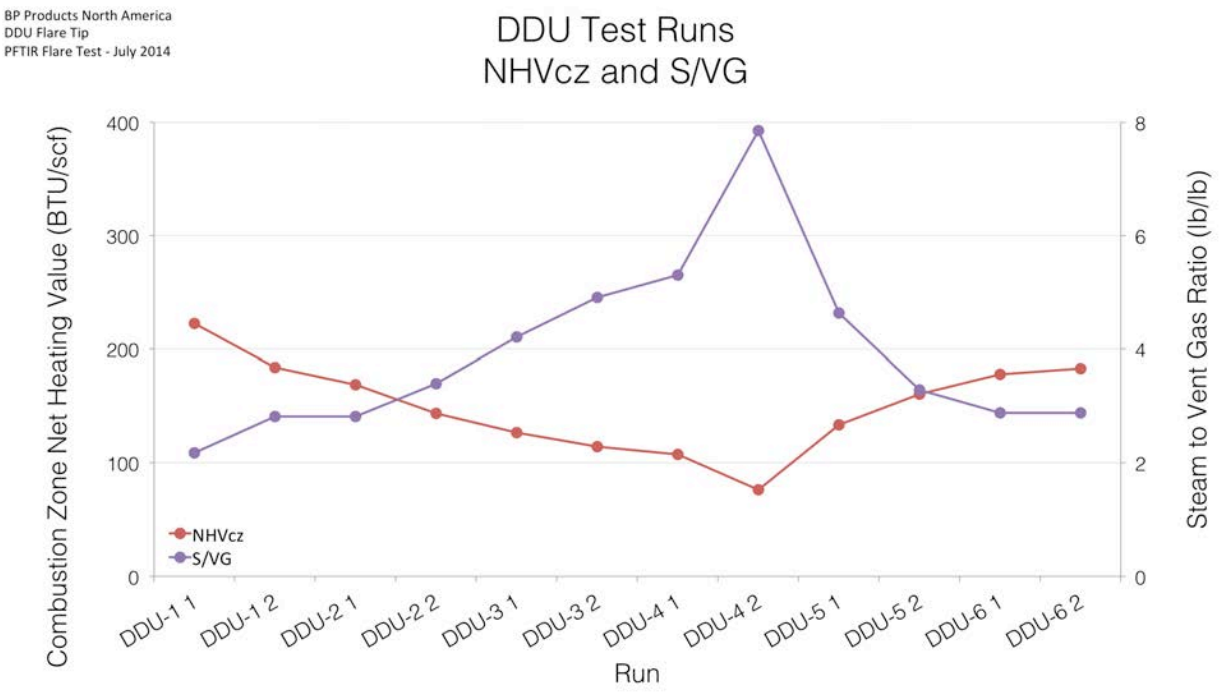

Figure 5.2.1-2: DDU Test Series NHVcz and S/VG (Mass Basis)

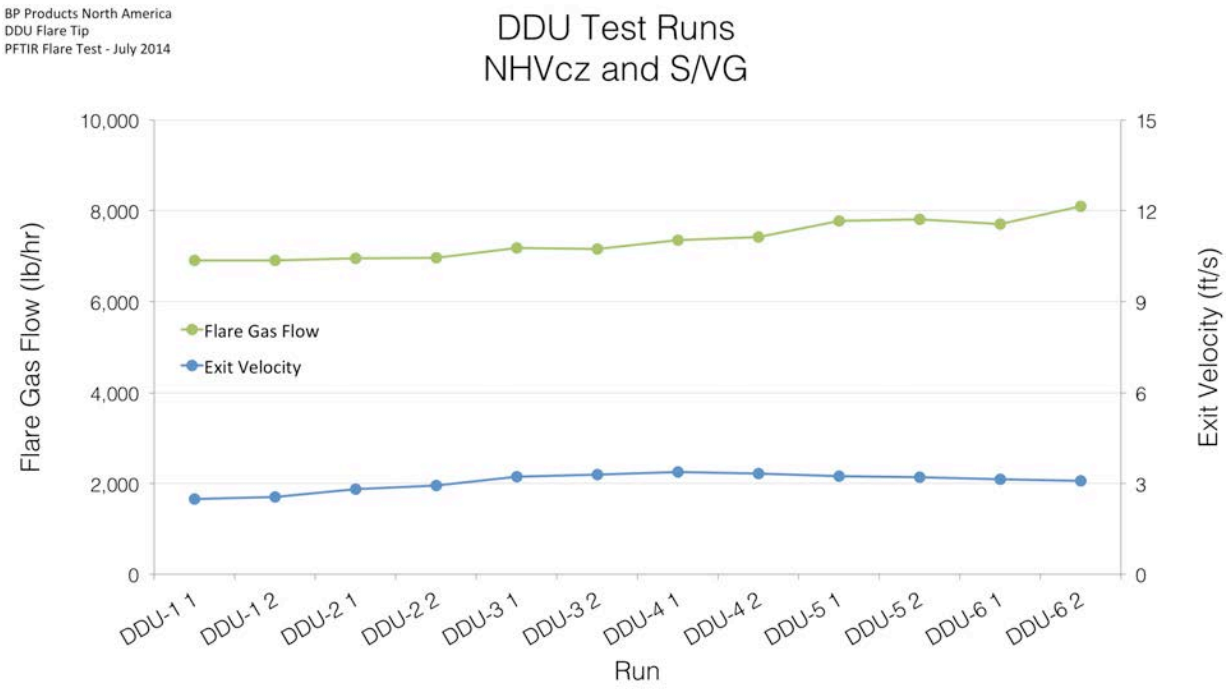

Figure 5.2.1-3: DDU Test Series Vent Gas Flow Rate & Exit Velocity

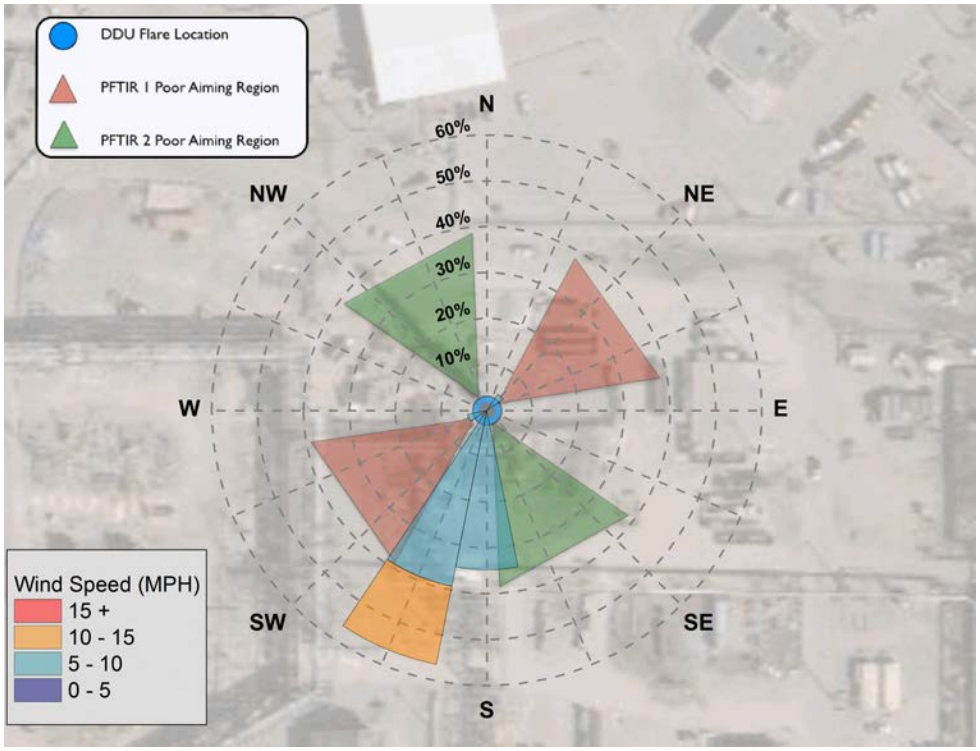

Figure 5.2.1-4: Test Run DDU-1 1 Windrose

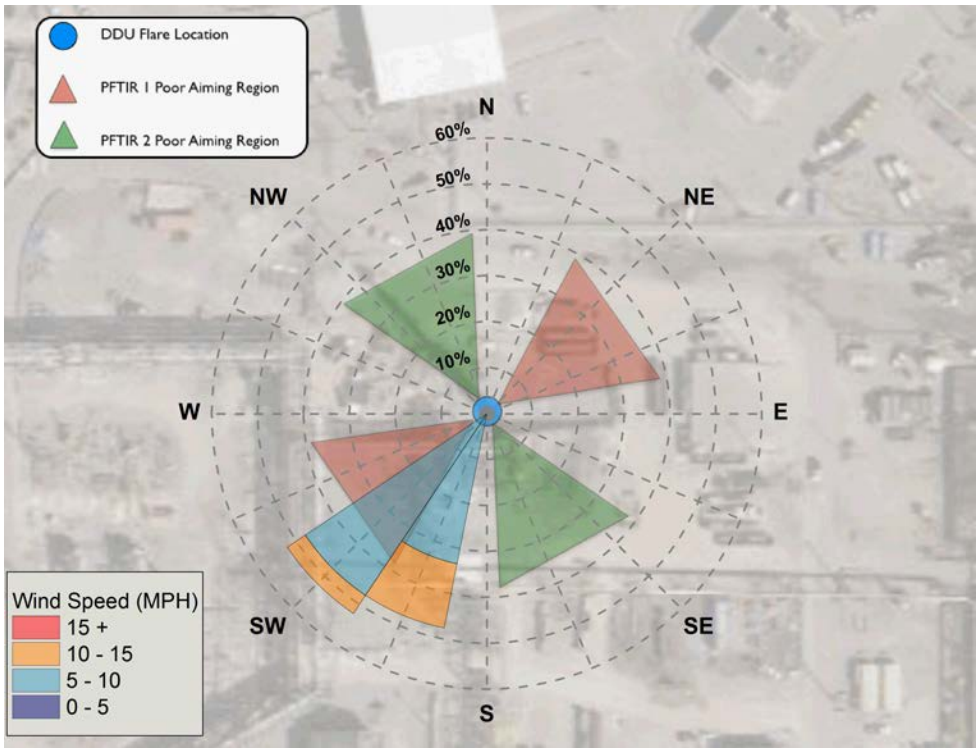

Figure 5.2.1-5: Test Run DDU-1 2 Windrose

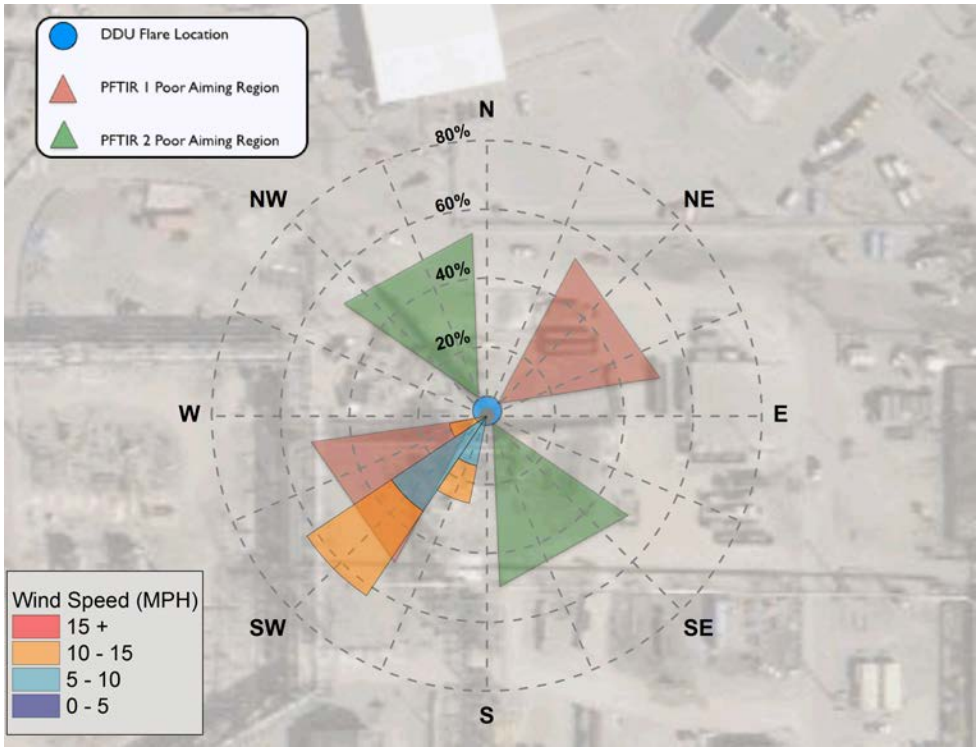

Figure 5.2.1-6: Test Run DDU-2 1 Windrose

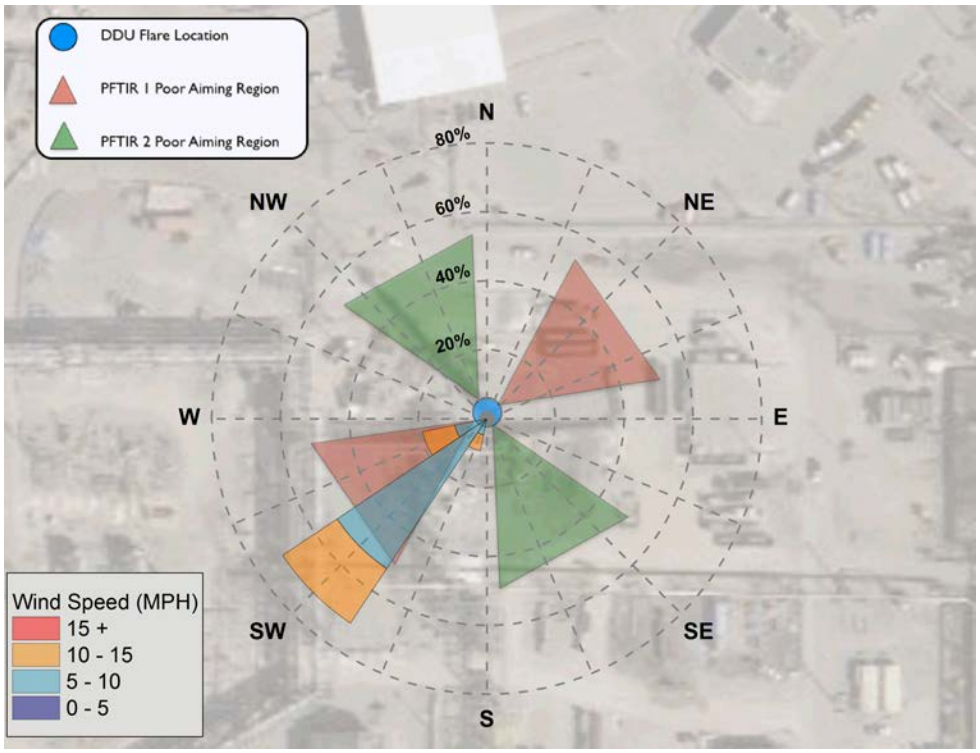

Figure 5.2.1-7: Test Run DDU-2 2 Windrose

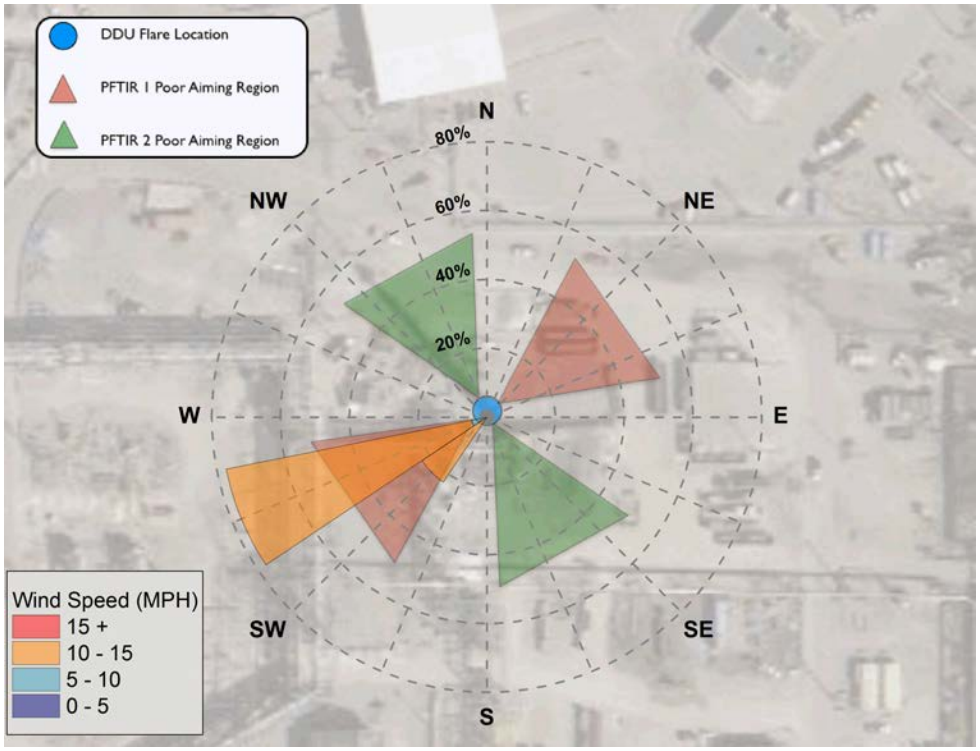

Figure 5.2.1-8: Test Run DDU-3 1 Windrose

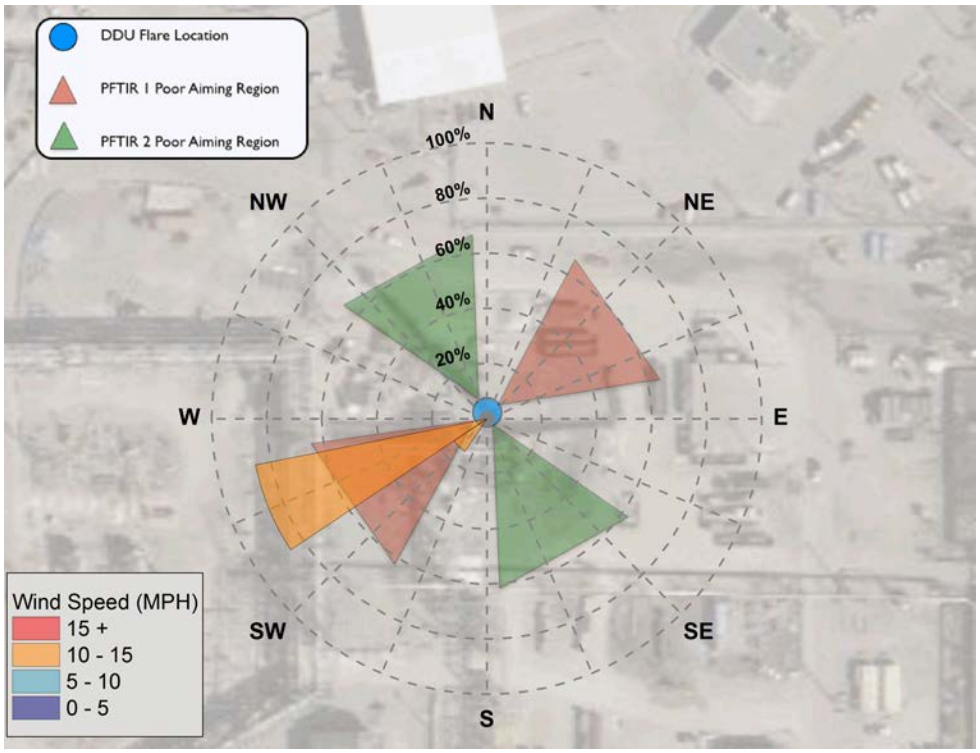

Figure 5.2.1-9: Test Run DDU-3 2 Windrose

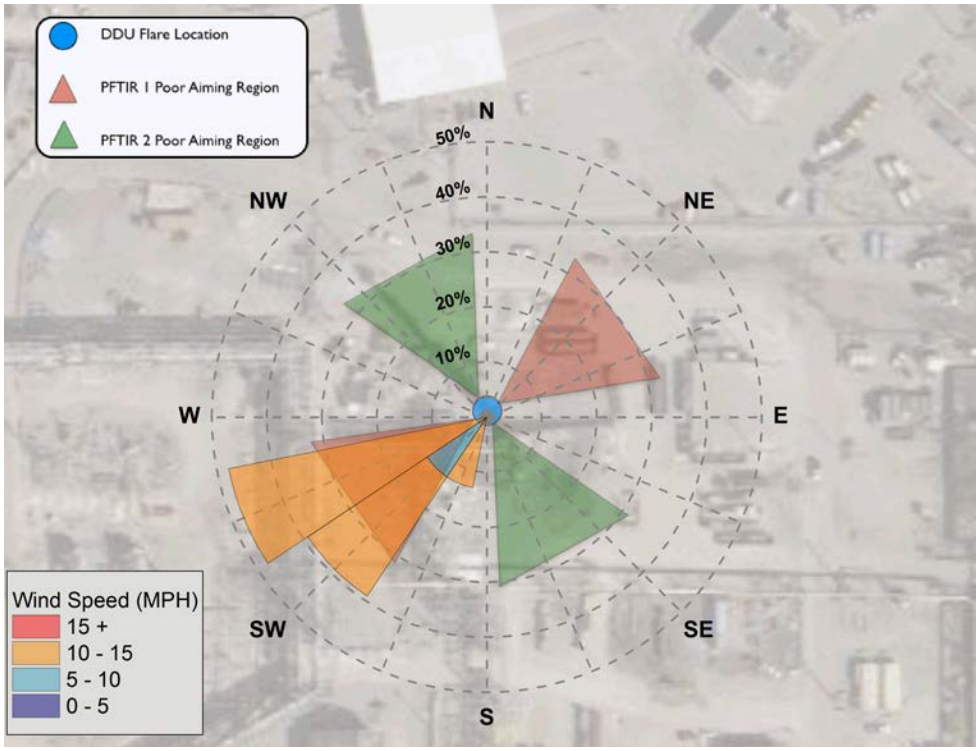

Figure 5.2.1-10: Test Run DDU-4 1 Windrose

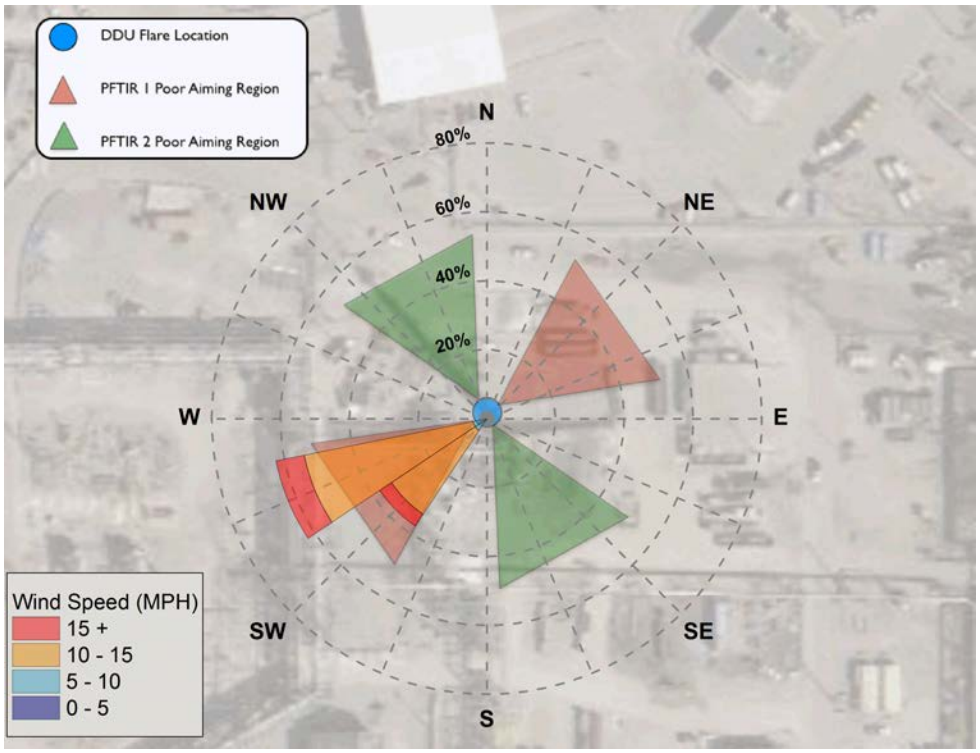

Figure 5.2.1-11: Test Run DDU-4 2 Windrose

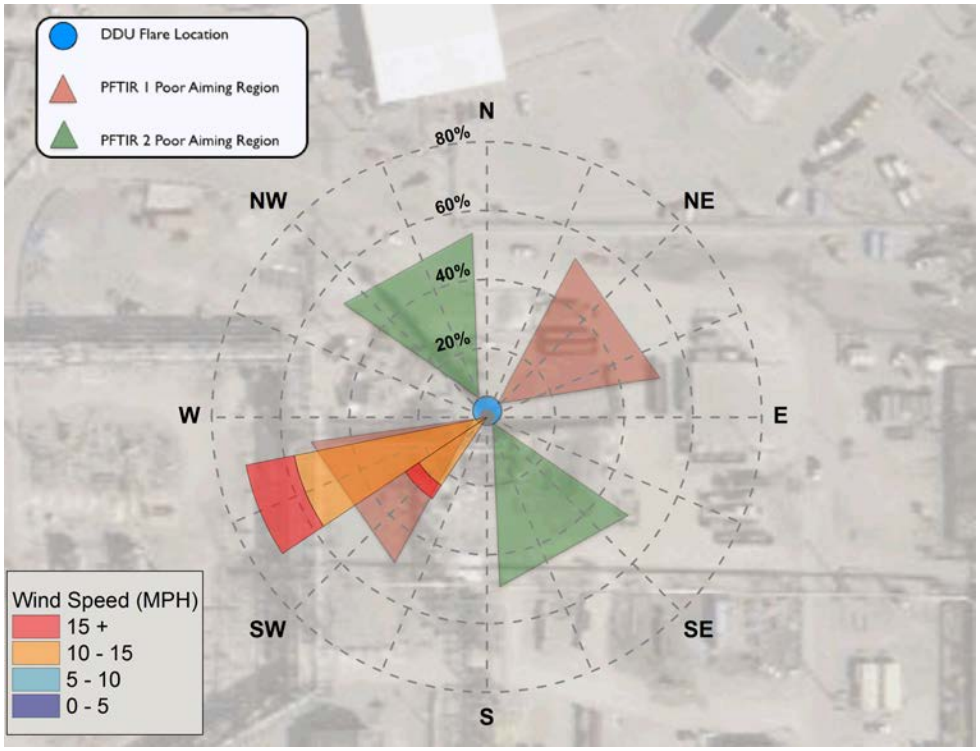

Figure 5.2.1-12: Test Run DDU-5 1 Windrose

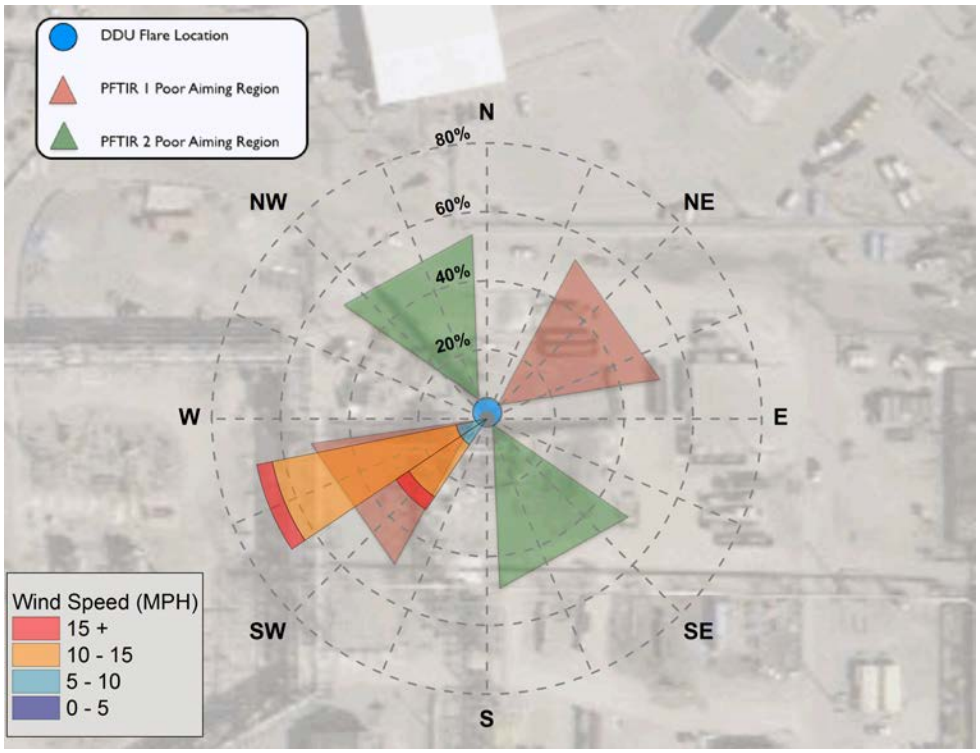

Figure 5.2.1-13: Test Run DDU-5 2 Windrose

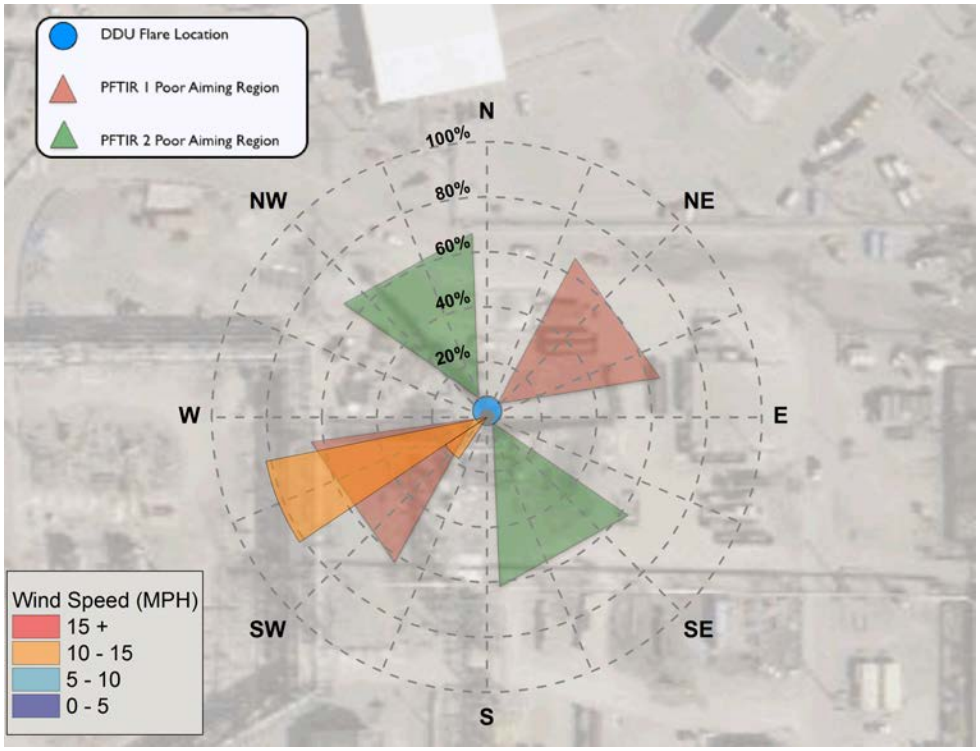

Figure 5.2.1-14: Test Run DDU-6 1 Windrose

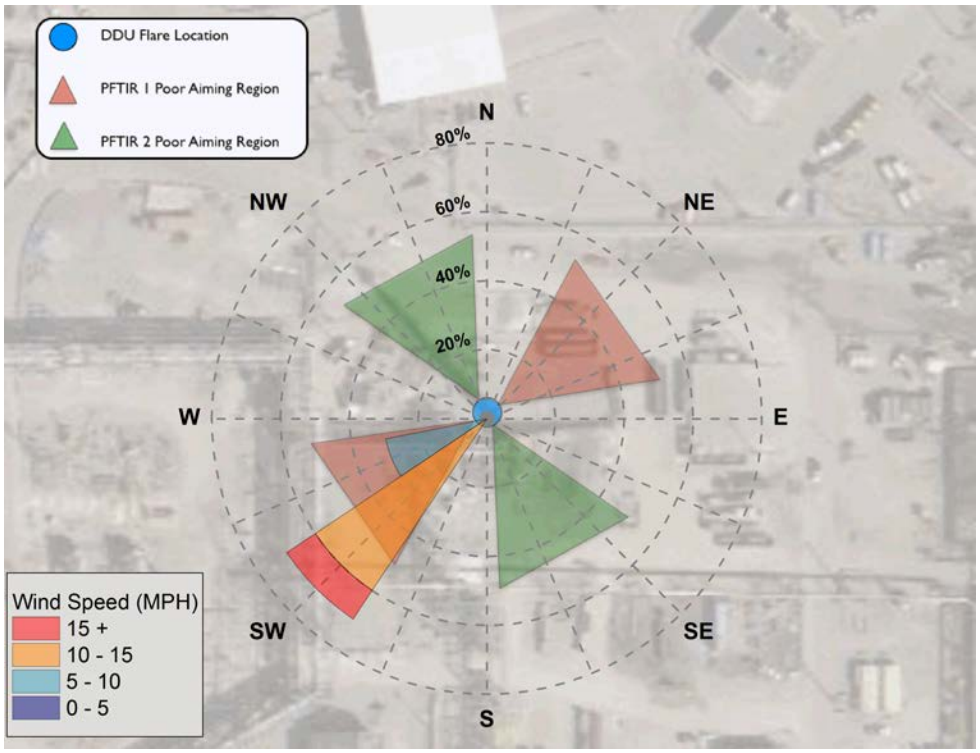

Figure 5.2.1-15: Test Run DDU-6 2 Windrose

Run Table

Table 5.2.1-1 details whether a run was considered valid, which PFTIR was used for each run, the run length, and any important notes.

Run	Validity	PFTIR Used	Run Length	Notes
DDU-1 1	Valid	PFTIR 2	20 minutes	Only PFTIR 2 operated.
DDU-1 2	Valid	PFTIR 2	20 minutes	Only PFTIR 2 operated.
DDU-2 1	Valid	PFTIR 2	27 minutes	Only PFTIR 2 operated. Software issue between 10:27 – 10:34. Poor Aiming at 12:41 and 12:43.
DDU-2 2	Valid	PFTIR 2	20 minutes	Only PFTIR 2 operated.
DDU-3 1	Valid	PFTIR 2	21 minutes	Only PFTIR 2 operated.
DDU-3 2	Valid	PFTIR 2	21 minutes	Only PFTIR 2 operated.
DDU-4 1	Valid	PFTIR 2	22 minutes	Only PFTIR 2 operated.
DDU-4 2	Valid	PFTIR 2	23 minutes	Only PFTIR 2 operated.
DDU-5 1	Valid	PFTIR 2	20 minutes	Only PFTIR 2 operated.
DDU-5 2	Valid	PFTIR 2	21 minutes	Only PFTIR 2 operated.
DDU-6 1	Valid	PFTIR 2	11 minutes	Only PFTIR 2 operated.
DDU-6 2	Valid	PFTIR 2	10 minutes	Only PFTIR 2 operated.

Table 5.2.1-1: Run Details for DDU Test Runs

5.2.2 ALKY Test Process and Wind Conditions

The purpose of the ALKY Test Series was to determine the performance curve of the ALKY flare tip under base load conditions.

Process Conditions

Figure 5.2.2-1 to 5.2.2-3 shows vent gas composition and process conditions for the ALKY Test Series. Figures 5.2.2-4 through 5.2.2-12 show wind speed and wind direction for the ALKY Test Runs.

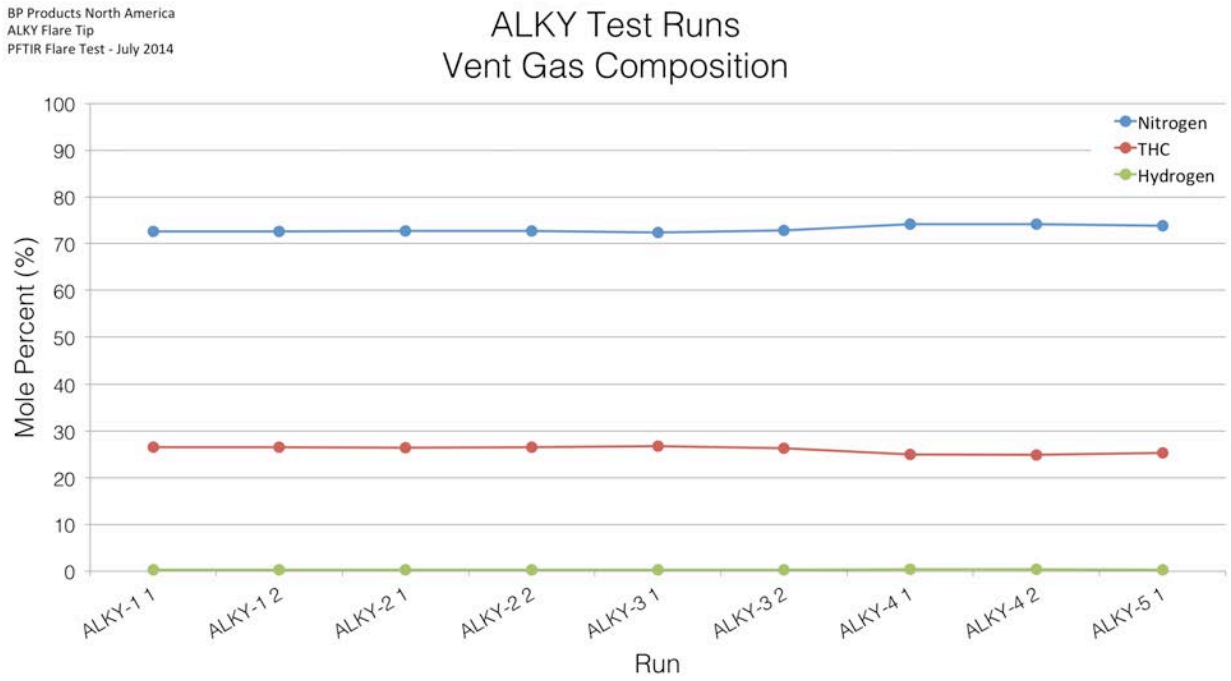

Figure 5.2.2-1: ALKY Test Series Vent Gas Composition

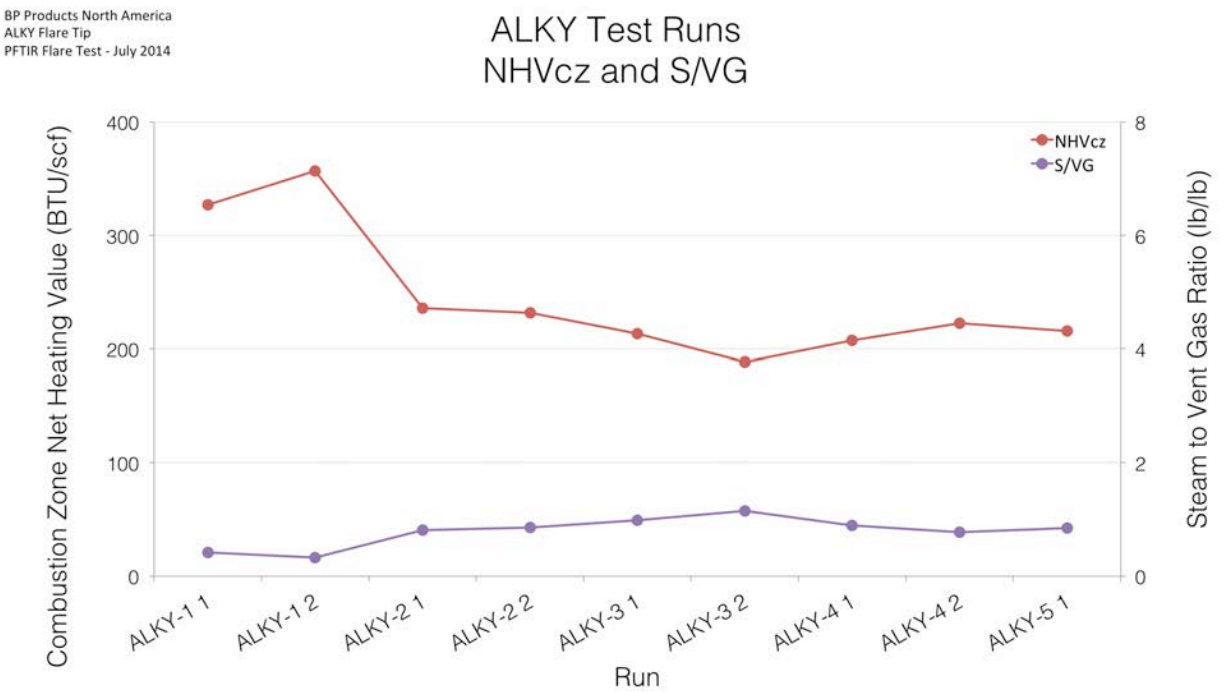

Figure 5.2.2-2: ALKY Test Series NHVcz and S/VG (Mass Basis)

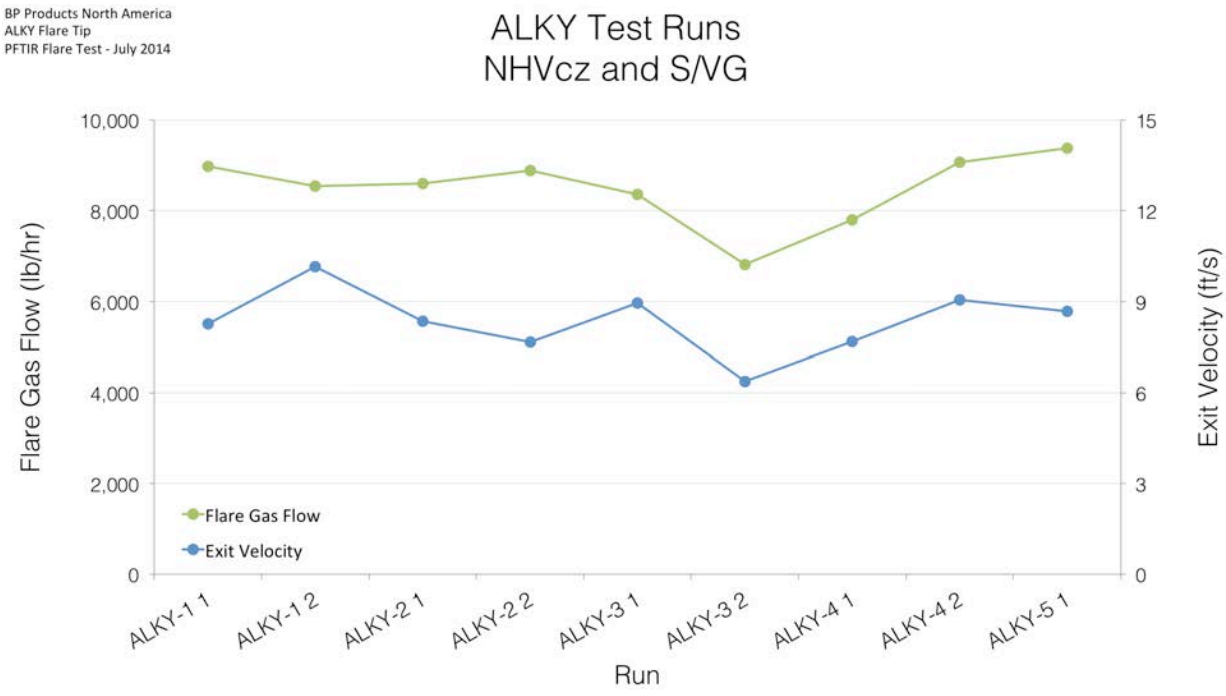

Figure 5.2.2-3: ALKY Test Series Vent Gas Flow Rate & Exit Velocity

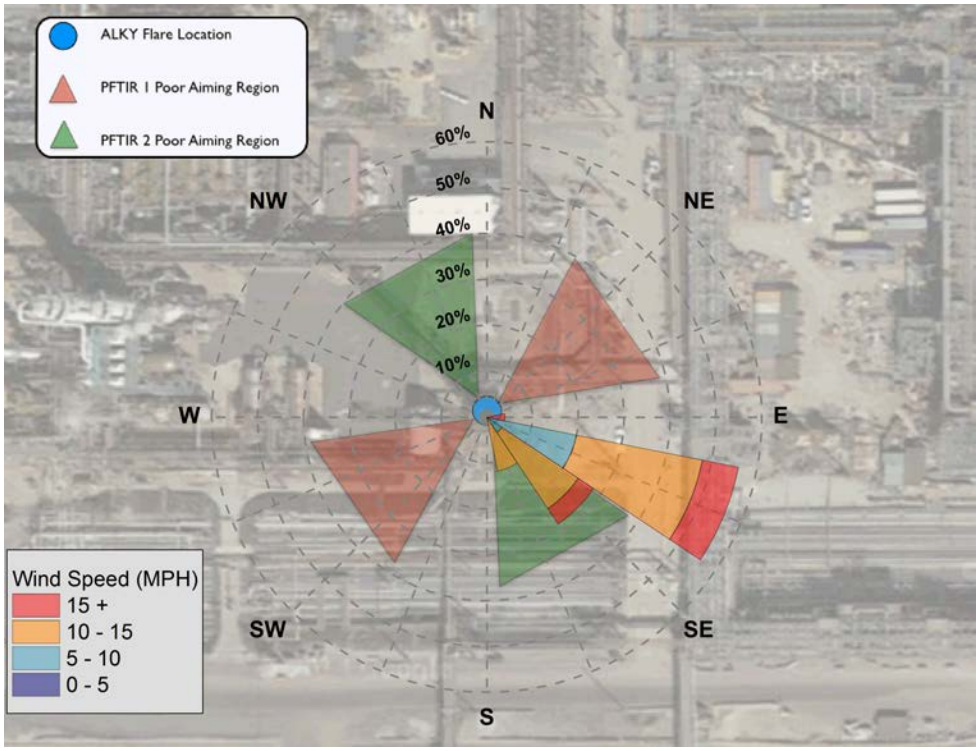

Figure 5.2.2-4: Test Run ALKY-1 1 Windrose

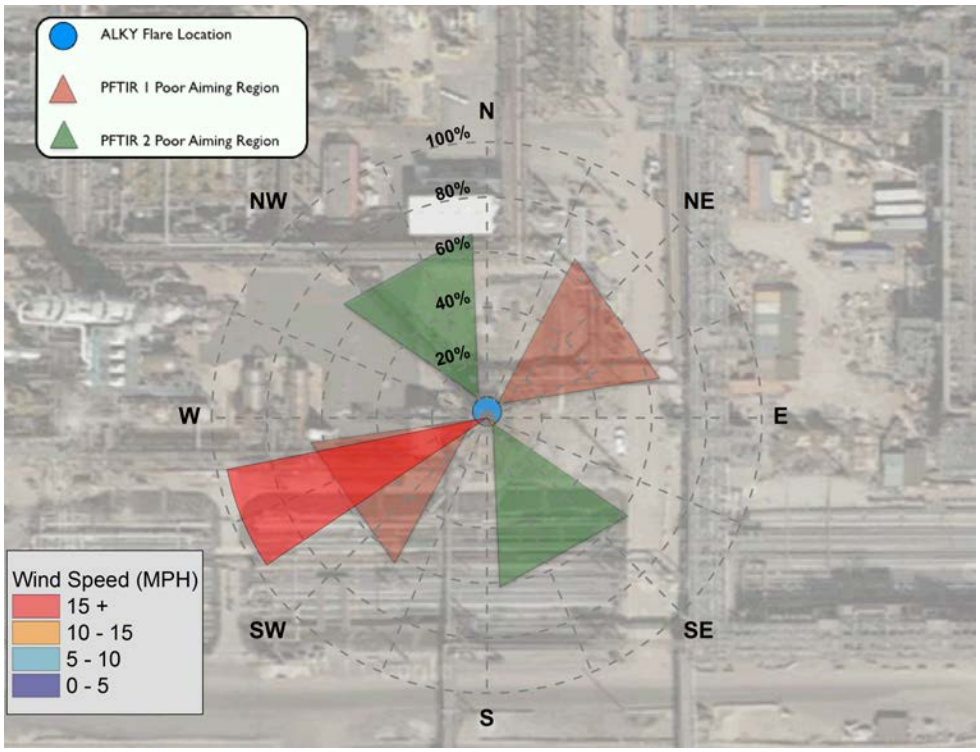

Figure 5.2.2-5: Test Run ALKY-1 2 Windrose

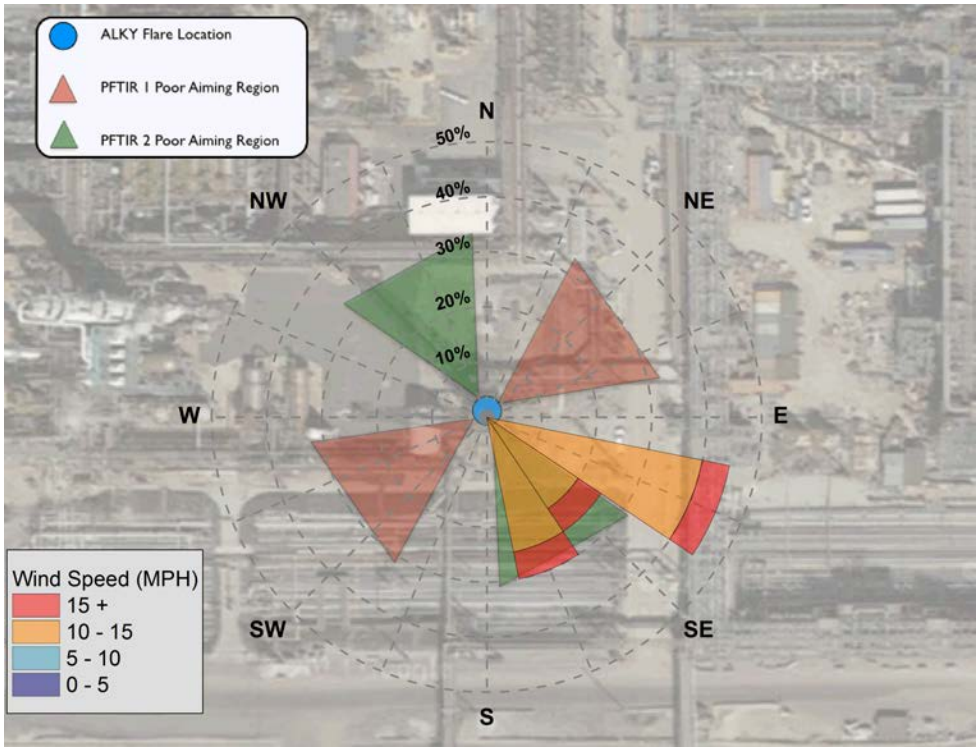

Figure 5.2.2-6: Test Run ALKY-2 1 Windrose

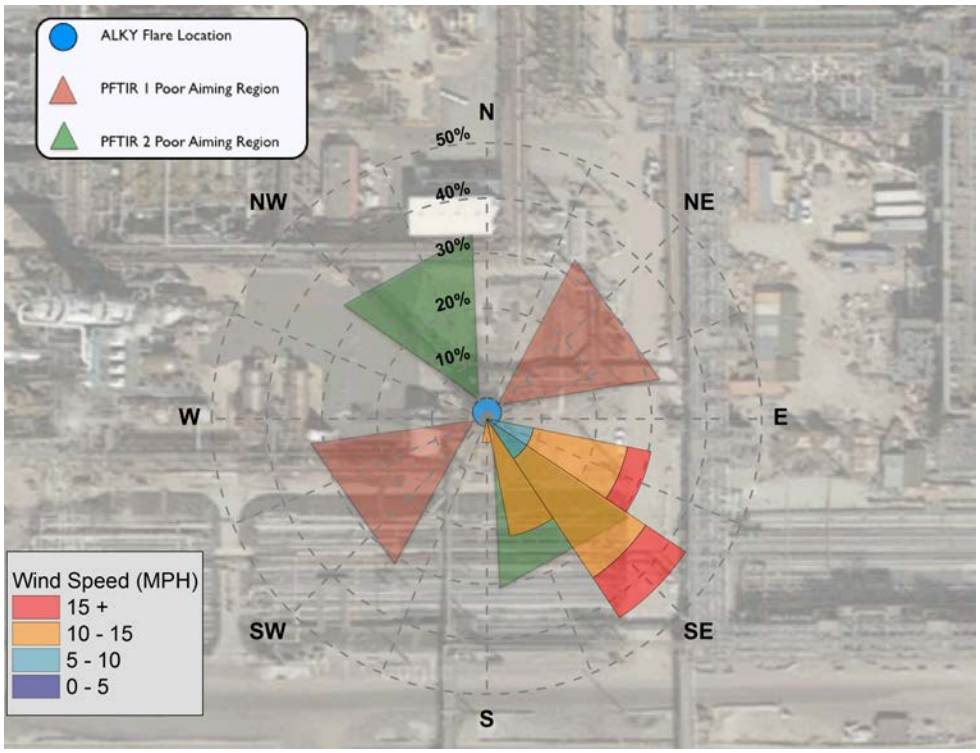

Figure 5.2.2-7: Test Run ALKY-2 2 Windrose

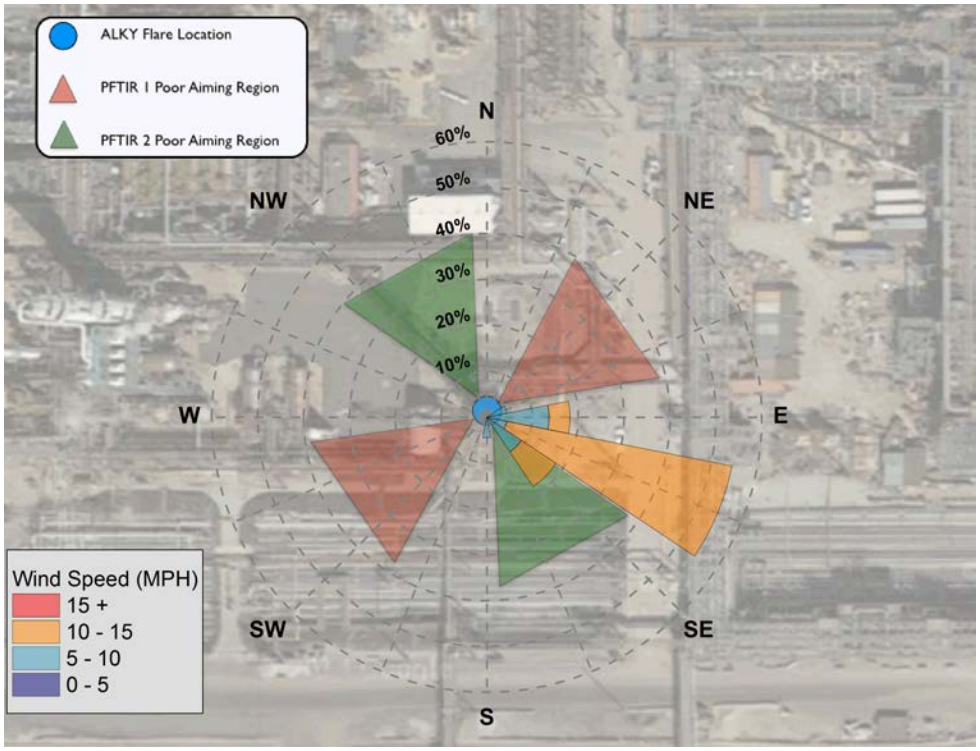

Figure 5.2.2-8: Test Run ALKY-3 1 Windrose

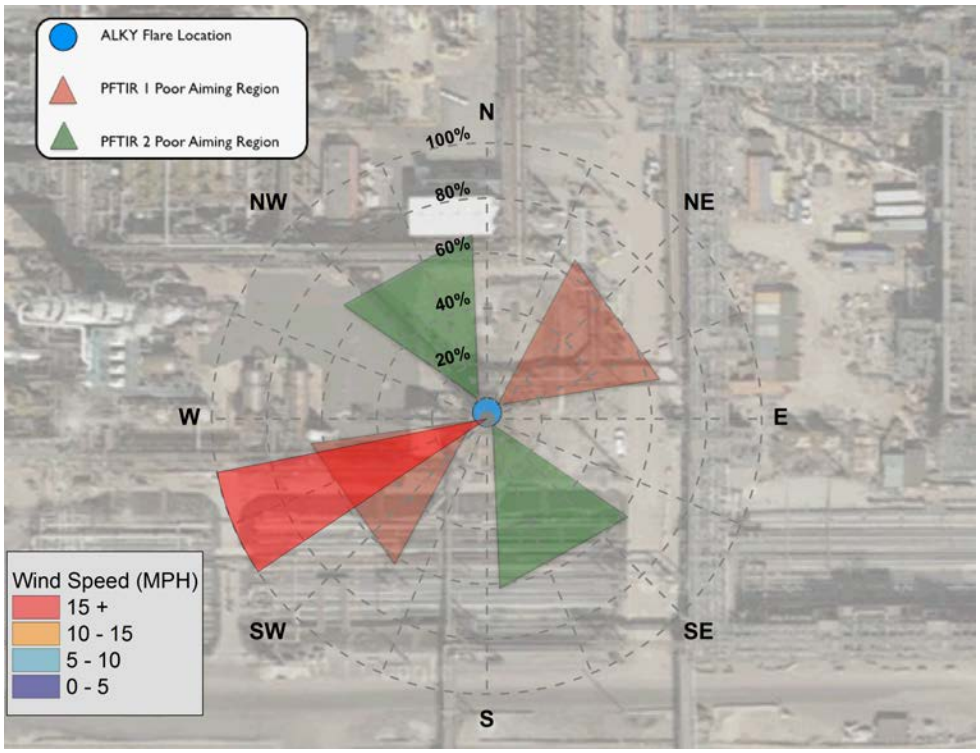

Figure 5.2.2-9: Test Run ALKY-3 2 Windrose

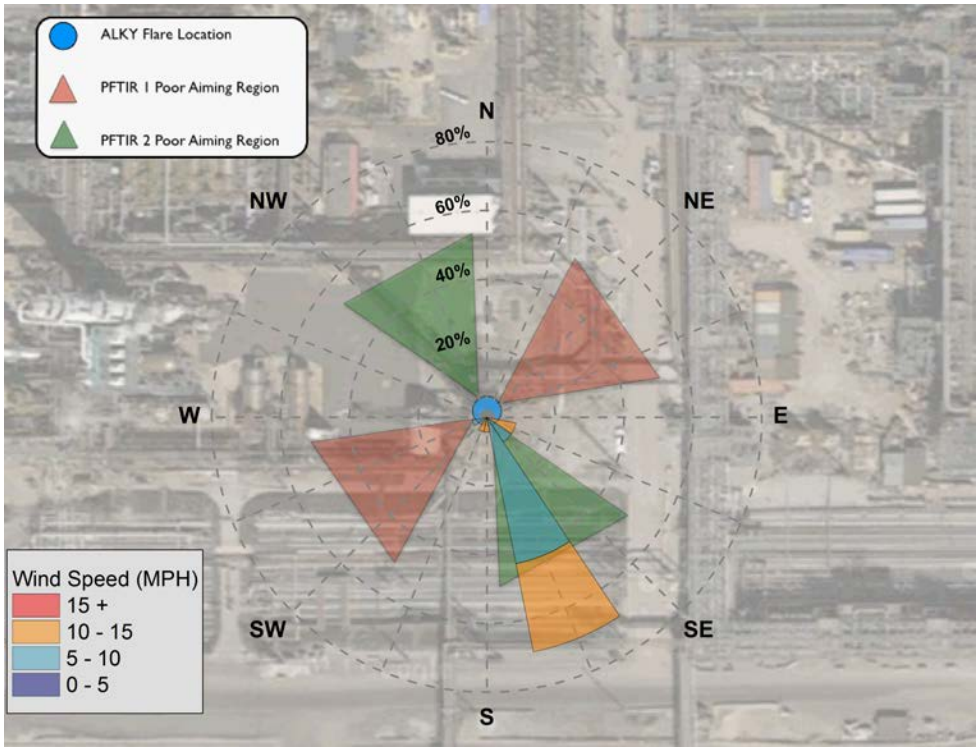

Figure 5.2.2-10: Test Run ALKY-4 1 Windrose

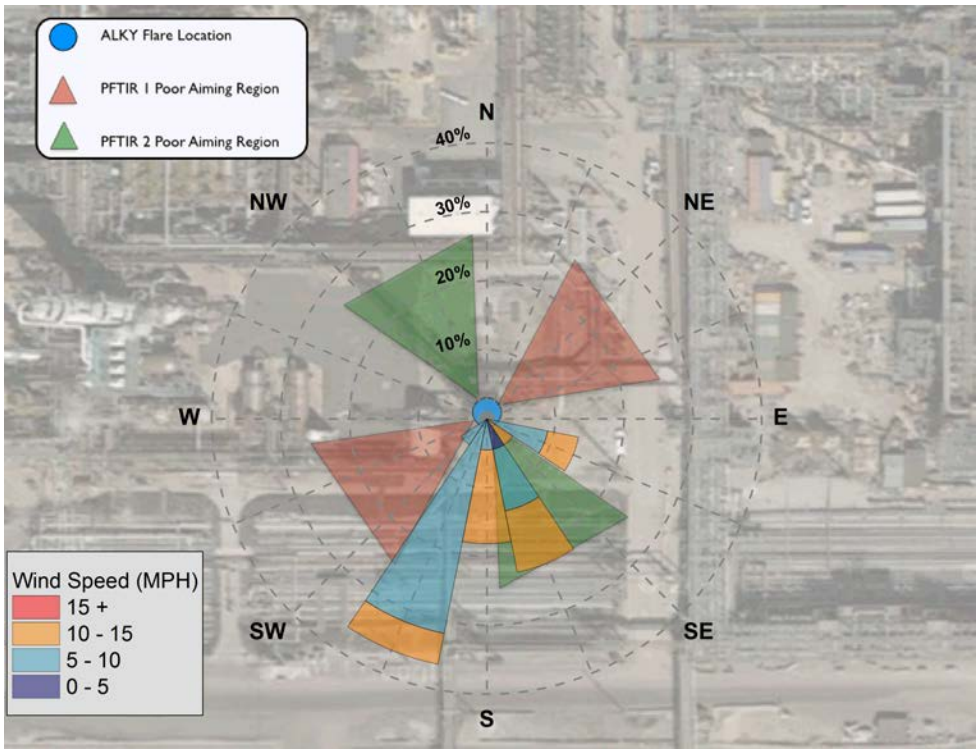

Figure 5.2.2-11: Test Run ALKY-4 2 Windrose

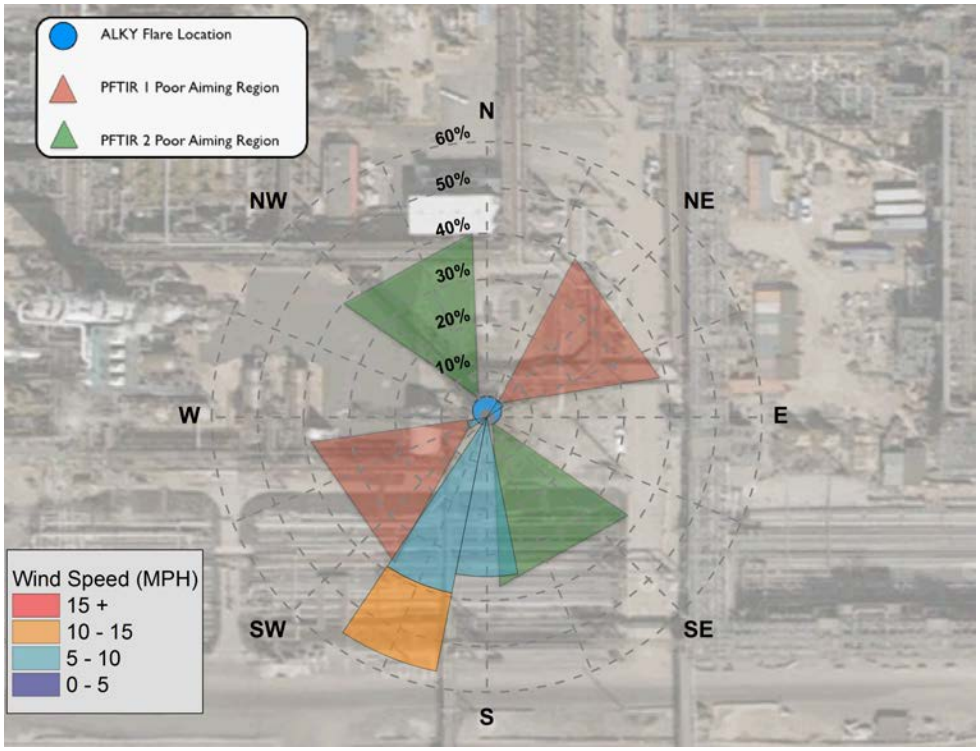

Figure 5.2.2-12: Test Run ALKY-5 1 Windrose

Run Table

Table 5.2.2-1 details whether a run was considered valid, which PFTIR was used for each run, the run length, and any important notes.

Run	Validity	PFTIR Used	Run Length	Notes
AKLY-1 1	Valid	PFTIR 2	25 minutes	Poor wind conditions at 12:16, 12:18-12:22, 12:26-12:27, and 12:29. Poor aiming at 12:15.
ALKY-1 2	Valid	PFTIR 2	26 minutes	Poor wind conditions at 12:43. Poor aiming at 12:48 and 13:03.
ALKY-2 1	Valid	PFTIR 2	21 minutes	Poor wind conditions at 13:38-13:39, 13:41,13:50, and 13:53-13:54.
ALKY-2 2	Valid	PFTIR 2	22 minutes	Poor wind conditions at 14:00-14:02, 14:04-14:05, 14:08-14:11, and 14:16-14:19.
ALKY-3 1	Valid	PFTIR 2	21 minutes	Poor wind conditions at 15:23, and 15:30-15:31. Poor aiming at 15:12
ALKY-3 2	Valid	PFTIR 2	22 minutes	
ALKY-4 1	Valid	PFTIR 2	23 minutes	Wind rose shows poor wind conditions even though PFTIR 2 had a good vantage point during the run.
ALKY-4 2	Valid	PFTIR 2	21 minutes	Poor wind conditions at 10:51, 10:54, 10:58, and 11:07-11:08.
ALKY-5 1	Valid	PFTIR 2	22 minutes	

Table 5.2.2-1: Run Details for ALKY Test Runs

A.0 Appendices

A.1 Calculations

The following calculations are used this report. In addition to the calculations listed below, many of the calculations used in reducing the PFTIR data are provided in Appendix A.2.

The Gas Chromatograph (GC) measured the following hydrocarbons.

i	Measured Component	MW (lb/lb-mol)	NHV (BTU/scf)	LFL (Vol. %)	C_y	H_z
1	Hydrogen	2.02	1212	0.040	0	2
2	Oxygen	32.00	0	∞	n/a	n/a
3	Nitrogen	28.01	0	∞	n/a	n/a
4	CO_2	44.01	0	∞	n/a	n/a
5	CO	28.01	316	0.125	n/a	n/a
6	Methane	16.04	896	0.050	1	4
7	Ethane	30.07	1595	0.030	2	6
8	Ethylene	28.05	1477	0.027	2	4
9	Acetylene	26.04	1404	0.025	2	2
10	Propane	44.10	2281	0.021	3	8
11	Propylene	42.08	2150	0.024	3	6
12	iso-Butane	58.12	2957	0.018	4	10
13	n-Butane	58.12	2968	0.018	4	10
14	Butenes (Combined)	56.11	2830	0.017	4	8
15	Hydrogen Sulfide	34.08	578	0.040	0	2
18	Pentane+ (C_5+)	72.15	3655	0.014	5	12
20	Water	18.02	0	∞	n/a	n/a

Table A.1-1. List of Compounds Measured by Gas Chromatograph (Range: 0-100 Mole %)

A.1.1 Vent Gas Molecular Weight

The vent gas molecular weight is calculated as:

$$MW_{vg} = \sum_{i=1}^{20} mol_i * MW_i \qquad \text{Equation A.1-1}$$

Where:

MW_{vg} = molecular weight of the vent gas (lb/lb-mol)
MW_i = molecular weight of each compound *i* from Table A.1-1 (lb/lb-mol)
mol_i = mole percent of each compound *i* from Table A.1-1 (%)

A.1.2 Net Heating Value of Combustion Zone

The Net Heating Value of the Vent Gas (NHVvg) is calculated and reported from the GC at the conclusion of each analytical cycle. The Net Heating Value is the Lower Heating Value or LHV defined as:

> *"Lower Heating Value" or "LHV" shall mean the theoretical total quantity of heat liberated by the complete combustion of a unit volume or weight of a fuel initially at 25° Centigrade and 760 mmHg, assuming that the produced water is vaporized and all combustion products remain at, or are returned to, 25° Centigrade; however, the standard for determining the volume corresponding to one mole is 20° Centigrade.*

The Combustion Zone Gas Net Heating Value is the flow-weighted average NHV of all combustion zone components. The contribution of pilot gas to the NHVcz is not considered significant.

$$NHV_{cz} = \frac{(Q_{vg} \cdot NHV_{vg})}{(Q_{vg}) + (Q_s) + (Q_{Air})} \qquad \text{Equation A.1-2}$$

Where:

NHV_{cz}	=	combustion zone gas net heating value " ("BTU"⁄scf)
Q_{vg}	=	volumetric vent gas flow rate (scf/hr)
NHV_{vg}	=	net heating value of vent gas (Btu/scf)
Q_s	=	volumetric steam flow rate (scf/hr)
Q_{Air}	=	volumetric air flow rate (scf/hr)

The calculation of each component is shown below.

Volumetric flow rates

Gas and steam flow data was provided in units of mass flow (lb/hr). This was converted to volumetric flow (scf/hr) by the following equation.

$$Q = \dot{m} \cdot \frac{385.5}{MW} \qquad \text{Equation A.1-3}$$

Where:

Q	=	volumetric flow rate for steam or vent gas (scf/hr)
$\dot{m}$	=	mass flow rate for steam or vent gas (lb/hr)
MW	=	molecular weight of steam or vent gas (lb/lb-mol)
385.5	=	molar volume of an ideal gas at 68 °F and 1 atm (scf/lb-mol)

Net heating value of the vent gas

$$NHV_{vg} = \sum_{i=1}^{20} x_i * NHV_i \qquad \text{Equation A.1-4}$$

Where:

NHV_{vg}	=	net heating value of vent gas (BTU/scf)
i	=	individual pure component in vent gas
x_i	=	concentration of individual pure component in vent gas (volume fraction)
NHV_i	=	net heating value of pure individual component *i* (Btu/scf)

A.1.3 Steam to Vent Gas Ratio (S/VG)

The Steam to Vent Gas Ratio is calculated (as the name implies) as follows:

$$\text{S/VG} = \frac{\dot{m}_{steam}}{\dot{m}_{vg}} \qquad \text{Equation A.1-5}$$

Where:

S/VG	=	steam to vent gas ratio (lb/lb)
$\dot{m}_{steam}$	=	steam mass flow rate (lb/hr)
$\dot{m}_{vg}$	=	vent gas mass flow rate (lb/hr)

Note: S/VG may also be calculated on a volumetric basis using steam and vent gas volumetric flow rates.

A.1.4 Total Hydrocarbons from PFTIR

The total hydrocarbon values reported by the PFTIR measurements are adjusted by carbon weighting as follows:

$$THC_w = C_{CH_4} + 2 \cdot C_{C_2H_4} + 3 \cdot C_{C_3H_6} + 4 \cdot \left(C_{But} + C_{1,3But}\right) + 5 \cdot C_{HC} \qquad \text{Equation A.1-6}$$

Where:

THC_w	=	weighted total hydrocarbons from PFTIR (ppm•m)
C_{CH4}	=	methane from PFTIR (ppm•m)
C_{C2H4}	=	ethylene from PFTIR (ppm•m)
C_{C3H6}	=	propylene from PFTIR (ppm•m)
C_{But}	=	butane from PFTIR (ppm•m)
$C_{1,3But}$	=	1,3 butadiene from PFTIR (ppm•m)
C_{HC}	=	pentane and larger hydrocarbons from PFTIR (ppm•m)
2,3,4,5	=	number of carbon atoms in each molecule"

A.1.5 Flare Combustion Efficiency

Combustion Efficiency means the efficiency of converting organic compounds to carbon dioxide as measured in the flare plume. Flare combustion efficiency is calculated as follows:

$$CE = \frac{CO_2}{CO_2 + CO + THC_w}$$ Equation A.1-7

Where:

CE	=	flare combustion efficiency (%)
CO_2	=	carbon dioxide from PFTIR (ppm•m)
CO	=	carbon monoxide from PFTIR (ppm•m)
THC_w	=	weighted total hydrocarbons from PFTIR (ppm•m)

A.1.6 Combustion Efficiency Multiplier

The Combustion Efficiency Multiplier is calculated as follows

$$A = \frac{NHV_{cz}^{*}}{NHV_{vg} * LFL_{vg}}$$ Equation A.3-8

Where

A	=	combustion efficiency multiplier
NHV_{vg}	=	net heating value of the vent gas
LFL_{vg}	=	lower flammability limit of the vent gas
NHV_{cz}^{*}	=	target net heating value of the combustion zone

For this calculation, NHV_{vg} and LFL_{vg} are determined from the vent gas composition. $NHVcz^{*}$ is the NHVcz where combustion efficiency dropped off during the test series.

A.2 PFTIR Theory and Operation

A.2.1 PFTIR Analytical Method and Procedure

Gases have highly variable absorption with wavelength. It is this variation that produces the absorption patterns that allow for their identification in the infrared. If the transmission of a gas is given by $\tau(\nu, T)$ then $[1 - \tau(\nu, T)]$ is the amount of absorption. The radiation the gas emits at temperature T is then given by:

$$N(\nu, T) = [1 - \tau(\nu, T)] \cdot N_{bb}(\nu, T) \qquad \text{Equation A.5-1}$$

For flare measurements, it is this signal that is being detected from the hot gases above the combustion zone.

As shown in Figure A.5.1-1, the total radiance measured by the PFTIR consists of:

1. The background radiance altered by its transmission through the flare plume and through the atmosphere between the plume and the PFTIR instrument.

2. The flare radiance altered by its transmission through the atmosphere between the plume and the PFTIR instrument.

3. The atmospheric radiance of the air between the flare plume and the PFTIR instrument.

4. The radiance from the PFTIR instrument itself.

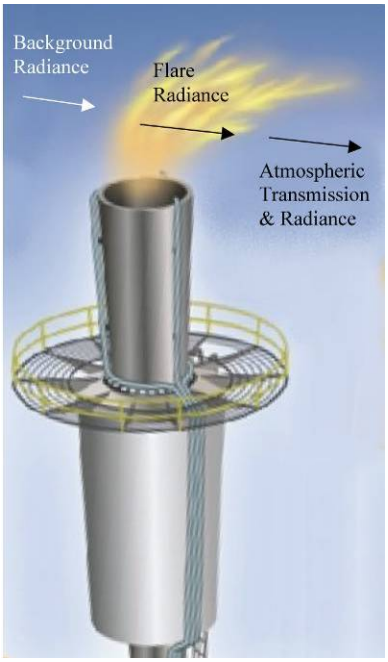

Figure A.5.1-1: Contributions to the measured flare radiance.

The total radiant signal received then consists of:

$$N_{total} = N_{bkg} \cdot \tau_{flr} \cdot \tau_{atm} + N_{flr} \cdot \tau_{atm} + N_{atm} + N_f \qquad \text{Equation A.5-2}$$

In Equation A.5-2, the arguments (ν, T) have been dropped for clarity and the individual terms are:

N_{total} = total radiance
N_{bkg} = background sky radiance
τ_{flr} = flare transmissivity
τ_{atm} = atmospheric transmissivity
N_{atm} = atmospheric radiance
N_f = radiance of the FTIR instrument itself

The actual measurements performed by the PFTIR consist of the following:

M_{flr} = the measured plume radiance
M_b = the measured background radiance taken by moving the PFTIR off the flare to monitor the sky background. This is given by:
$M_b = N_{bkg} \cdot \tau_{atm} + N_{atm} + N_f$
M_n = a measurement made looking at the calibration source (see below) with a cold (liquid nitrogen) emitter in place of the normal (black body)
M_{bb} = a measurement made looking at the calibration source with a commercial black body emitter in the source
τ_{atm} = measured atmospheric path transmission

A.2.2 From Radiance to Transmission Spectra

Based on these measurements Equation A.5-2 can be rearranged to give the plume transmission as:

$$\tau_{flr} = \frac{C \cdot \left(M_{flr} - M_n\right) - N_{BB}^{flr} \cdot \tau_{atm}}{C \cdot \left(M_b - M_n\right) - N_{BB}^{flr} \cdot \tau_{atm}} \qquad \text{Equation A.5-3}$$

In this equation, the superscript on the Planck function radiance (N_{BB}) denotes that this is the Planck function computed at the temperature of the flare. *C* is a calibration measurement made with a black body calibration source. This is the initial derivation that has had some proprietary modifications to improve stability and performance.

Atmospheric transmission τ_{atm} is also measured using the calibration source. In this case the black body is replaced by a standard infrared source and the measurement is made at a path length roughly equal to that of the slant-path from the PFTIR to the flare.

Atmospheric transmission is then given by:

$$\tau_{atm} = \frac{M_{IR} - M_n}{I_0}$$ Equation A.5-4

M_{IR} is the measured signal from the calibration source using the IR source and M_n is the measured cold source as defined earlier. The only term not defined is I_0. This is the so-called synthetic background. It is frequently used in open-path FTIR measurements to convert a measured spectrum to transmission. It represents the shape of the spectrum that the PFTIR would measure if no gases were present. It can be synthesized from the $(M_{IR} - M_n)$ measurement by doing a mathematical fit to points in the spectrum known to be free of molecular absorptions. An example is given in Figure A.2-2. In this figure, the bottom plot is the measured spectrum (here a relatively clean spectrum done in the laboratory), the middle plot the points chosen for fitting, and the top plot the mathematical fit to the chosen points. The top plot is the I_0 spectrum.

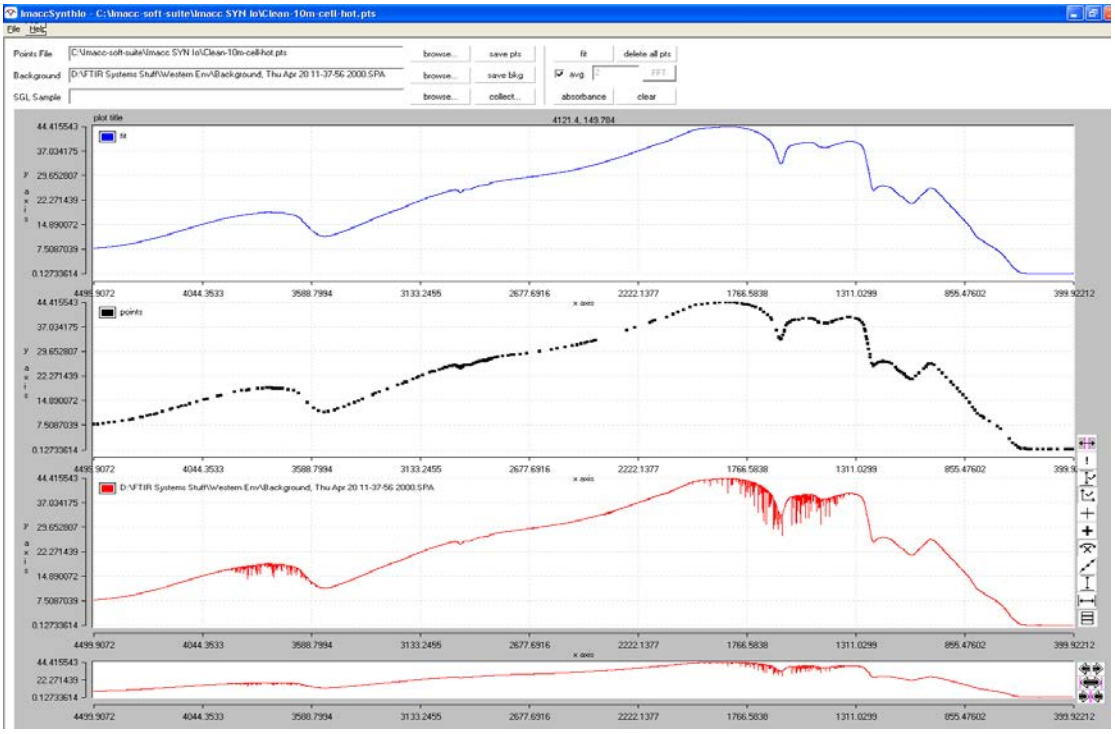

Figure A.5.2-1: Development of synthetic spectrum

A.2.3 Determination of Flare Temperature

With Equations A.5-3 and A.5-4, Equation A.5-2 then contains only measured or computed terms. However, to compute the Planck function at the temperature of the flare, N_{BB}^{flr}, the flare gas temperature must be known. Fortunately, this can be measured using features in the PFTIR data itself. One convenient feature is the CO band near 2150 cm^{-1}. Figure A.2-3 shows this band at two different temperatures. The upper plot is at ambient temperature (300 K) and the bottom plot is at 550 K. The effect of increasing temperature is to expand the band shifting the peak position away from band center while increasing the strength of the weaker lines farther

from band center. This is a sensitive function of temperature, so the shape of the band essentially measures temperature.

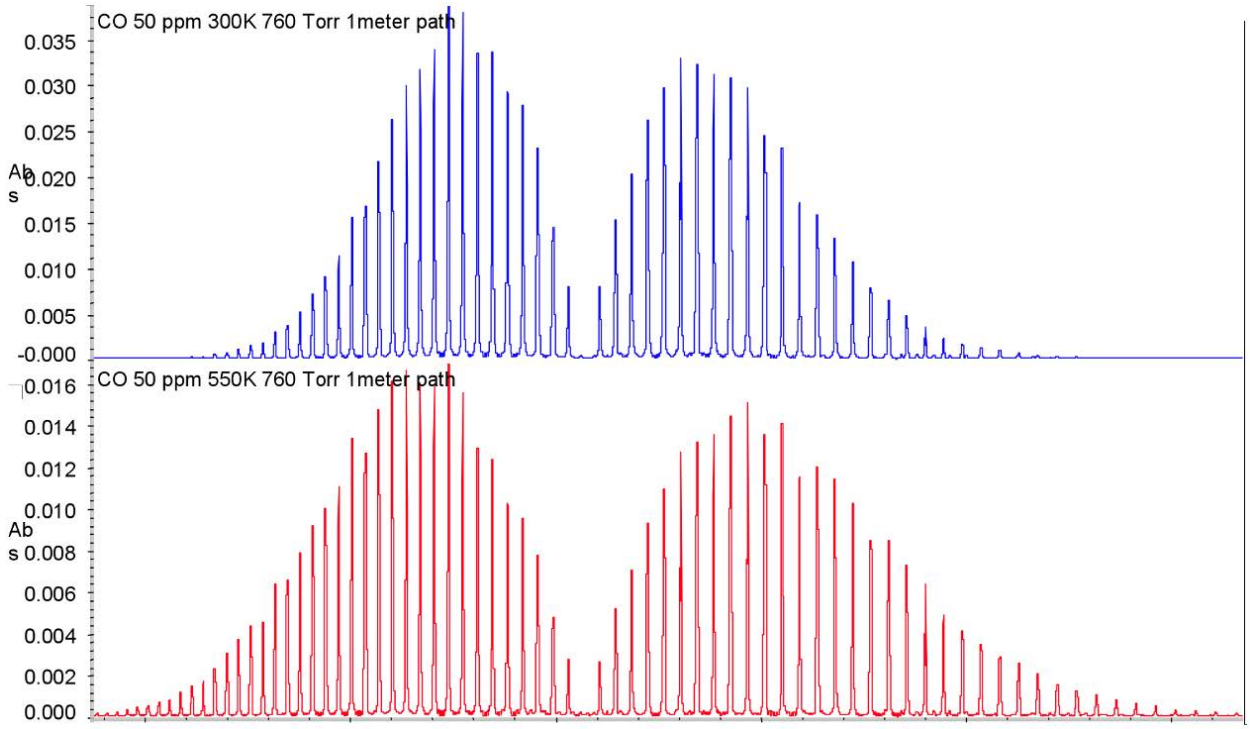

Figure A.5.3-1: Structure of the Fundamental CO Band at 300K (top) and 550K (bottom) showing alteration of band shape with temperature

The CO lines arise (in emission) from a transition of the molecule from a higher vibration/rotation state to a lower one. The transitions are dictated by quantum mechanics. However, the intensities of the individual lines are strongly influenced by the number of molecules in the initial state available to make the transition. This "population" of the initial states is dictated by the Boltzmann distribution which is given by:

$$N_{J"} = N_0 \cdot \frac{2 \cdot J" + 1}{Q} \cdot e^{\frac{-E"}{k \cdot T}} \qquad \text{Equation A.5-5}$$

Here $N_{j"}$ is the number of molecules in the initial rotational state defined by the rotational quantum number $J"$. N_0 is the total number of molecules available, $E"$ the energy of the initial state, k Boltzmann's constant, T the absolute temperature, and Q a "partition sum." The partition sum is just the sum of the exponential term over all possible energy levels. If the log of the measured intensity of the CO lines is plotted against the initial state energy, the plot is linear and its slope is proportional to

$$\frac{hc}{kT} \qquad \text{Equation A.5-6}$$

Where h is Planck's constant and c the speed of light.

Temperature can therefore be determined by measuring the slope of the plot. An example of this process is shown in Figure A.5.3-2. In this case the temperature was 225°C and the group of lines to the left in Figure A.5.3-2 was used. These are defined as the R-branch lines of the CO band.

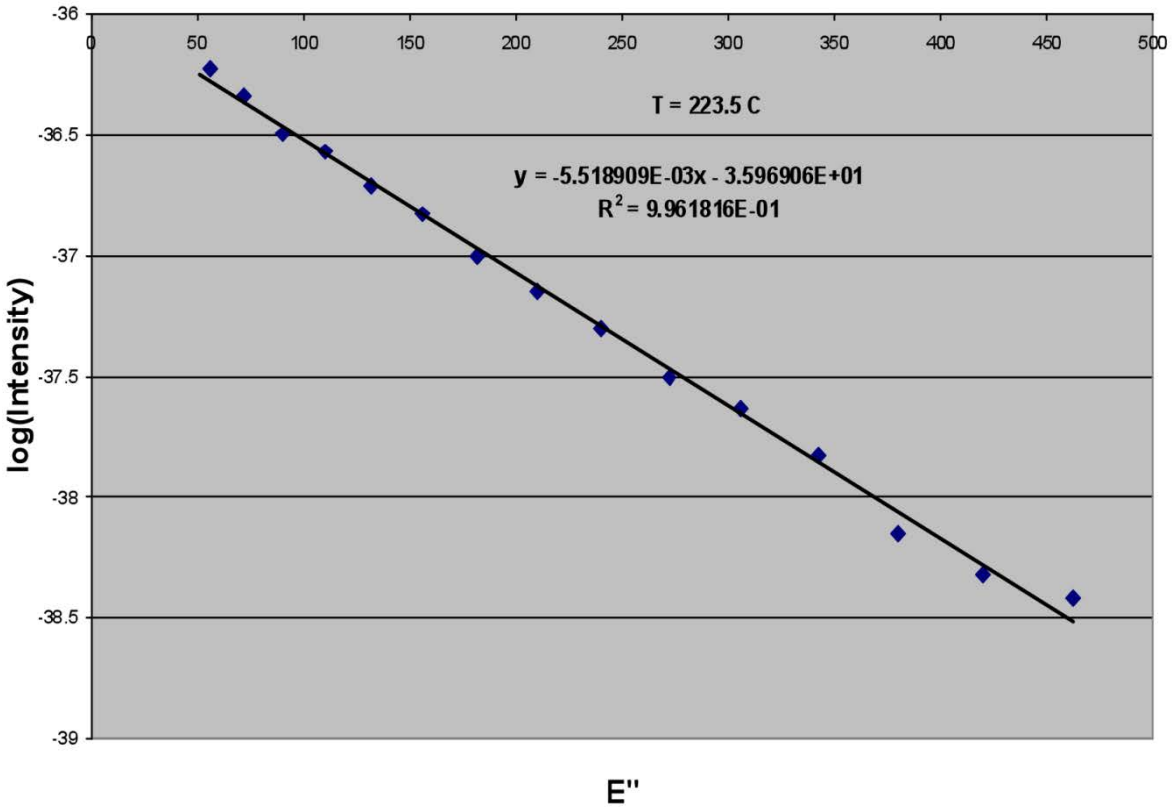

Figure A.5.3-2 Plot of the log of the measured intensity of the CO lines vs. initial state energy

Given temperature, all terms in Equation A.5-3 can be determined. Equation A.5-3 represents the transmission spectrum, just as would be observed if an active FTIR were used and an IR beam propagated through the plume. As a result, the same algorithms used in normal spectroscopy can be used to analyze this transmission spectrum.

A.2.4 From Transmission to Absorption Spectra

As in normal absorption spectroscopy, the transmission is exponential in gas concentration. That is transmission is given by:

$$\tau_{plume} = e^{-K(\nu)\cdot c\cdot l} \qquad \text{Equation A.5-7}$$

Where $K(\nu)$ is the absorption coefficient for the spectral line, c the gas concentration, and l the path length in the gas. Effectively $K(\nu)$ is the reference standard in the FTIR for the gas being monitored. Taking the negative log of this equation gives what is called Absorbance. For historical reasons, log base 10 is used and thus gives:

$$Absorbance(\nu) = (0.434) \cdot K(\nu) \cdot c \cdot l \qquad \text{Equation A.5-8}$$

Where the constant 0.434 is the log base 10 of e. Absorbance is linear in concentration times path length and the absorbance spectrum is analyzed using standard Classical Least Squares (CLS) procedures to get the individual gas concentrations in the spectrum.

A.3 VOC Emissions Calculations

A.3.1 Total VOCs

Annual emissions for total volatile organic compounds (VOCs) are based on daily emissions data, which is ultimately calculated from daily averaged process data and flare combustion efficiencies. Since methane and ethane are not considered VOCs due to their negligible ozone formation potential, any total VOC calculation excludes these compounds. The term "VOC" in the following paragraphs is equivalent to non-methane, non-ethane hydrocarbons.

Total VOC emissions are calculated using combustion efficiency (CE), which is required by the consent decree (CD). If vent gas composition and flow to the flare is continuously measured, total annual VOC emissions (EF_{VOC}) can be determined as follows:

$$E_{VOC} = 0.0005 \cdot \sum_{p=1}^{n} \left[Q_{vg} \cdot VOC_{vg} \cdot MW_{VOC} \cdot 0.0026 \cdot (1 - CE) \right]_p \qquad \text{A.3.1-1}$$

Where:

E_{VOC}	VOC emissions for a specific fuel type (short tons / year)
Q_{vg}	Vent gas flow rate (scfh)
VOC_{vg}	VOC volume fraction in the vent gas normalized to the sum of the volume fractions of all constituents measured in the vent gas. See Equation 2.
MW_{VOC}	Molecular weight of VOCs measured in the vent gas (lb / lb-mole). See Equation 3.
0.0005	Unit conversion factor (1 short ton / 2000 lb)
0.0026	Molar volume conversion factor (1 lb-mole / 385.5 scf)
CE	Combustion efficiency (fraction). See Table A.3.1-1 for CE determination.
p	Measurement period index
n	Annual operating periods

VOC_{vg} is calculated in Equation (1) by summing the measured volume fractions (%) of all individual VOCs and dividing the sum by the total volume fraction (%) as determined from the measurement of all vent gas constituents. This normalization is primarily done to account for uncertainty in the individual compound measurement results, which on occasion could result in total volume fractions not equal to 100%.

$$VOC_{vg} = \frac{\sum_k x_{VOC,k}}{\sum_i x_i} \qquad (1)$$

Where:

VOC_{vg}	VOC volume fraction normalized to the sum of the volume fractions of all constituents measured in the vent gas (including methane, ethane, and inerts)
$x_{VOC,k}$	Volume fraction of each individual VOC measured in the vent gas stream (%)
x_i	Volume fraction of each constituent measured in the vent gas stream (%)
i	Index for all compounds in the vent gas.
k	Index for all VOC in the vent gas.

The hourly averaged total VOC molecular weight contained in the vent gas is determined via Equation (2) by weighting each individual VOC molecular weight by the corresponding volume fraction. The resulting term is divided by the total VOC volume fraction (%) in order to normalize the molecular weight.

$$MW_{VOC} = \frac{\sum_k \left(x_{VOC,k} \cdot MW_{VOC,k}\right)}{\sum_k x_{VOC,k}} \quad (2)$$

Where:

MW_{VOC}	Molecular weight of VOC measured in the vent gas (lb / lb-mole)
$MW_{VOC,k}$	Molecular weight of each individual VOC measured in the vent gas stream (lb / lb-mole)
$x_{VOC,k}$	Volume fraction of each individual VOC measured in the vent gas stream (%)
k	Index for all VOC in the vent gas.

The hourly averaged combustion efficiency (CE) is a function of the average combustion zone net heating value (NHV_{cz}) during the same time frame. Table provides CE for different ranges of NHV_{cz}.

Table A.3.1-1. Combustion efficiency (CE) as a function of Net Heating Value of the Combustion Zone (NHV_{cz})

NHV_{cz} (BTU/scf)	**CE (Fraction)**
$NHV_{cz} < 96$	0.0
$96 \leq NHV_{cz} < 300$	$[0.16 \cdot (-95 + NHV_{cz})]/[1 + 0.16 \cdot (-95 + NHV_{cz})]$
$300 \leq NHV_{cz} < 350$	0.98
$350 \leq NHV_{cz} < 425$	0.985
$425 \leq NHV_{cz} < 500$	0.9875
$500 \leq NHV_{cz} < 600$	0.99
$600 \leq NHV_{cz}$	0.995

A.3.2 Speciated VOCs

Combustion efficiency (CE) and destruction efficiency (DE) are two different parameters used to characterize how efficiently a flare is operating. CE is the percentage of hydrocarbons being sent to the flare that is converted to carbon dioxide (CO_2) through complete combustion. DE is the percentage of hydrocarbons being sent to the flare that is either converted to CO_2 through complete combustion or converted to carbon monoxide (CO) through incomplete combustion. Emissions of individual VOC and hydrocarbon compounds should be reported using destruction efficiency (DE) rather than combustion efficiency (CE). This represents a more accurate approach to reporting emissions, as it does not include the incomplete combustion product carbon monoxide (CO) which biases emission estimates high. Consequently, substituting CE with DE in Equation A.3.2-1 yields a more accurate expression for flare emissions[1]. This calculation uses the global DE value for all compounds and does not attempt to estimate individual DE for each compound.

$$E_{VOC,k} = 0.0005 \cdot \sum_{p=1}^{n} \left[Q_{vg} \cdot \frac{x_{VOC,k}}{\sum_i x_i} \cdot 0.0026 \cdot MW_{VOC,k} \cdot (1 - DE) \right]_p \qquad \text{A.3.2-1}$$

Where:

$E_{VOC,k}$	Annual emissions of one individual VOC/HC (short tons / year)
Q_{vg}	Vent gas flow rate (scfh)
$x_{VOC,k}$	Volume fraction of each individual VOC measured in the vent gas stream (%)
x_i	Volume fraction of each constituent measured in the vent gas stream (%)
$MW_{VOC,k}$	Molecular weight of individual VOC/HC in the vent gas (lb / lb-mole)
0.0005	Unit conversion factor (1 short ton / 2000 lb)
0.0026	Molar volume conversion factor (1 lb-mole / 385.5 scf)
DE	Destruction efficiency (fraction)
p	Measurement period index
n	Annual operating periods.
i	Index for all compounds in the vent gas.
k	Index for all VOC in the vent gas.

It has been shown that DE scales linearly with CE for a variety of flare tip designs and operating conditions. For a CE range of 0.965 to 1, Equation A.3.2-2[1] is used to calculate DE as a function of CE.

$$DE = 0.8382 \cdot CE + 0.1622 \quad for \quad 0.965 \leq CE < 1 \qquad \text{A.3.2-2}$$

CE is a function of the average net heating value of the vent gas in the combustion zone (NHV_{cz}). Use hourly averaged NHV_{cz} values in conjunction with Table A.3.1-1 to determine the corresponding hourly averaged CE.

1. Pearson, D., and S. Evans. *A comparison of combustion efficiency and destruction efficiency.* Marathon Petroleum Company, LLC, Detroit, Michigan: Prepared for Marathon Petroleum Company, LLC, 2013.

A.4 Personnel Involved with Flare Performance Test

BP Products North America
Dave Ringwald
Dave Fashimpaur
Rohini Sengupta
Jim Keating
Ken Come

Clean Air Engineering, Inc.
Dan Pearson
Scott Evans
Tony Milianti
Mike LeResche
Roy Scandrol

A.5 Minute Data of Runs

Minute data spreadsheets and charts are located on the digital media provided with this report.

A.6 Video Data of Runs

Videos of Test Runs are located on the digital media provided with this report.

A.7 PFTIR Raw Data and Spectra

PFTIR Raw Data and Spectra are located on the digital media provided with this report.

A.8 Background Times and Spectra

Background Times and Spectra are located on the digital media provided with this report.

A.9 Daily Calibration Data and Spectra

Daily Calibration Data and Spectra are located on the digital media provided with this report.

A.10 Flare Visual Rating Data Sheets

Flare Visual Rating Data Sheets are located on the digital media provided with this report.

A.11 Gas Calibration Sheets for Hot Cell Calibrations

Gas Calibration Sheets are located on the digital media provided with this report.

A.12 Tracerco Correction Factors

A Tracerco study conducted at Whiting indicated that the reported flow rates of steam and vent gas may not be accurate. Adjustment factors were applied to these measurements. All data contained in the main body of this report uses the flow correction factors obtained from the Tracerco study. Table A.12-1 shows the correction factors used to corrected the DDU and ALKY vent gas and steam flow rates. These correction hours are based on standard volume flowrates Figures A.12-1 through A.12-5 show the impact of the Tracerco correction factors on key test parameters.

	Flow	Correction Factors
ALKY	Vent Gas	1.98
	Steam	2.84
DDU	Vent Gas	0.81
	Steam	1.21

Table A.12-1: Tracerco Correction Factors

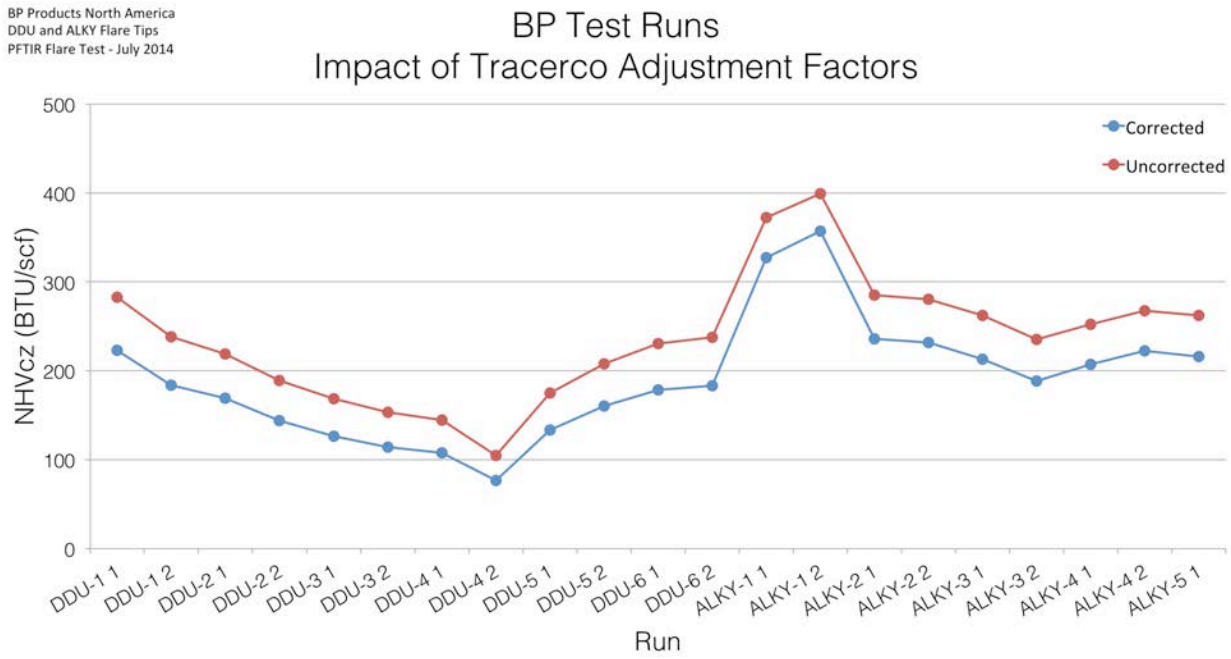

Figure A.12-1: Impact of Tracerco Correction Factors on NHVcz

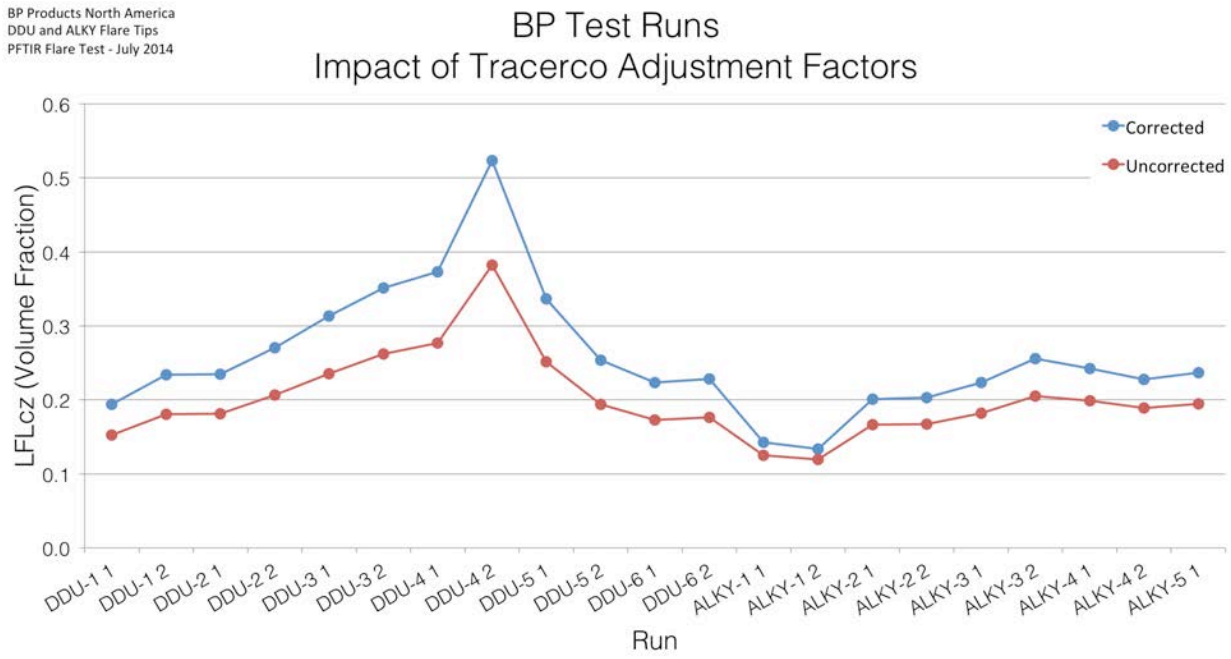

Figure A.12-2: Impact of Tracerco Correction Factors on LFLcz

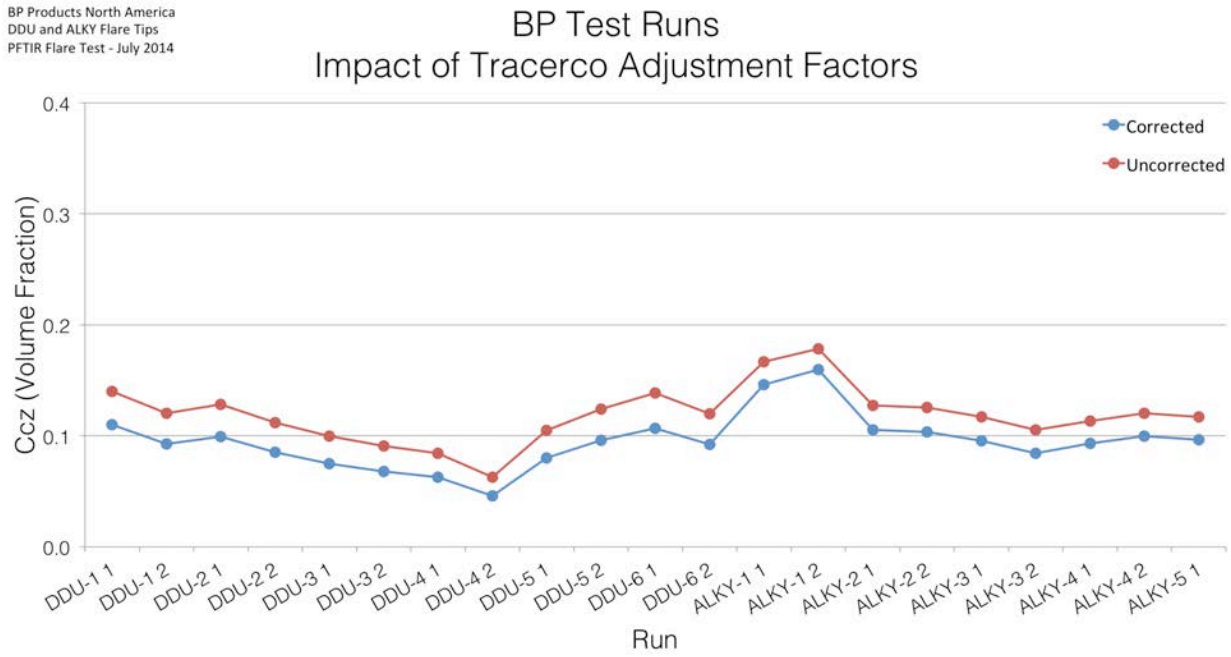

Figure A.12-3: Impact of Tracerco Correction Factors on Ccz

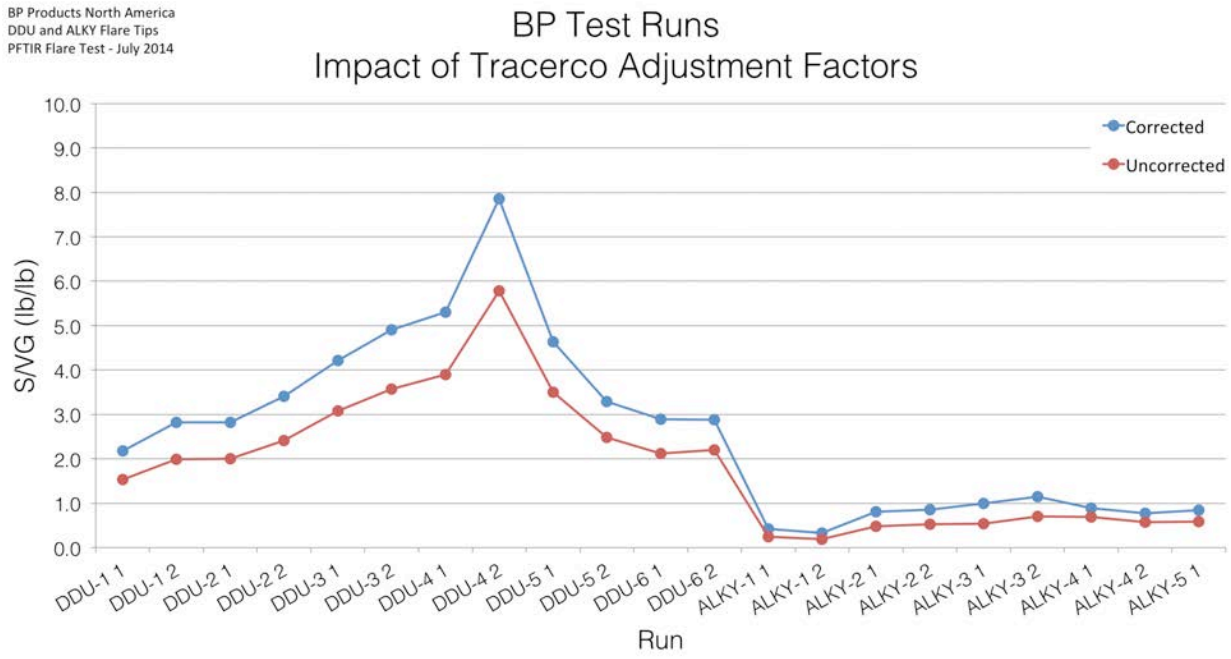

Figure A.12-4: Impact of Tracerco Correction Factors on S/VG (lb/lb)

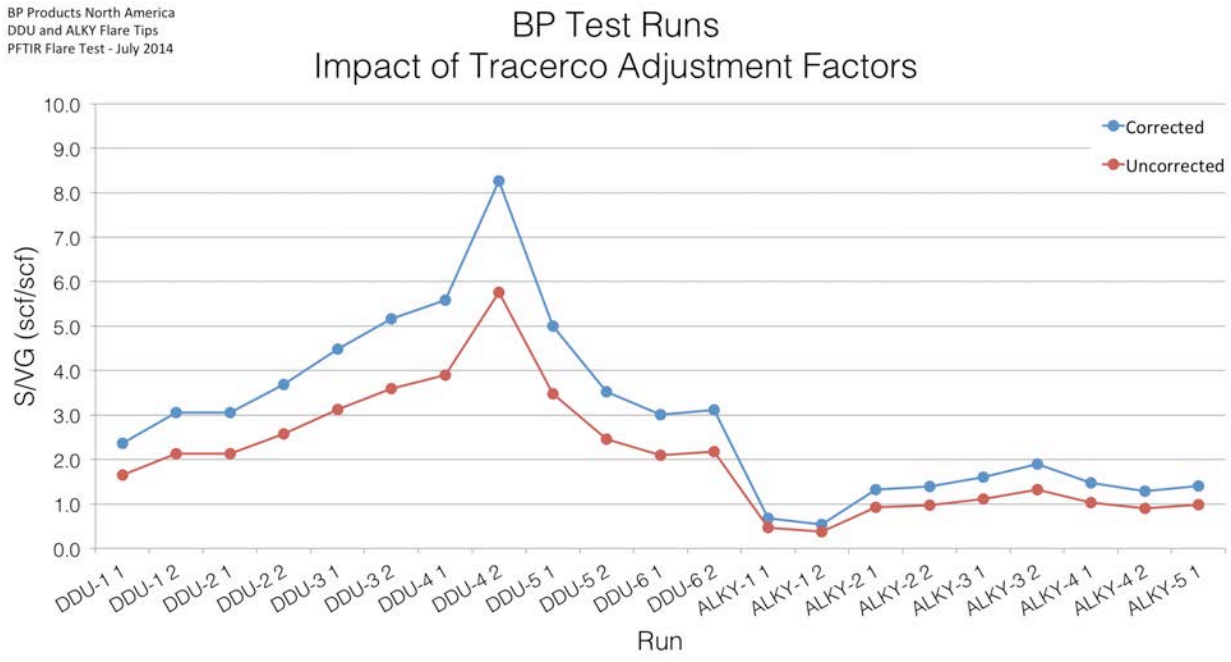

Figure A.12-1: Impact of Tracerco Correction Factors on S/VG (scf/scf)

A.13 Vent Gas Composition

Figure A.13-1 shows the vent gas component distribution for each run. Figure A.13-2 shows the net heating value contributions of each vent gas component for each run. Table A.13-1 lists the vent gas component distribution for each run. Table A.13-2 lists the net heating value contributions of each vent gas component for each run.

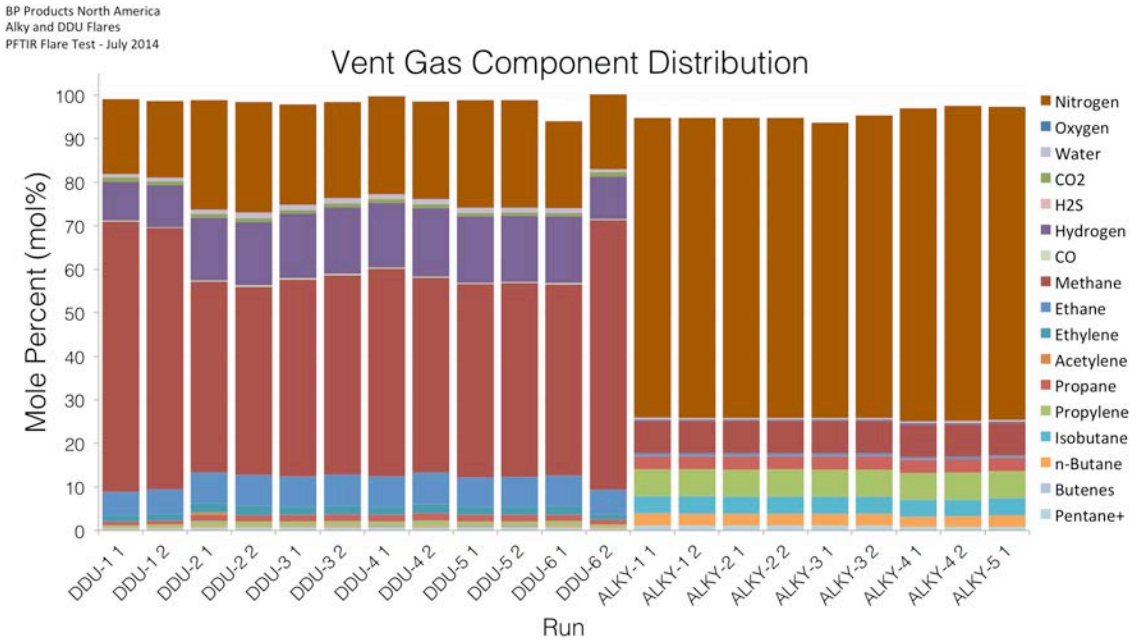

Figure A.13-1: Vent Gas Component Distribution for Each Run

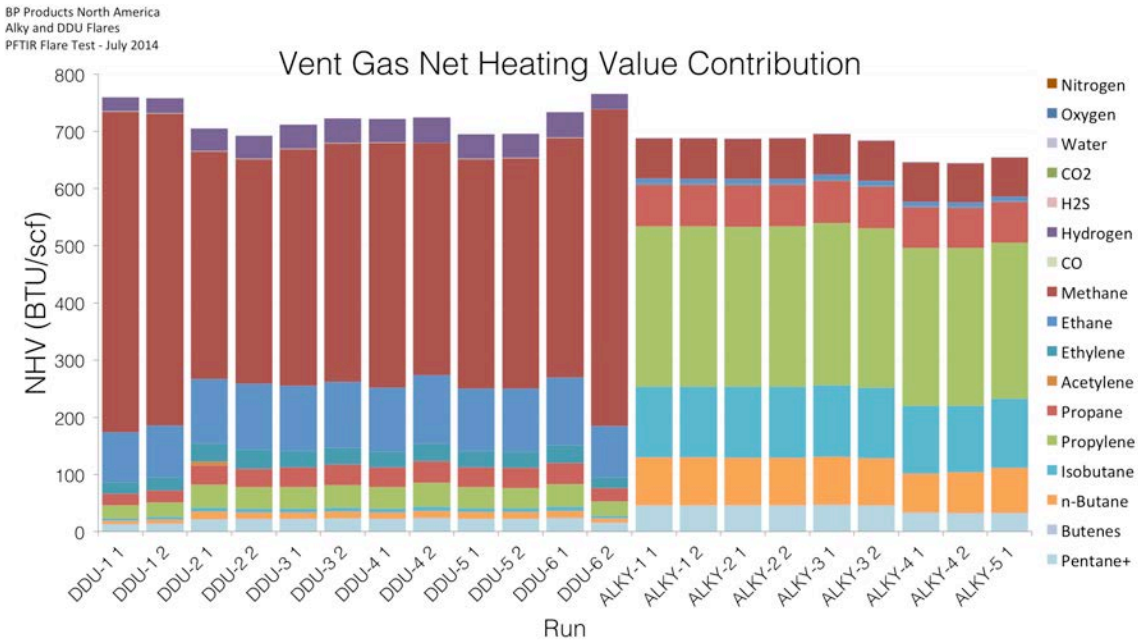

Figure A.13-2: Vent Gas Net Heating Value Contributions for Each Run

Condition --	Run --	Nitrogen (mol %)	Oxygen (mol %)	Water (mol %)	Carbon dioxide (mol %)	Carbon monoxide (mol %)	Hydrogen sulfide (mol %)	Methane (mol %)	Ethane (mol %)	Hydrogen (mol %)	Ethylene (mol %)	Acetylene (mol %)	Propane (mol %)	Isobutane (mol %)	n-Butane (mol %)	Butenes (combined) (mol %)	Propylene (mol %)	n-Pentane+ (mol %)	Total (mol %)	Molar Weight (lb/lb-mol)
DDU-1	1	17.3	0.0	0.8	1.0	0.2	0.0	62.1	5.4	8.9	1.4	0.0	0.9	0.1	0.2	0.0	0.5	0.3	99.1	19.3
DDU-1	2	17.6	0.0	0.8	1.0	0.2	0.0	60.1	5.6	9.6	1.5	0.0	0.9	0.2	0.2	0.1	0.6	0.3	98.6	19.2
DDU-2	1	25.1	0.0	1.0	1.0	0.3	0.0	43.9	7.0	14.4	2.1	0.5	1.5	0.2	0.4	0.1	0.9	0.5	98.9	19.1
DDU-2	2	25.3	0.0	1.3	0.9	0.3	0.0	43.2	7.1	14.6	2.3	0.0	1.4	0.2	0.4	0.1	0.9	0.5	98.4	19.0
DDU-3	1	22.9	0.0	1.2	0.8	0.2	0.0	45.2	7.0	14.9	1.9	0.0	1.5	0.2	0.4	0.1	0.8	0.5	97.8	18.9
DDU-3	2	22.0	0.0	1.2	0.8	0.2	0.0	45.8	7.1	15.4	2.0	0.0	1.5	0.2	0.4	0.1	0.9	0.6	98.4	18.9
DDU-4	1	22.4	0.0	1.1	0.8	0.2	0.0	47.7	7.0	14.9	1.9	0.0	1.5	0.2	0.4	0.1	0.9	0.6	99.7	18.8
DDU-4	2	22.4	0.0	1.2	0.8	0.3	0.0	44.7	7.4	15.8	2.1	0.0	1.6	0.2	0.4	0.1	1.0	0.6	98.5	18.8
DDU-5	1	24.7	0.0	1.2	0.8	0.2	0.0	44.4	6.8	15.3	1.9	0.0	1.5	0.2	0.4	0.1	0.8	0.6	98.9	18.7
DDU-5	2	24.7	0.0	1.1	0.8	0.2	0.0	44.5	6.9	15.2	1.9	0.0	1.5	0.2	0.4	0.1	0.8	0.6	98.9	18.7
DDU-6	1	19.9	0.0	1.1	0.8	0.3	0.0	44.0	7.0	15.3	2.0	0.0	1.5	0.2	0.4	0.1	0.9	0.6	94.0	18.6
DDU-6	2	17.2	0.0	0.7	0.9	0.2	0.0	62.0	5.6	9.9	1.2	0.0	1.1	0.2	0.3	0.1	0.6	0.4	100.2	18.6
ALKY-1	1	68.9	0.0	0.4	0.1	0.0	0.0	7.4	0.5	0.3	0.1	0.0	3.0	4.0	2.7	0.0	6.2	1.2	94.8	36.4
ALKY-1	2	68.9	0.0	0.4	0.1	0.0	0.0	7.4	0.5	0.3	0.1	0.0	3.0	4.0	2.7	0.0	6.2	1.2	94.8	36.1
ALKY-2	1	68.9	0.0	0.4	0.1	0.0	0.0	7.4	0.5	0.3	0.1	0.0	3.0	4.0	2.6	0.0	6.2	1.2	94.8	33.9
ALKY-2	2	68.9	0.0	0.4	0.1	0.0	0.0	7.4	0.5	0.3	0.1	0.0	3.0	4.0	2.7	0.0	6.2	1.2	94.8	33.6
ALKY-3	1	67.8	0.0	0.4	0.1	0.0	0.0	7.4	0.5	0.3	0.1	0.0	3.0	4.0	2.7	0.0	6.2	1.2	93.7	33.0
ALKY-3	2	69.4	0.0	0.4	0.1	0.0	0.0	7.4	0.5	0.3	0.1	0.0	3.0	4.0	2.6	0.0	6.2	1.2	95.3	34.0
ALKY-4	1	71.9	0.1	0.3	0.1	0.0	0.0	7.4	0.5	0.4	0.1	0.0	3.0	3.9	2.2	0.1	6.3	0.8	97.0	34.6
ALKY-4	2	72.3	0.0	0.3	0.1	0.0	0.0	7.4	0.5	0.4	0.1	0.0	3.0	3.8	2.4	0.1	6.3	0.8	97.5	34.5
ALKY-5	1	71.9	0.1	0.3	0.1	0.0	0.0	7.4	0.5	0.3	0.1	0.0	3.0	4.0	2.6	0.0	6.2	0.8	97.3	31.4

Table A.13-1: Vent Gas Component Distribution for all Test Runs

Condition --	Run --	Nitrogen NHV BTU/scf	Oxygen NHV BTU/scf	Water NHV BTU/scf	Carbon dioxide NHV BTU/scf	Carbon monoxide NHV BTU/scf	Hydrogen sulfide NHV BTU/scf	Methane NHV BTU/scf	Ethane NHV BTU/scf	Hydrogen NHV BTU/scf	Ethylene NHV BTU/scf	Acetylene NHV BTU/scf	Propane NHV BTU/scf	Isobutane NHV BTU/scf	n-Butane NHV BTU/scf	Butenes (combined) NHV BTU/scf	Propylene NHV BTU/scf	n-Pentane+ NHV BTU/scf	Total NHVvg BTU/scf
DDU-1	1	0.0	0.0	0.0	0.0	0.6	0.0	561.0	87.6	24.7	20.6	0.0	19.9	4.1	6.4	1.2	22.5	11.6	760.2
DDU-1	2	0.0	0.0	0.0	0.0	0.7	0.0	545.7	91.0	26.7	23.0	0.0	21.0	4.5	6.9	1.4	25.1	12.6	758.7
DDU-2	1	0.0	0.0	0.0	0.0	0.8	0.0	397.9	113.2	39.8	31.8	6.8	33.6	6.5	13.4	1.7	40.0	20.0	705.8
DDU-2	2	0.0	0.0	0.0	0.0	0.9	0.0	393.2	114.6	40.6	34.1	0.0	31.7	6.8	10.8	2.5	38.0	19.7	692.9
DDU-3	1	0.0	0.0	0.0	0.0	0.8	0.0	414.2	114.5	41.7	28.6	0.0	35.0	6.7	11.2	1.9	37.2	20.4	712.1
DDU-3	2	0.0	0.0	0.0	0.0	0.8	0.0	417.3	115.5	42.9	29.7	0.0	35.7	7.0	11.7	1.9	39.3	21.3	723.2
DDU-4	1	0.0	0.0	0.0	0.0	0.8	0.0	428.8	111.9	40.9	27.8	0.0	34.4	6.7	11.3	2.0	37.0	20.4	722.0
DDU-4	2	0.0	0.0	0.0	0.0	0.8	0.0	406.4	119.1	43.9	31.3	0.0	37.6	7.3	12.0	2.2	41.9	21.9	724.5
DDU-5	1	0.0	0.0	0.0	0.0	0.8	0.0	402.2	109.3	42.4	28.4	0.0	34.3	6.9	11.4	1.9	36.8	20.8	695.1
DDU-5	2	0.0	0.0	0.0	0.0	0.8	0.0	403.6	110.5	42.0	28.3	0.0	34.6	6.9	11.5	1.7	35.6	20.7	696.2
DDU-6	1	0.0	0.0	0.0	0.0	0.9	0.0	419.0	118.9	44.7	30.9	0.0	37.0	7.2	12.1	2.1	39.5	21.9	734.3
DDU-6	2	0.0	0.0	0.0	0.0	0.6	0.0	554.2	89.6	27.0	18.4	0.0	24.0	4.7	7.6	1.6	24.9	13.8	766.3
ALKY-1	1	0.0	0.0	0.0	0.0	0.0	0.0	70.3	8.2	0.8	2.2	0.0	72.9	123.7	83.8	1.3	280.5	44.9	688.8
ALKY-1	2	0.0	0.0	0.0	0.0	0.0	0.0	70.3	8.2	0.8	2.2	0.0	72.9	123.9	83.5	1.3	280.5	44.9	688.4
ALKY-2	1	0.0	0.0	0.0	0.0	0.0	0.0	70.2	8.2	0.8	2.2	0.0	73.0	124.1	82.8	1.3	280.4	44.9	687.9
ALKY-2	2	0.0	0.0	0.0	0.0	0.0	0.0	70.3	8.2	0.8	2.2	0.0	72.9	124.0	83.2	1.3	280.4	44.9	688.2
ALKY-3	1	0.0	0.0	0.0	0.0	0.0	0.0	71.1	8.3	0.8	2.2	0.0	73.9	125.5	84.1	1.4	283.8	45.4	696.5
ALKY-3	2	0.0	0.0	0.0	0.0	0.0	0.0	69.9	8.1	0.8	2.2	0.0	72.6	123.4	82.5	1.3	278.9	44.6	684.4
ALKY-4	1	0.0	0.0	0.0	0.0	0.0	0.0	68.2	7.5	1.1	1.7	0.0	71.4	118.0	68.2	1.7	277.2	31.6	646.5
ALKY-4	2	0.0	0.0	0.0	0.0	0.0	0.0	68.0	7.5	1.1	1.6	0.0	70.5	115.7	71.8	1.8	276.8	30.3	645.1
ALKY-5	1	0.0	0.0	0.0	0.0	0.0	0.0	68.3	8.0	0.8	1.7	0.0	71.1	121.2	79.4	1.3	272.8	30.8	655.3

Table A.13-2: Vent Gas Net Heating Value Contribution for all Test Run